N O T I C E

THIS DOCUMENT HAS BEEN REPRODUCED FROM MICROFICHE. ALTHOUGH IT IS RECOGNIZED THAT CERTAIN PORTIONS ARE ILLEGIBLE, IT IS BEING RELEASED IN THE INTEREST OF MAKING AVAILABLE AS MUCH INFORMATION AS POSSIBLE

8.1 - 1 0 0.2 9.
CR-1635-29

REMOTE SENSING APPLICATIONS TO

RESOURCE PROBLEMS IN SOUTH DAKOTA

For

National Aeronautics and Space Administration
Office of University Affairs
Washington, D.C.

July 1, 1979 to June 30, 1980

Annual Progress Report
Grant No. NGL 42-003-007

Remote Sensing Institute
South Dakota State University
Brookings, South Dakota 57007

Abstract

'· Cooperative projects between RSI and numerous South Dakota agencies have provided an important means of incorporating remote sensing techniques into operational programs. In Fiscal Year 1980 eight projects have been completed; each project is abstracted in the following, titled paragraphs.

Detection of High Moisture Zones Near Interstate 90

High moisture zones adjacent to Interstate 90 in western South Dakota are associated with highway warping and/or pavement breakup. Location of the high moisture zones indicates possible areas where drainage tiles can be installed to ease the problem. Thermal, midday and predawn, and color infrared imagery were collected at three altitudes (305, 914, 2472 m) on two dates (5/24/79 and 9/14/79) over a primary study area, a 20-mile segment of I-90 near Rapid City. An 8-mile segment of I-90 near Chamberlain was also flown on 9/15/79 at 914 m; day and predawn thermal data and CIR photography were collected. Visual analysis and level slicing (thermal imagery only) revealed that predawn, September 9 thermal imagery (2 a.m. LST) appeared best for locating high moisture zones in the Rapid City area. Color infrared imagery was of valuable assistance with the thermal imagery in the Rapid City site, and by itself in the Chamberlain area it was more useful than either midday or predawn thermal imagery for locating high moisture zones. Further analysis and field data are needed to verify the utility of the September predawn thermal data in the Rapid City area.

Thermal Infrared Census of Canada Geese in South Dakota

Current methods for censusing Canada goose concentrations on the mainstem reservoirs in South Dakota have sizeable errors. Significant errors occur because many geese are feeding away from the reservoir during counts and return only in the evening. The objective of this project is to determine the feasibility of an operational inventory utilizing aerial thermography collected during the night when all geese are resting on the water. The thermal infrared emissivity of central flyway geese was measured at .962 ± .017. There were no significant differences in emissivities between species of Canada and Snow geese or between adults and immature. The apparent temperature of Canada geese was measured at varying environmental temperatures. The results of this data were used in conjunction with test flights to determine ambient temperature constraints for successful aerial thermal infrared data collection. Geese could be distinguished from the background of water or ice on aerial thermal infrared imagery collected with a trimetal detector at altitudes less than 455 m AGL. There was a 10.98% error between estimates of goose numbers from thermal imagery and the actual number of geese determined from counts made on aerial photographs.

Dutch Elm Disease Detection in Urban Environment

Dutch elm disease is fatal to nearly all elm trees. The disease is transmitted by beetles which survive in the dead or dying trees. Removal of infected trees is the only effected method to control the disease. Economic loss, including removal of dead trees was $22 million in South Dakota in 1978. The city of Watertown and South Dakota Division of Forestry are cooperating with the Remote Sensing Institute to use remote sensing data for early detection and removal of infected trees before the disease is spread. Aerial photography collected in August 1979 proved to be basically unusable because of camera malfunction. The film was used primarily for training in basic species identification. New photography was collected on June 28, 1980. The data has been reviewed and is suitable for objectives of the project.

A Feasibility Study for Monitoring Effective Precipitation in South Dakota Using TIROS-N

A study is in progress to evaluate the potential for using weather satellite (TIROS-N) data to monitor effective precipitation. TIROS-N imagery were compared with ground measurement of precipitation and soil moisture. No patterns associated with moisture variations were found on the standard image products. Digitally enhanced imagery are currently being produced and will be analyzed.

Open and Abandoned Dump Sites in Spink County

There are numerous open and abandoned solid waste dump sites in existance which are utilized without sound environmental practices. Several government agencies are addressing this solid waste management problem. One major problem is determining how many and where they exist. Remote sensing techniques have successfully been used to identify the location of these sites and provide other resource information concerning pollution potential.

Influence of Soil Reflectance on Landsat Signatures of Crops

Ten photo-interpreted strata were evaluated within a study area in eastern South Dakota as a means of partitioning Landsat data into relatively homogeneous regions. Economics, Statistics, and Cooperatives Service provided the ground sample scheme in which 255 segments were spread across the 6-county study area. Ground data, collected in last week of July and first week of August, included field boundaries, crop type, and crop stage on aerial photographs (1:15840). Corn and sunflower digital data were extracted from an August 25, 1979 Landsat Computer Compatible Tape. Analysis of variance for corn data indicated that there were significant differences among strata and among crop stages. Multiple comparison testing for corn grouped strata that were not statistically significant; five to seven groups were indicated, dependent upon Landsat MSS band. Sunflower data have not yet been analyzed; however, expansion of the ground data provided a current areal estimate of sunflowers for use by several South Dakota agencies. Multivariate analyses are needed for a comparison between corn and sunflower results.

Model Implementation Program - Lake Herman Watershed

The Lake Herman watershed in southeastern South Dakota was selected as one of seven watersheds in the United States for involvement in the national pilot Model Implementation Program (MIP). Remote Sensing Institute is cooperating with numerous other states and local agencies to provide baseline and continuous resource information for watershed management. An information system including land cover, soil series, slope, drainage and land treatment is being used to locate land in need of treatment, sites suitable for sediment control structures and estimate sediment delivery to the lake.

Six-Mile Investigation Follow-On

An investigation of Six-Mile Creek Watershed, located in southeastern South Dakota, was conducted in FY79 to develop and apply remote sensing techniques to assess the geohydrology and the environment of the watershed to evaluate the impact of a proposed dam and recreation site on Six-Mile Creek. As part of the original investigation, SCS geologists used thermal imagery to select sites for drilling observation wells to provide information for designing seepage and cutoff controls. A follow-on to the original investigation was requested to document the results of the drilling. The drilling, which occurred in August 1979, verified the presence of permeable alluvium and near-surface groundwater in the vicinity of the proposed dam.

TABLE OF CONTENTS

TABLE OF CONTENTS (Continued)

TABLE OF CONTENTS (Continued)

LIST OF FIGURES

LIST OF FIGURES (Continued)

LIST OF TABLES

LIST OF TABLES (Continued)

ACKNOWLEDGEMENTS

REMOTE SENSING APPLICATIONS TO
RESOURCE PROBLEMS IN SOUTH DAKOTA

The Remote Sensing Institute has cooperated with numerous local, state, and federal agencies in South Dakota to effect the transfer of remote sensing techniques. The cooperative projects have been made possible through the funding of NASA, the State of South Dakota, and numerous cooperating agencies. The overall objectives embodied in the NASA Applications Program are: 1) introduce remote sensing techniques to local, state, or federal agencies in addressing certain resource problems of South Dakota; and/or 2) provide alternative methods of improving current practices or procedures. In FY 1980 eight projects have been completed.

DETECTION OF HIGH MOISTURE ZONES
NEAR INTERSTATE 90

INTRODUCTION

The deteriorating condition of many highways in South Dakota is a very severe problem. The role of the state's highways in transportation is further emphasized in 1980 due to the reduction of railway services and concomitant increase in heavy truck traffic. While much of the deterioration of the highways is due to age and the economics of maintenance (i.e. inflation and lowered taxes), numerous areas of the I-90 system in western South Dakota have had a warping or break up problem due to the geologic nature of this region.

Fractures, joints, and bedding planes in the Pierre shale have contributed to differential weathering and ultimately to variable expansion-contraction of materials under and near I-90 in western South Dakota. Several research and characterization studies have been undertaken to more fully understand the nature of these phenomena (Bruce and Scully, 1966; McDonald, 1970; and Hoskins and Hammerquist, 1970). These studies have accomplished much in describing the morphology and genesis of Pierre shale as it relates to highway breakup and/or warping.

It is generally accepted that the so-called highway bumps are the result of two major mechanisms: 1) differential expansion of weathered shale and clayey textured soils at the interface of cut-and-fill sections, and 2) very commonly, faults in the Pierre shale and the

resultant "gouge" zones of 2:1 clays. The presence of soil moisture is a triggering factor in bump formation. Hoskins and Hammerquist (1969) reported water in 4 of 9 trenches which were "... dug in a rather scattered manner ..."; some perched water tables were also noted. One source of water is the dam-like effect of bumps in highway ditches, i.e. drainage from highway ditches is blocked by the swelling of the gouge material. In many cases, the gouge areas expand more and faster than the surrounding material (Hammerquist and Hoskins, 1969). Primary and secondary discontinuities also provide mechanisms for water movement in the Pierre Formation (Bruce and Scully, 1966).

McDonald (1970) has outlined three possible approaches to eliminate water accumulation in the lower portions of roadbeds located in Pierre shale problem areas. Very briefly the methods are: 1) an asphalt blanket over the in-slope, ditch bottom, and part of the backslope; 2) a drain or tile utilizing granular materials; and 3) increasing the gradient in the ditches to facilitate better drainage.

Assuming that the above methods of combating the high moisture zones associated with highway bumps are successful, it follows that these procedures should be implemented at the earliest sign of a problem. Hoskins et al. (1971) reported the usefulness of low altitude color and color infrared (CIR) photography to locate fracture zones associated with I-90 near Rapid City. Other remote sensing studies have indicated the potential of thermal infrared imagery for locating zones of high moisture (Rib, 1975; Stallard and Myers, 1972).

The major objective of this study was to investigate the utilization of CIR photography and thermal infrared imagery as tools in locating problem areas related to highway warping or breakup associated with the Pierre Formation. Other objectives included a comparison of the remote sensing variable (i.e. altitudes, CIR and thermal, date of collection) and the transfer of the data to DOT personnel.

STUDY AREA

A 20-mile segment of I-90 near Rapid City, representative of highway breakup problems, was selected as the primary study area (Figure 1). Fracture zones in parts of this area have been previously documented (Hoskins et al., 1971). This area is in a warm, very dry plain with an annual rainfall of 35 to 43 cm. Soils have formed in Pierre shale and in high terraces.

A secondary site west of Chamberlain was added to the project in mid-summer due to cooperator interest (Figure 2). This site lies in a warm, dry plain with a rainfall of near 43 cm. Soils have formed in the Pierre shale. The rolling to steeply breaking topography often exposes several members of the Pierre Formation. This region has a high landslide potential.

PENNINGTON COUNTY STUDY AREA

Rain
Recording
Stations

SOIL ASSOCIATION

Terrace Soils
  18. Satanta, gently undulating

Clay uplands
  24. Pierre-Samsil, undulating
  26. Samsil-Pierre, rolling
Badlands
  30. Badlands, steep
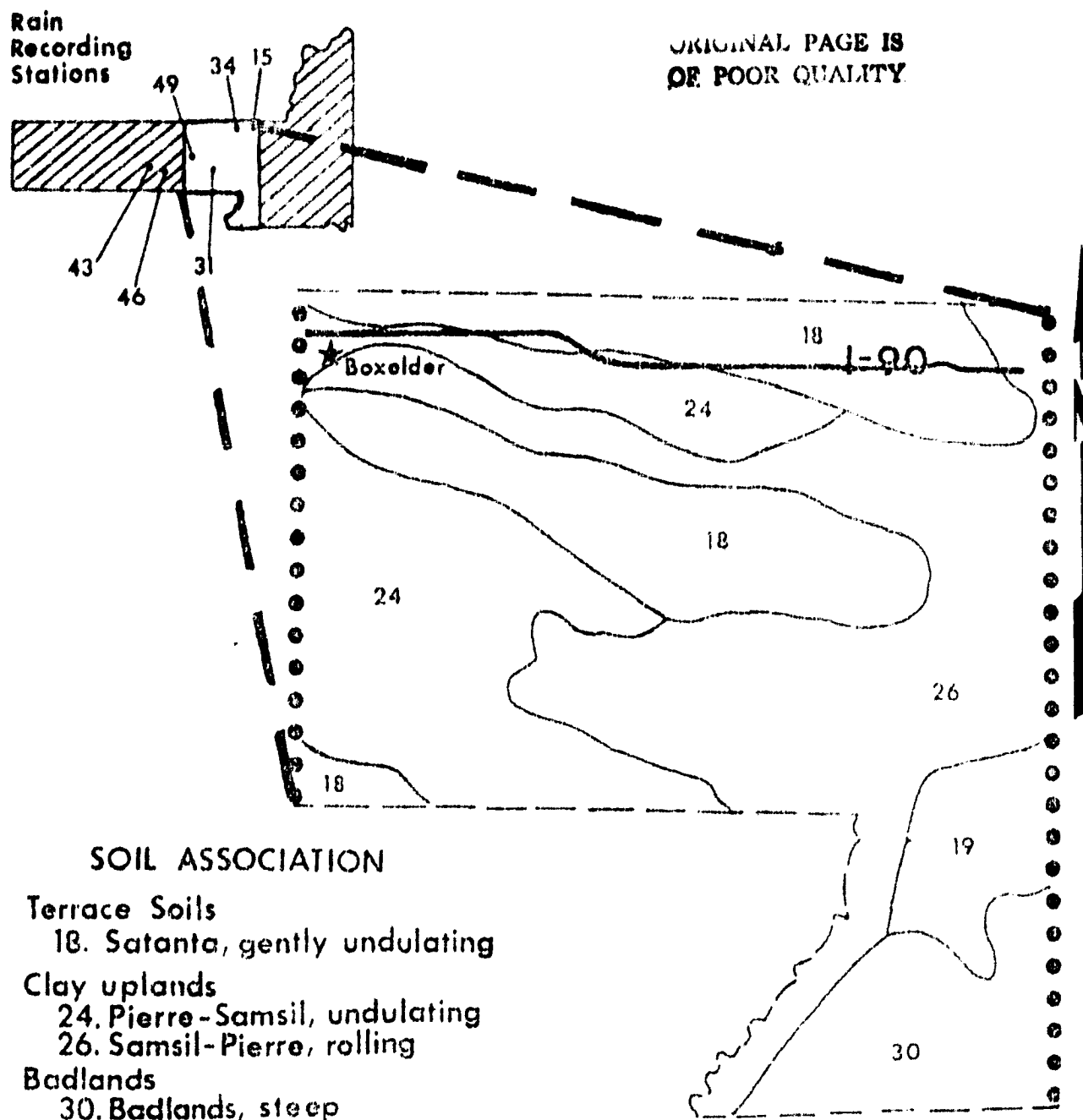
Figure 1. Location of I-90 study section and the soils of surrounding
region. Precipitation recording stations are also located.
(See Table 2).

CHAMBERLAIN STUDY AREA

LYMAN COUNTY

MISSOURI RIVER

I-90

. 20

. 25

. 17

NT-PS . 8

Z3-NT

RJ

. 13

I .

Oacoma

NT PS

M9-HG

N

SOIL ASSOCIATIONS

Uplands, Clayey
NT-PS   Opal-Promise
Z3-NT   Sansarc-Opal

Uplands, Silty
RJ Reliance

Bottomlands, Loamy
M9-HG Munjor-Haverson
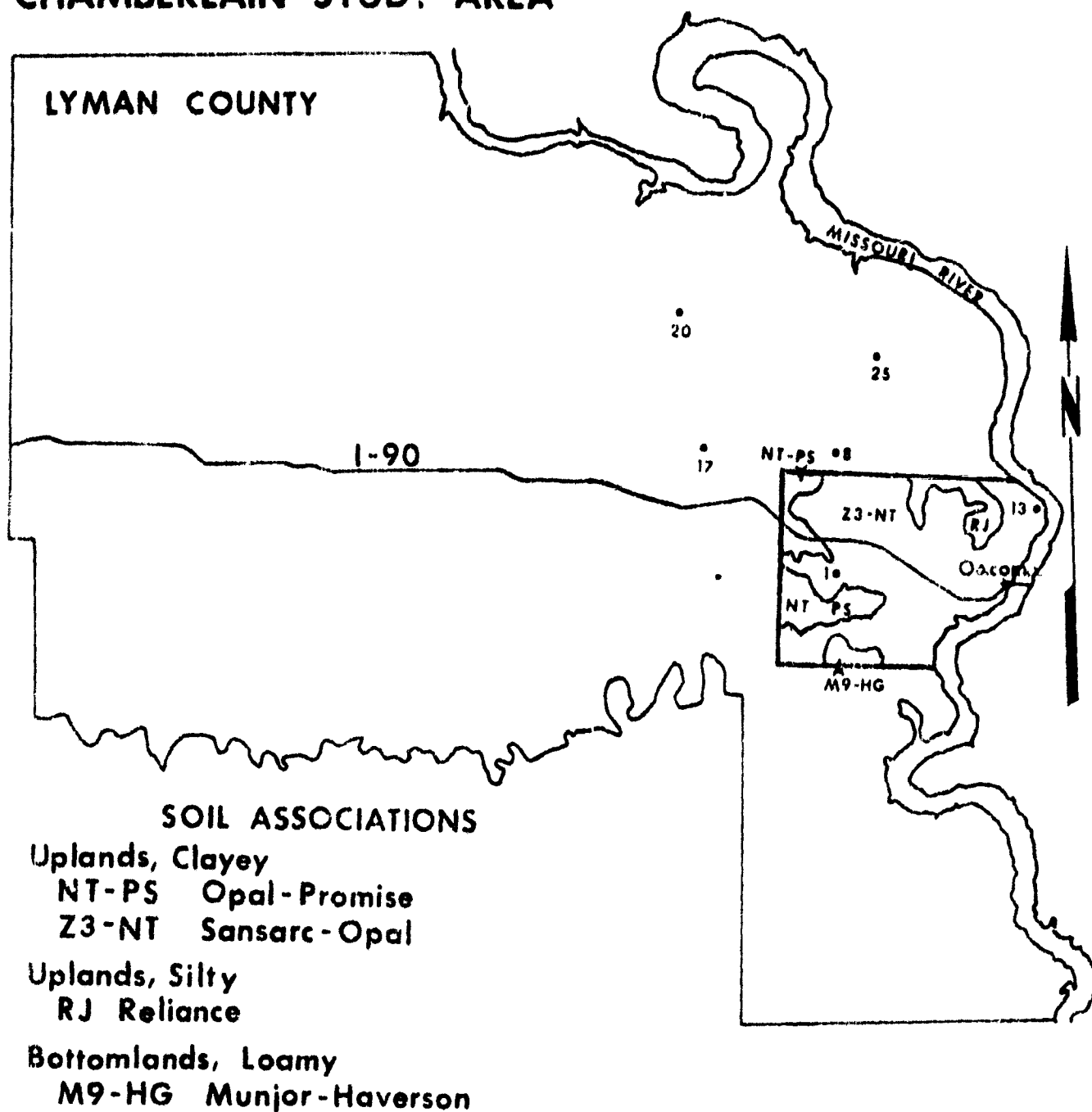
Figure 2. Location of Chamberlain study area. Precipitation recording
stations are the numbered positions in and surrounding the
study site. (See Table 2).

METHODS AND MATERIALS

Thermal imagery and CIR photography were collected twice for the
Rapid City site and once for the Chamberlain site. Further pertinent
details of each flight are outlined in Table 1. All flights took place
under cloudless skies. The 4.5 to 5.5 µm thermal detector was used in
the initial flight due to malfunction in the 8.7 to 11.5 µm thermal
detector.

Neither of the sites had received any rainfall immediately prior
to the aerial data collection. Precipitation recorded during the
growing season is detailed by monthly totals and recording station
(Table 2).

Photo-interpretation of the remote sensing data was accomplished
using visual analysis. The CIR photography in its original, film-
positive format was systematically and stereoscopically interpreted.
Landform, surficial drainage, soils, and vegetation were the major
indicators used in the delineation of potential high moisture zones.
Thermal imagery was level sliced to accentuate the apparent temperature
zones of interest, i.e. cool areas during day flights and warm areas
during night flights are zones of potentially high water tables.
Positive prints (approximately 1:10,000 scale) of the September-collected
thermal and CIR imagery were delivered to DOT personnel.

Limited field checking of the remote sensing interpretations was
accomplished by DOT personnel. Field checks were visual; the correspondence
of several interpreted high moisture zones on the September data (i.e. day

Table 1. Aircraft data collected for 1980 DOT project.

Data	Site	Date	Altitude Above Ground Level (m)			Range of Apparent Ground Temp.†	Notes
			305	914	2742		
Thermal (4.5-5.5 μm)	Rapid City	5/24/79	x	x	x	20 to 44° C, 14 to 35.5° C, 10 to 32° C	Day flight§
Color infrared photography†† (.51 to .91 μm)	Rapid City	5/24/79		x			
Thermal (4.5-5.5 μm)	Rapid City	5/25/79	x			10 to 20° C	Predawn flight
Thermal (8.7-11.5 μm)	Rapid City	9/14/79	x	x	x	6 to 46° C, 6 to 46° C, 6 to 46° C	Day flight
Color infrared photography (.51 to .91 μm)	Rapid City	9/14/79		x			
Thermal (8.7-11.5 μm)	Rapid City	9/15/79	x	x		-4 to 16° C, -4 to 16° C	Predawn flight, Temp. inversion
Thermal (8.7-11.5 μm)	Chamberlain	9/15/79	x	x		20 to 50° C, 20 to 50° C	Day flight
Color infrared photography (.51 to .91 μm)	Chamberlain	9/15/79		x			
Thermal (8.7-11.5 μm)	Chamberlain	9/16/79	x	x		1 to 21° C, 1 to 21° C	Predawn flight, Temp. inversion

† As instrumented on the thermal scanner.

†† One pass centered on highway with 60% endlap.

§ All day flights took place at approximately 2 p.m. local standard time (LST) while night or predawn flights took place at approximately 2 a.m. LST.

Table 2. Precipitation records for area around study sites (1979 data provided courtesy of Department of Water and Natural Resources, Pierre).

			Precipitation (cm)				
Station	April	May	June	July	Aug.	Sept.	Totals
Pennington County							
15	2.1	2.9	13.2	8.7	4.5	.2	31.6
31	.6	2.9	10.3	13.7	5.7	0	33.2
34	1.3	3.3	12.6	10.1	4.7	0	32.0
43	N/A	1.3	13.1	12.4	6.8	0	33.6
46	N/A	N/A	10.3	11.6	7.0	.1	29.0
49	4.4	2.7	9.1	8.5	4.9	6.2	35.8
Lyman County							
01	4.6	5.0	5.3	13.2	5.7	0	33.8
08	5.4	N/A	6.3	13.9	9.3	0	34.9
13	7.3	5.8	10.3	N/A	5.2	N/A	28.6
17	.8	6.1	6.2	12.2	6.9	0	32.2
20	4.2	5.2	14.7	12.8	7.7	N/A	44.6
25	5.7	7.3	10.7	20.5	6.4	0	50.6

See Fig. 1 and Fig. 2 for station location.

CIR and predawn thermal) to ground features was checked in the Rapid City site during June, July 1980. Drilling programs to verify shallow water tables have not been undertaken. Consequently, interpretations based on the CIR and the thermal data were not fully authenticated. However, DOT personnel will be utilizing the interpretations when drilling programs are undertaken in the Rapid City study area.

RESULTS AND DISCUSSION

In order to fulfill the major objective of this study, three flight altitudes, day and night flights, thermal and CIR data, and two flight periods were included. It was established, within reasonable limits, that the remote sensing data had merit, in accord with the major objective. This was accomplished by: 1) reference to a previous project in the Rapid City study area (Hoskins et al., 1971); 2) position of interpreted areas to highway patches; and 3) communication with DOT personnel who were familiar with the area. The next evaluation was the selection of the best set of variables, i.e. altitude, etc.

The comparison was accomplished in a two-step procedure. First, possible high moisture zones were located on the remote sensing data; this was relatively easy since several problem areas in the study site had previous documentation (Hoskins and Hammerquist, 1969; Hoskins et al., 1971). The second phase of comparison was photo-interpretation of various highway segments where high moisture zones were indicated. Qualitative comparison among the remote sensing variables took place; this was accomplished by answering the following two questions: 1) was the possible high moisture zone recorded on all the imageries, and 2) if it was, how easy was it to locate. The indicators of possible high moisture zones were presented to DOT personnel for their use with photographic prints.

Rapid City Site

The comparison of the variables was accomplished strictly in a visual manner. The results for the Rapid City site are listed as follows, by the "best" variable: 1) altitude-914 meters; 2) remote sensing data-predawn thermal; and 3) season of flight-early September. The selection of the most useful variable is obviously limited by the number of variables. Other factors also limited the extent to which the foregoing results could be extrapolated.

The results apply only to the variables tested (e.g. a 1500 m altitude may be a better compromise between cost and resolution than 914 meters). The results are applicable only within the constraints of the antecedent climatic events (Table 2). Two thermal detectors of different spectral response were used, thereby, causing extrapolative problems in comparing the spring vs fall data. However, acquisition of thermal data in the fall has been shown to be useful for locating shallow aquifers (Myers and Moore, 1972). Additionally, the CIR photography, while not rated as the "best" variable, provided complementary information to the thermal data as well as a means of registering the thermal data to ground locations.

Knowledge of basic soil thermal properties and characteristics is useful in interpreting the thermal data. The conductivity and storage of heat in the soil is differentiated to a large degree by the content of soil air and soil moisture. A large volume of soil air is a result

of low soil moisture (this is variable with texture) and as such the thermal conductivity and heat capacity are reduced. Consequently, the heat capacity in a dry soil is diminished, and the transfer of the heat to deeper portions of the soil is restricted, relative to a case where soil moisture is abundant. As a result (i.e. when comparing "dry" to "wet" soils) the maximum day soil temperature will occur in the dry soil because heat capacity and thermal conductivity are low. Whereas, at night when the soil is radiating to a clear sky, the wet soil will be warmer than the dry soil because of greater heat storage (Van Wijk and DeVries, 1963). In other words, soil with a water table within capillary rise of near the surface will be cooler during the day and warmer at night than a soil without such a water table. It must be noted, however, that daytime thermal patterns are strongly influenced by actively transpiring plants and the direction and steepness of slopes, among other considerations.

The use of CIR photography was very useful in recording differential vigor of vegetation. In this study, we looked for non-alluvial pockets of actively growing vegetation to indicate a favorable moisture regime, or shallow water table (Fig. 3). Growing vs non-growing vegetation is easily distinguishable on CIR photography. If seepage or a shallow water table has occurred, the vigor of vegetation drawing upon the additional soil moisture was often easily perceived on the September CIR photography and thermal imagery (Fig. 4). The daytime thermal patterns also record this cooler surface, but the thermal imagery is

Fig. 3. Actively growing vegetation (A) is recorded by CIR photography
(14 September 1979). Anomalous, nonalluvial vegetative growth
often indicates the availability of additional soil moisture.
Magenta or red tones are actively growing vegetation. Blue-
green is bare soil and is of a smoother texture than rangeland.
Light-toned areas are harvested crops. Scale is approximately
1:5500 (18 cm/km).

Color infrared photography
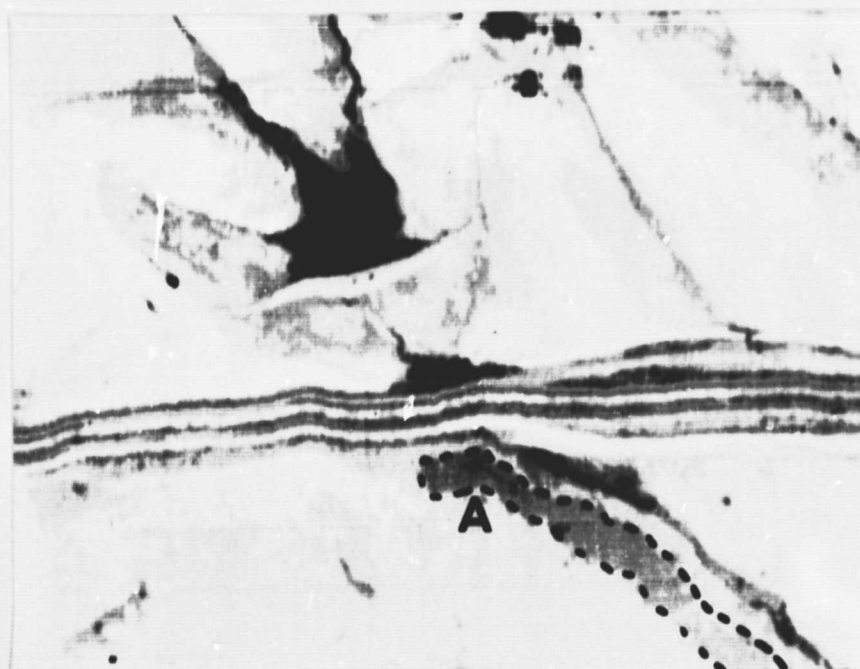
September 14 day thermal; dark is cool, white tones >39°C

Fig. 4. Growing vegetation on a sideslope (A) is shown on CIR photography
and day and predawn thermal imagery. Highway patches in this
vicinity indicate this high moisture zone may be contributing to
the highway problem. A small saline seep is noticeable on the
CIR photography (B). The apparent temperature of the ground is
represented on the thermal prints by six tones, each of which
relates to a range of temperatures. Approximate scale is
1:5500 (18 cm/km).
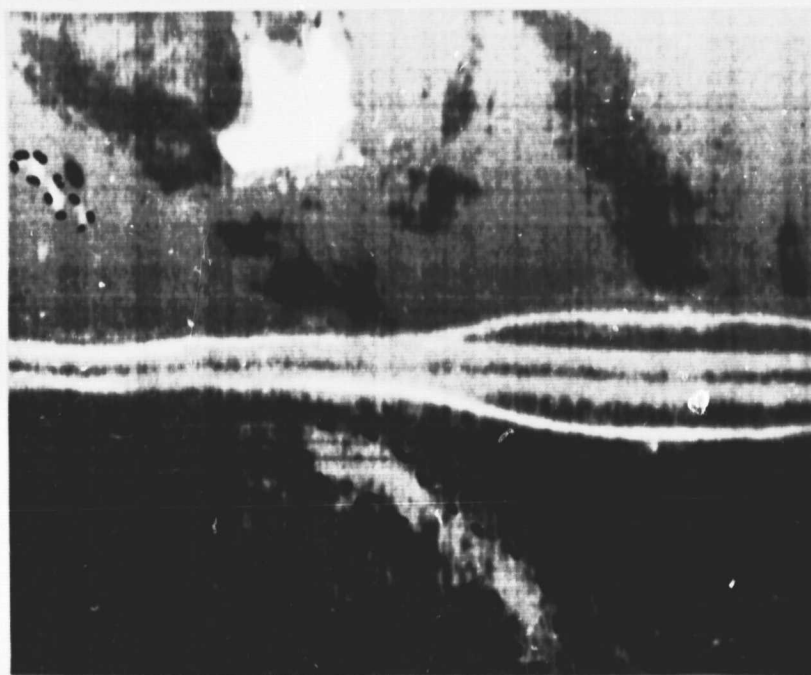
September 15 predawn thermal; dark is cool, black tones <6°C

Fig. 4. Continued.

not limited by the necessity of having a transpiring surface. The May CIR photography (not shown) recorded the influence of the spring snow melt on vegetative growth in the road ditches; this is not an indicator of high moisture zones. Many elements were considered when the interpretation was being undertaken such as landscape position, slope, shape of the surface (i.e. concave vs convex), and other mitigating features.

Some patterns on the predawn thermal imagery and the day CIR photography did not correspond (Fig. 5). While the drainage pattern is indicative of shale (Fig. 5a), the thermal patterns (i.e. warm areas) in this area seemed to encircle several gravelly "caps" (Fig. 5b). Shallow water tables are indicated by warm apparent temperatures; however further ground investigation, including drilling, is needed for full corroboration.

The complexity of vegetated surfaces is apparent on the CIR photography (Fig. 6a). However, unless the vegetation is indicative of the subsurface phenomenon of interest, this detail is not useful (ad hoc). The complexity of this surface can be reduced to series of discrete ranges of apparent ground temperatures (Fig. 6b), but aspect of slope, slope, and shape of slope (i.e. concave vs convex slope) present confounding thermal patterns. Further reduction of complexity is accomplished by using predawn thermal data (Fig. 6c). The predawn thermal data is less biased by the confounding factors, as listed above, and therefore, it empirically provides the most useful information. The photographic tones which correspond to 12.5 to 14.5° C
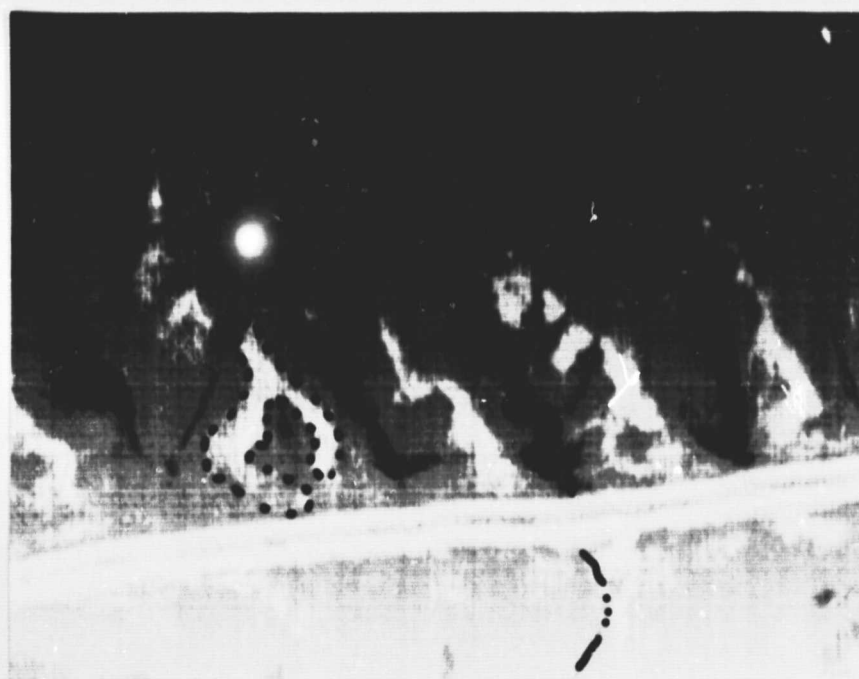
14 September

15 September; dark is cool, 6 to 16°C

Fig. 5. Potential high moisture zones are revealed on the predawn thermal imagery but not on the CIR photography. Warm areas (possible high moisture zones) excluding the highway pavement are predominantly north of the highway in a north-south orientation. Light tones are warm on the thermal imagery. Scale of CIR print is approximately 1:5500 (18 cm/km); scale of thermal prints is approximately 1:4500 (22 cm/km).
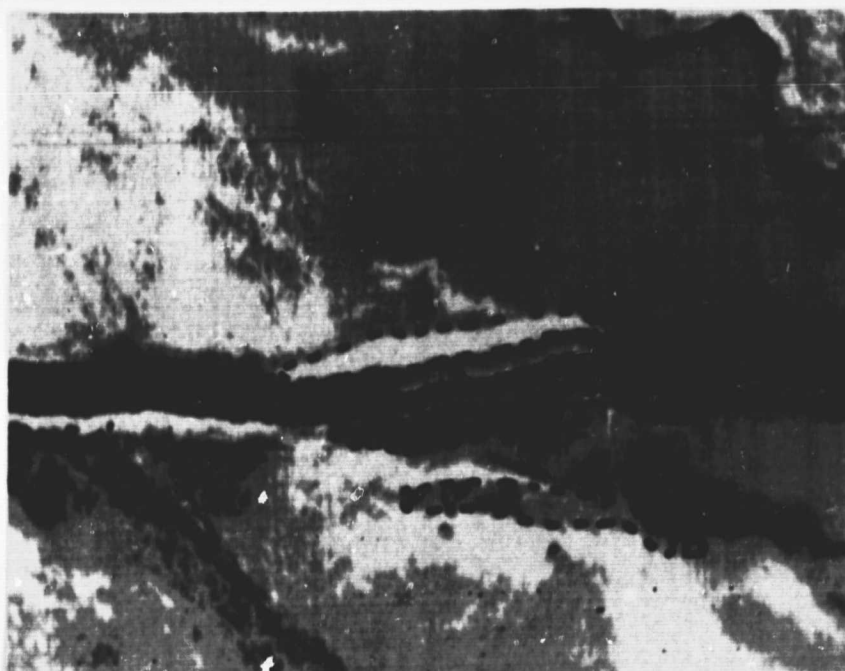
14 September day thermal; dark is cool

Fig. 6. The influence of aspect on road cuts (A) is shown on CIR and thermal data; the predawn thermal is the least sensitive to aspect variation in this area. A potential high moisture zone is indicated on the predawn thermal imagery (B). Scale of CIR is approximately 1:5500. Scale of thermal prints is approximately 1:5000 (20 cm/km).
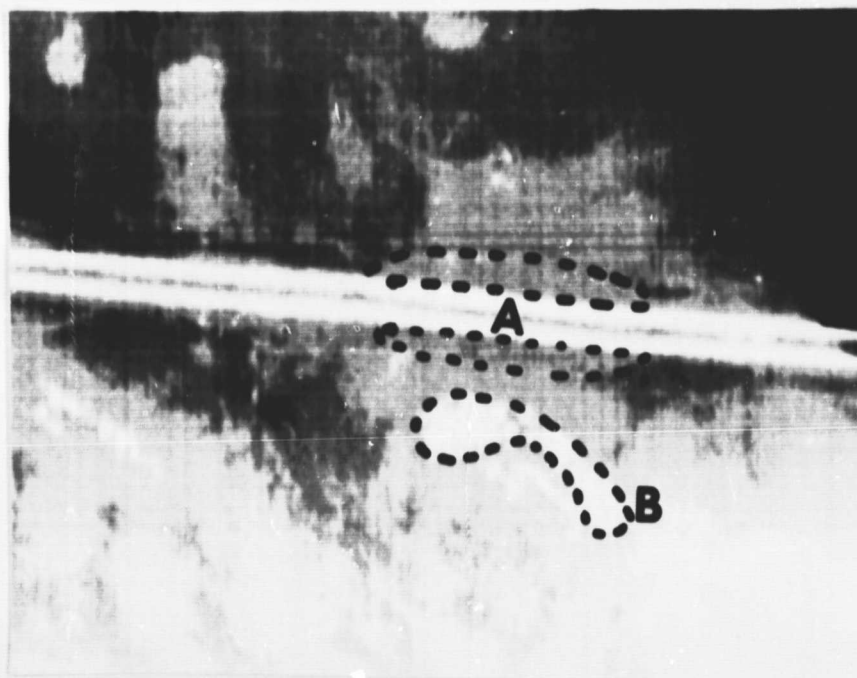
15 September predawn thermal; dark is cool

Fig. 6. Continued

Fig. 7. The complexity of the topography in the Chamberlain site
is shown. Sharon Springs member of the Pierre Formation (A)
outcrops near the entire study area. Salinity associated with
water movement is shown (B). Scale is approximately 1:12000
(8.5 cm/km).

apparent ground temperature on the predawn, 15 September 1979, thermal imagery were interpreted as indicative of a shallow water table in the absence of other mitigating factors, e.g. open water.

Chamberlain Site

This region provided a landscape of much variability compared to the Rapid City site. While the Pierre shale remained as the major parent material, the exposure of numerous members of the Pierre shale and the steepness of the topography contributed to the surficial complexity (Fig. 7). Due to these factors, the CIR photography provided the more useful information in the Chamberlain site. Additionally, a temperature inversion (predawn flight) may have reduced the usefulness of the thermal data. There were no comparisons other than CIR photography vs thermal imagery because only one flight took place (Table 1). Ground verification was limited to visual comparison of imagery tones to ground features. DOT personnel are intimately familiar with this area and they were able to provide much pertinent information about this area which was gathered in the construction phase. Again, no dulling programs were undertaken, and the information gathered from remote sensing did not add substantially to what was already known.

Major indications of high moisture zones in this area on the CIR photography are as follows: 1) lush vegetation on sideslopes (Fig. 8), 2) salinity (Fig. 7), and 3) salt-affected vegetation.

The location of high moisture zones in both areas, other than alluvial soils, is not necessarily directly related to the alleviation
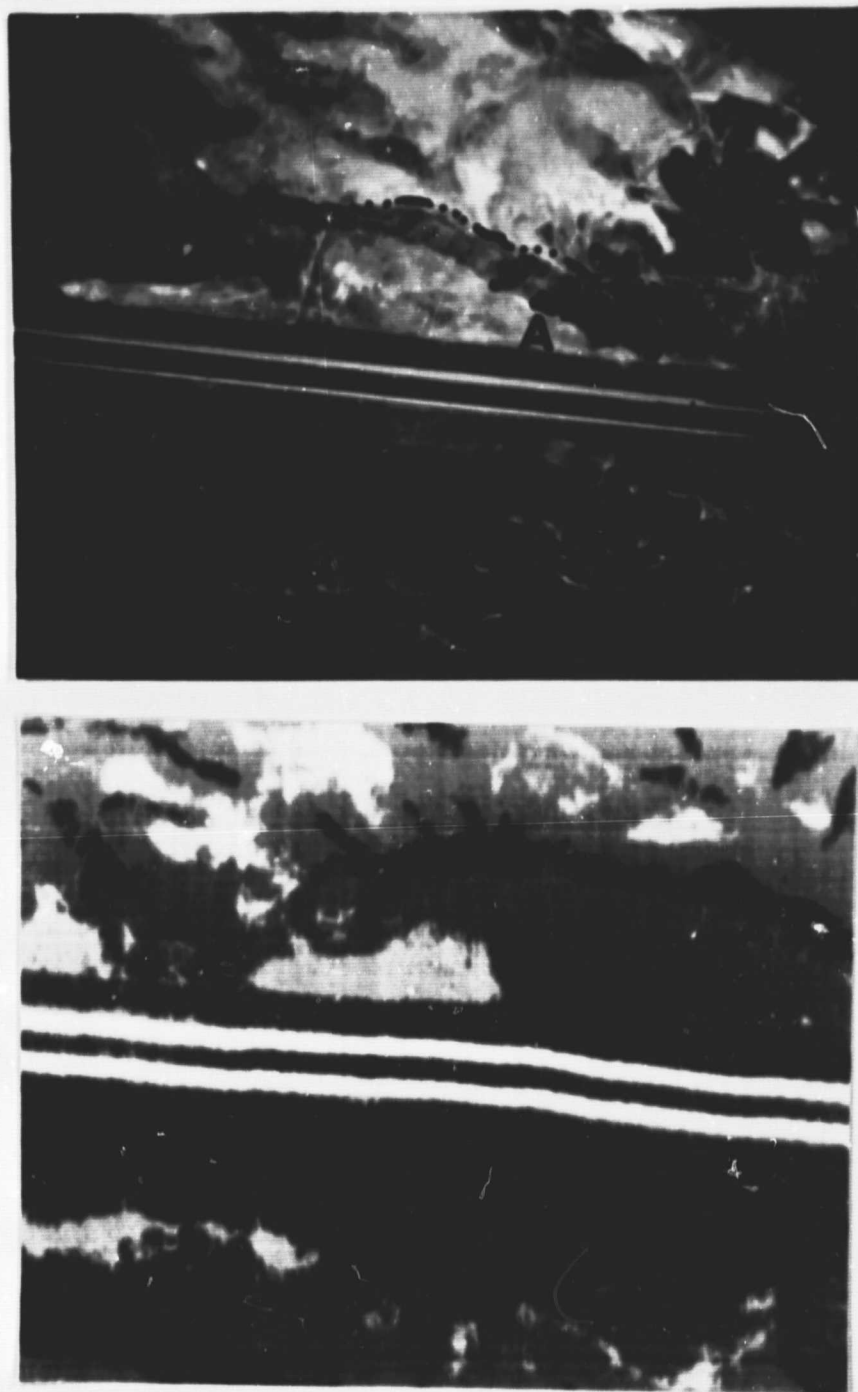
Predawn thermal; dark is cool

Fig. 8. A comparison of CIR photography and predawn thermal imagery is exhibited from the Chamberlain site. Lush vegetative growth (A) is easily distinguishable on the CIR photography but not apparent on the thermal imagery. Warm areas on the thermal imagery may or may not be associated with high moisture zones. Scale of CIR print is approximately 1:9000 (11 cm/km) and scale of thermal print is approximately 1:6000.

of the highway breakup. Locating high moisture zones provided only
an indication of the moisture supply that may provide the driving force
behind differential expansion and contraction of the soil. We were
unable to locate fracture zones; however, ground experience indicates
that fault zones are often difficult to observe on the ground. Further
field investigation by DOT personnel is scheduled in Rapid City area,
and location of fracture zones on the imagery will be emphasized.

CONCLUSIONS

The major objective, that is, location of high moisture zones
with remote sensing data, was accomplished short of drilling programs.
Comparisons among variables indicated that predawn thermal data taken
in September at 914 meters provided the best information for the Rapid
City site. However, the CIR photography taken in September complemented
the thermal data. The relation of photographic tones on thermal prints
with an appropriate level or range of apparent ground temperature was
determined.

The Chamberlain site had a comparison of CIR photography and
thermal infrared data from only one flight. The CIR photography was
the better remote sensing product due to the confounding thermal
complexities in the study site, i.e. parent material differences and
steep slopes. Photographic indications of high soil moisture on the
CIR imagery were: 1) salinity, 2) spots of lush vegetation in side-
slopes, and 3) salt-affected vegetation in the highway ditches and

meridians. The indication of high soil moisture on thermal prints was related to warm areas on the predawn, September imagery.

The remote sensing data were useful for locating indications of shallow water tables. Shallow water tables or seepage are expressed on landscape in several fashions as well as by a changing thermal regime. These indicators were noted in both study sites, and it remains for the actual determination of the shallow water table (i.e. drilling to take place (Appendix A). Fault zones were not located on any of the imagery, but further field observations hold some promise for this determination.

REFERENCES

Bruce, R.L., and J. Scully. 1966. Manual of landslide recognition in Pierre shale, South Dakota. Final Report. S. Dak. Dept. of Highways, Pierre. 70p.

Hammerquist, D.W., and E.R. Hoskins. 1969. Correlation of expansive soil properties and soil moisture with pavement distress in roadways in western South Dakota. Final Report on HP5890(03). S. Dak. School of Mines and Tech., Rapid City. 61p.

Hoskins, E.R., and D.W. Hammerquist. 1970. Investigation of alternative chemical treatments for controlling expansive soil in roadways in western South Dakota. Final Report on HP5898(04). S. Dak. Dept. of Highways, Pierre. 40p.

Hoskins, E.R., D.W. Hammerquist, and P.H. Rahn. 1971. A preliminary investigation of terrestrial and low altitude aerial infrared photography as an aid in determining water table depths and buried geologic structures in the Pierre shale in western South Dakota. Final Report on HP5806(5115)P. S. Dak. Dept. of Transportation, Pierre. 59p.

McDonald, E.B. 1970. Determination of water accumulation adjacent to and in normal earth embankments constructed in Pierre shale. Final Report. S. Dak. Dept. of Highways, Pierre. 49 p.

Myers, V.I., and D.G. Moore. 1972. Remote sensing for defining aquifers in glacial drift. p715-728. In Proc. 8th International Symposium for Remote Sensing of Environment. ERIM, Ann Arbor, Mich.

Rib, H.T. 1975. Engineering: Regional inventories, corridor surveys, and site investigations. p.1881-1946. In R.B. Reeves (ed.). Manual of Remote Sensing. Amer. Soc. Photogram., Falls Church, VA.

Stallard, A.H., and L.P. Myers. 1972. Soil identification by remote sensing techniques in Kansas, Part 1. State Highway Commission of Kansas in Cooperation with Fed. Highway Admin. (Abstract)

Van Wijk, W.R., and D.A. DeVries. 1963. Periodic temperature variations in a homogeneous soil. p102-143. In W.R. Van Wijk (ed.). Physics of Plant Environment. North-Holland Publishing Company, Amsterdam.

APPENDIX A

SOUTH Dakota
Department of Transportation
Division of Highways
Pierre, South Dakota 57501
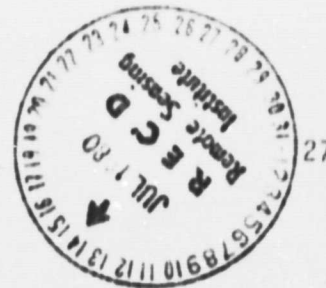
July 10, 1980

Mr. Kevin Dalsted
Remote Sensing Institute
South Dakota State University
Brookings, South Dakota 57007

Re: Detection of High Moisture Zones Under Interstate Highways.

Dear Kevin:

As part of our 3-R Interstate Program, we will be evaluating subgrade problems to determine any corrective action which may be necessary to restore the riding quality of the surface. This may even extend to removal of the pavement in certain locations and reworking the subgrade.

The first project to receive this consideration will be from Box Elder east 9 miles on I-90 in Pennington County. The Thermal Imagery and Color IR you have supplied to us for this location will be one of the information sources to be examined in determining the degree and type of corrective work. Your assistance would be much appreciated in making any specific recommendations or in the interpretation of this remote sensing data in order that we might make effective use of it.

Yours truly,

MATERIALS AND SOILS PROGRAM

Donald W. Anderson
Materials Engineer

DWA:jr
CC: M. Buhler

THERMAL INFRARED CENSUS OF
CANADA GEESE IN SOUTH DAKOTA

By

Robert Best and Ron Fowler

INTRODUCTION

Canada geese concentrate on the mainstem reservoirs of the Missouri River in central South Dakota, during fall migration. A significant portion of these Canada geese are relatively large birds and are hunted and shot by large numbers of hunters who consider the birds as trophies. Commercial or controlled goose hunting operations are becoming more common and increasingly efficient at providing geese for hunters to shoot. The goose harvest and the potential for larger harvest is increasing. This is cause for concern by goose managers in both state and federal wildlife management agencies, in regard to (1) extent of present harvest in relation to that which the goose population can withstand; (2) the proper distribution of harvest among areas, states and people; and (3) the population size in relation to potential population size or population goal based on available nesting habitat.

Goose population distribution, trend and status is determined by visual estimates made by trained observers in small aircraft, during daylight flights. The trend of population distribution is toward fewer and larger concentrations due primarily to increased concentration and availability of food as in controlled goose

hunting areas. Accurate estimates of numbers of birds in these concentrations, and thus the entire population, are becoming more difficult, or impossible, to make. Photographic spot checks of visual estimates have indicated that visual estimates may be 50-75 percent lower than the actual numbers of birds in a concentration. Also, the degree of error probably varies among observers thereby resulting in inconsistent estimates.

Furthermore, varying numbers of geese feed in surrounding agricultural areas during the day, and are not present on the water or immediate area when counts are made. A technique for estimating goose numbers which relies on remotely sensed imagery collected at night when all geese are resting on the reservoirs would provide for more accurate censusing and result in a more reliable basis for regulation of harvest to meet population and harvest goals.

The development of airborne thermal infrared sensors has provided a potential method for censusing warm-blooded animals whose behavior would allow them to be more accurately censused during periods of darkness. Thermal infrared imagery has been used, with varying degrees of success, for the census of white-tailed deer (Croon et al. 1968, McCullough et al. 1968, Graves et al. 1972); elk, moose and deer (Wride and Baker 1977); harp seals (Lavigne and Ronald 1975); and polar bears (Brooks 1970). Wyatt et al (1980) recently statistically evaluated the use of remotely sensed thermal data for deer census. The effectiveness depends on the thermal characteristics of the animal and its habitat and the characteristics of the scanner.

The objectives of this project are to: (1) develop operational procedures to use predawn aerial thermography to census Canada geese (*Branta canadensis*); (2) determine which of two wavelength detectors (4.5-5.5 μm, 8.7-11.5 μm) will provide maximum apparent temperature contrast; (3) evaluate optimal altitude-resolution parameters for data collection; (4) establish an ambient temperature range at which procedures will be most effective; (5) determine the effect of climatic factors on data collection including: temperature, cloud cover, and wind velocity; (6) develop an emperical relationship between the thermal anomalies produced by the geese and goose numbers; (7) develop procedures to obtain contiguous aerial thermography over water resting areas; and (8) measure the approximate emissivity of goose integument.

PROCEDURES

The infrared emissivity and radiant heat loss at varying environmental temperatures were measured to supplement the collection of aerial thermography. The exact procedures used are detailed by Best and Fowler (1980b) which is attached in Appendix A.

Aerial thermography was collected five times over goose concentrations on the Missouri River reservoirs in the Pierre, South Dakota area utilizing a Daedalus* thermal scanner (Table 1). A brief description

_____

*Inclusion in this report of registered trade names or trade marks does not constitute an endorsement by the authors or the Remote Sensing Institute.

Table 1. Thermal infrared data collection missions.

Date	Time (CST)	Ground Level Ambient Temperature	Sensors (μm)	Altitudes (AGL)
11-16-79	1530 hr	18° C	8.7-11.5 4.5-5.5	303 m 455 m 758 m
11-16-79	2100 hr	8° C (10° inversion at altitude)	8.7-11.5	303 m 455 m 758 m
1-30-80	1400 hr	-5° C	8.7-11.5	303 m 455 m
1-30-80	2400 hr	-13° C	8.7-11.5	303 m
1-31-80	1130 hr	-15° C	8.7-11.5	303 m 455 m

of the characteristics of the Daedalus thermal scanner and detectors
was reported by Best and Fowler (1980a). Aerial photography was exposed
concurrently with the thermal imagery during all daylight missions.
Daylight missions were flown to develop interpretation procedures and
to establish the goose density relationship. The photovoltaic detector
(4.5-5.5 μm) was used during the first daylight data collection mission
only. The trimetal detector (8.7-11.5 μm) was used on all data
collection missions. A 10° C temperature inversion was present at
303 m (1000 ft) AGL during the 16 November 1978 night data collection
mission.

Overlapping data must be collected if the area of geese is
larger than the field of view of the scanner. Contiguous coverage

could easily be collected if sufficient moonlight was present to allow visual navigation. Overlapping coverage could be collected on dark nights by using lights at farmsteads for navigation points. A line can be drawn between obvious thermal anomalies in the overlap area on the imagery and counts can be made on opposite sides of the line on overlapping images in order to prevent duplication of counts.

Thermal data were processed into a photographic format which was scaled to base maps and aerial photographs. The thermal data was 'level sliced' into equal temperature increments during the processing. The 'level slicing' process divides the voltage signal from the scanner into 6 equal voltage increments which produced discrete gray tones on the photographic imagery. Each of the gray levels represent an equal apparent temperature increment. Any one or more consecutive levels can be further divided into 6 more levels to increase apparent temperature resolution.

Goose counts were made on enlargements of aerial photography using the technique developed by Chatten (1952). Ten random counts were made within each region of relatively uniform goose density. The areas of each density region were measured with a Numonics electronic digital planimeter and goose totals were calculated directly from these figures. Chatten (1952) found that the results from this technique were accurate to 15% or less.

Aerial measurements of goose concentrates on enlargements of aerial thermography and average goose densities determined from the

aerial photography were used to estimate total goose numbers from the thermography for purposes of comparison. An average density of geese weighed for areal density differences was calculated from counts made on aerial photographs.

RESULTS AND DISCUSSION

The major factors contributing to heat loss from a goose are conduction, convection, radiation and evaporation. The temperature profile near the skin is determined solely by conduction (Birkebak et al. 1966). A major proportion of the sensible (non-evaporative) heat loss from the back of a Canada goose resting on water can be attributed to a combination of convection and radiation. The radiated component, which can be measured with remote sensors, should be the most significant because the environment acts as an infinite heat sink. Kelly et al. (1954) discussed the importance of heat loss by radiation in the energy balance of animals. Latent (evaporative) heat loss is insignificant at low temperatures (Salt and Zeuthen 1960). Heat loss from the bill was negligible because resting or sleeping geese generally place their bill under their wing during cold weather.

The energy emitted from the surface of a goose depends not only on the temperature of the feathers, but also the emissivity of the surface as expressed by the Stephan-Boltzman Law (Campbell 1977):

$$R = \varepsilon \sigma T^4$$

where:

    R = energy emitted by non-blackbody W m^{-2}

    ϵ = emissivity of the surface

    σ = Stephan-Boltzman constant 5.67×10^{-8} W m^{-2} K^4

    T = absolute temperature in °K

It is necessary to measure the infrared emissivity and the apparent temperature of the Canada goose in order to determine if sufficient thermal contrast exists between the goose and the background so it can be distinguished on thermal imagery. The infrared emissivity and radiant heat loss from Canada geese were measured as part of this project (Best and Fowler 1980b, attached in Appendix A). The mean emissivity was $0.962 \pm .017$ and was not significantly different from other species of geese. Canada geese have an insulating integument to minimize heat loss and reduce the temperature differential with the environment. However, Best and Fowler (1980b) found that Canada geese have a relatively high radiant temperature relative to ambient air temperature, which should provide sufficient thermal contrast to distinguish geese from the background on thermal data. The rate of radiant heat loss depends on the potential or temperature difference between the goose and the environment. The potential increases rapidly as ambient temperatures decrease.

The apparent temperature difference between Canada geese and the ambient temperature is not constant and increases with decreasing ambient temperatures (Figure 1). This relationship must be considered
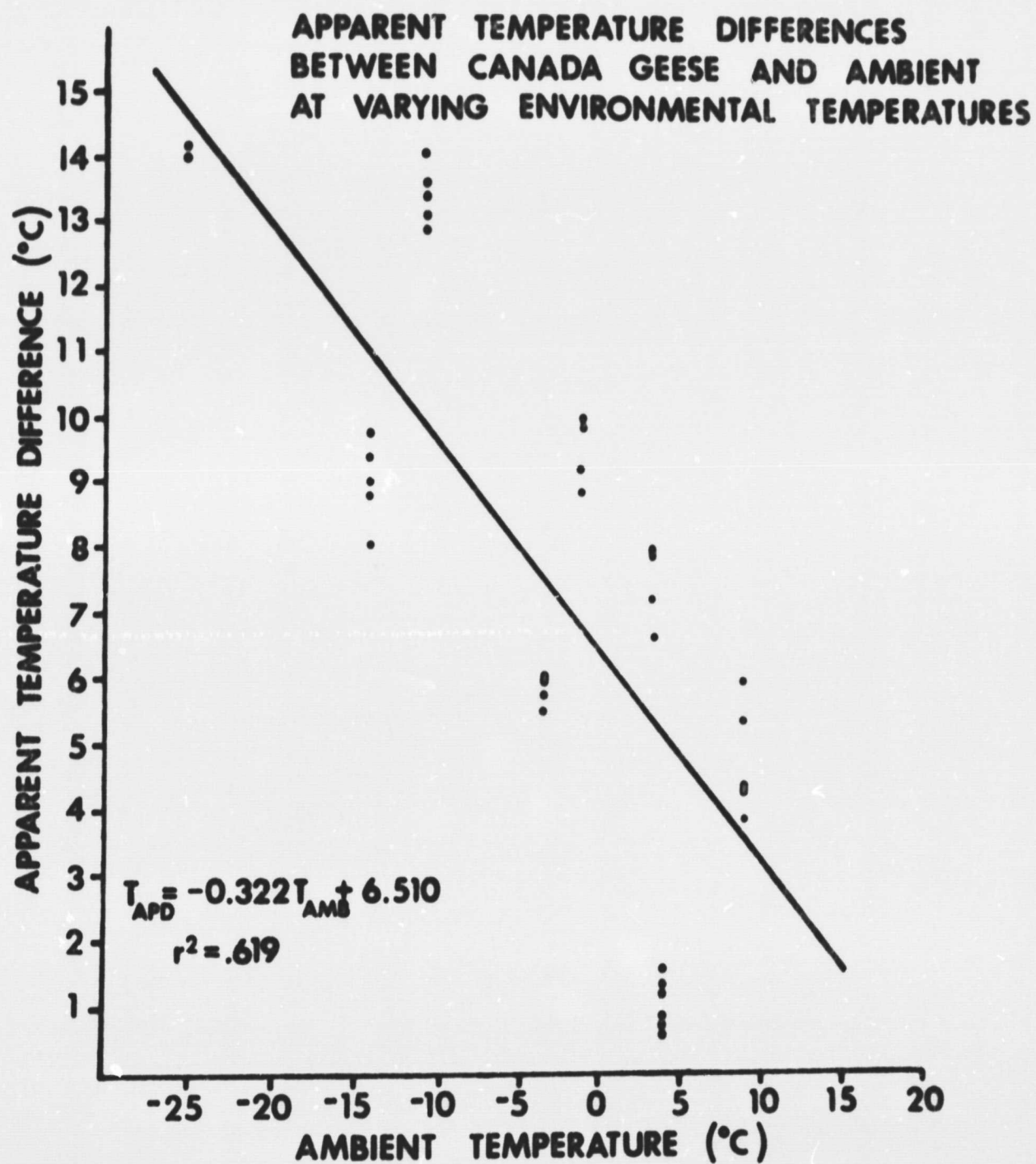
Figure 1. Apparent goose temperature, ambient temperature differences determined with PRT radiometer.

in flight planning to determine if the apparent temperature of the geese will be significantly different from the background temperature at a specific ambient temperature. It is an approximately linear relationship and can be calculated from the following statistical model:

$$T_{APD} = -0.322 \; T_{AMB} + 6.510$$

where:

T_{APD} = apparent temperature difference between goose and ambient (°C)

T_{AMB} = ambient temperature (°C)

The results of a statistical evaluation of thermal data for deer census by Wyatt et al. (1980) indicate that deer can be detected most successfully against a snow cover background which has a relatively uniform radiance. The background from which the geese must be differentiated is open water during fall and early winter and water and ice during late winter. Both water and ice have a very uniform radiance and provide an ideal background. The emissivity of water is very close to that of a perfect blackbody so the apparent background temperature is very close to the sensible temperature and can be measured with an immersed thermometer.

Background temperature used in conjunction with apparent goose temperature data can be used to determine optimal conditions for aerial thermal data collection (Figure 2). The "cross hatched" region of Figure 2 indicates ambient temperature - water temperature constraints

**AMBIENT TEMPERATURE CONSTRAINTS FOR COLLECTING
AERIAL THERMOGRAPHY FOR CENSUSING CANADA GEESE**
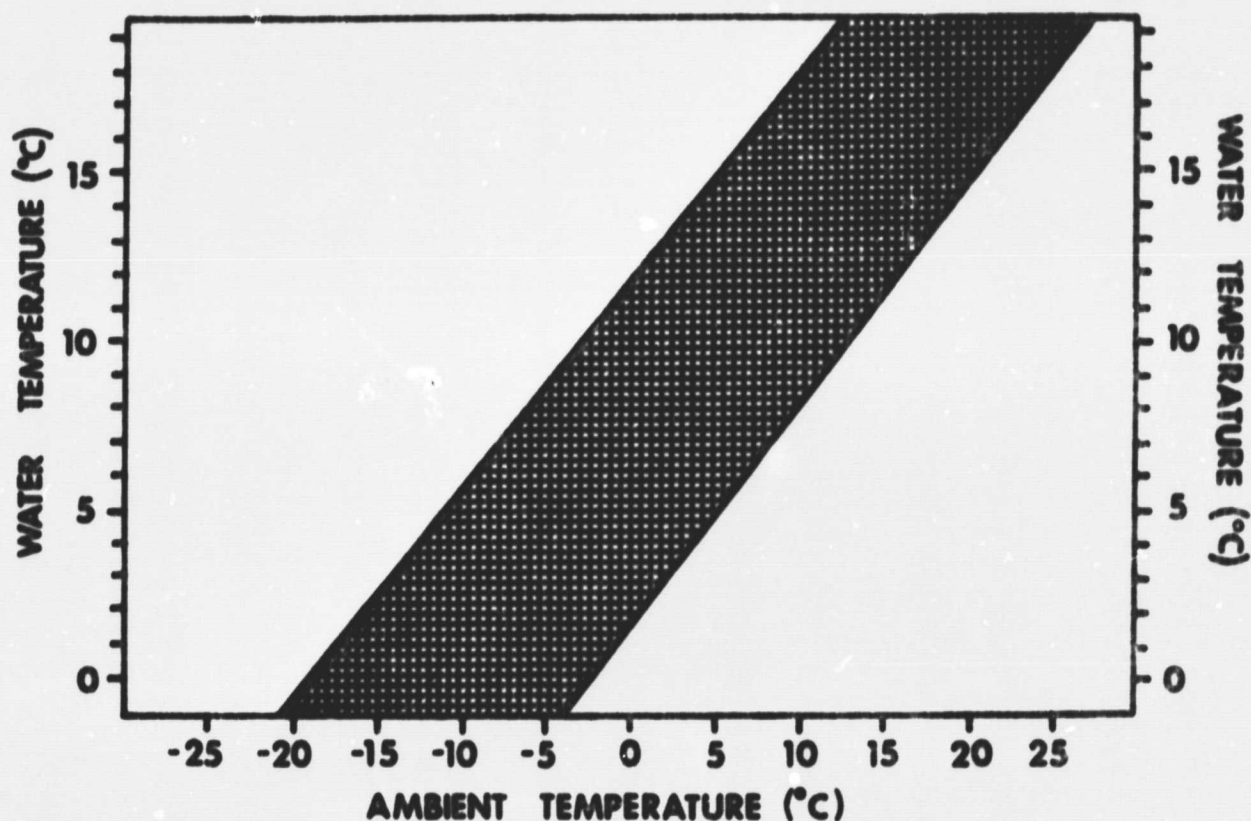
Figure 2.   Ambient temperature/background temperature constraints
for collecting aerial thermography for detecting geese.
The crosshatched region represents ambient/water temperatures
where sufficient contrast would not be present to distinguish
geese.

where the thermal contrast between geese and water background would not be sufficient to detect geese on thermal data. These data are based on the assumption that a minimum apparent temperature difference of 5° C is necessary to distinguish geese from an open water background.

The minimum temperature that can be resolved by the Daedalus thermal scanner used in this project is 0.5° C and the spatial resolution is 0.48 m at an altitude of 303 m. Consequently, the signal recorded by the scanner is an average of the apparent temperature of all objects within a resolution cell. The results of this study indicate that the apparent temperature of the goose must be at least 5° C different from the background in order to produce a response which is different than the background alone. Croon et al. (1968) reports that single animals smaller than a fox probably can not be detected with present thermal scanning equipment. The objective of this project is not to enumerate individual geese, but to determine the areal extent of goose concentrations and estimate total numbers as the product of area and goose density as determined from aerial photographs.

In addition to ambient temperature, other climatic factors will effect the radiant heat loss for Canada geese. Moen (1974) and Moen and Jacobsen (1974) found that there was an increase in the radiant temperature on the surface of the integuments of white-tailed deer (*Odocoileus virginianus*), mule deer (*O. hemionus*), snowshoe hare (*Lepus americanus*), cottontail rabbit (*Sylirlagus floridanus*), and red fox (*Vulpus fulva*) when wind velocities increased. They reported

that changes at lower wind velocities had a relatively greater effect than changes at higher wind velocities. Parker and Harlan (1972) and Moen and Jacobsen (1974) found that direct-beam solar radiation would result in a higher radiant temperature which may increase apparent temperature contrasts during daylight data collection missions. Marble (1967) identified cloudy days as best for detecting big game animals from a snow background with a thermal scanner.

Spatial resolution of the thermal scanner is a function of the altitude. The size of the resolution cell increases proportionally with the altitude. Geese could not be resolved on thermography collected at altitudes above 758 m (2500 ft) AGL. Goose concentrations could be delineated on altitudes of 455 m (1500 ft) and 303 m (1000 ft) AGL. Data collected at 303 m (1000 ft) AGL had the smallest spatial resolution and was best suited for delineating geese, especially when they occurred in low densities.

Geese could not be distinguished from the background at any altitude on thermography collected with the photovoltaic detector (4.5 to 5.5 μm). The signal to noise ratio was very low, resulting in data with very low temperature contrasts. This may be attributed to the very strong thermal absolution band due to water vapor that begins at about 5 μm (Figure 3). There is also some absorbance by carbon monoxide. The effects of ozone absorbtion would be minimal on the trimetal detector because of the low concentrations of ozone at the altitude flown.
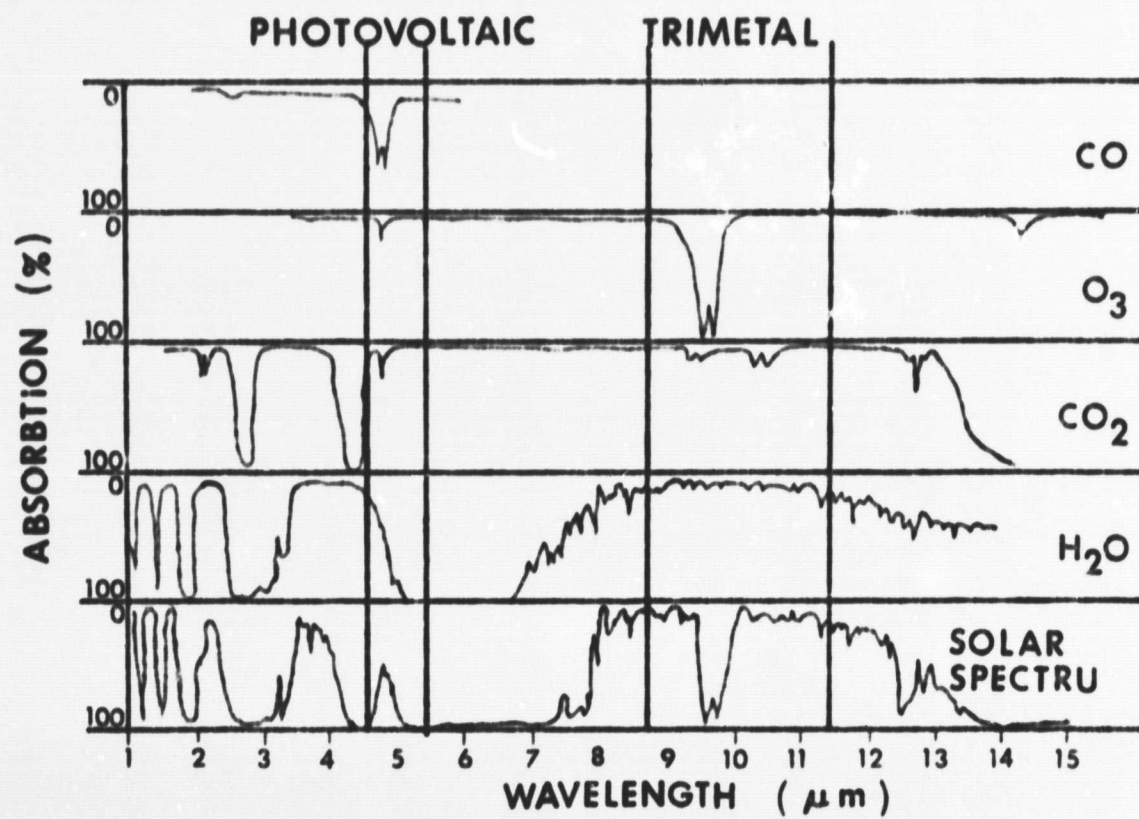
Figure 3. Thermal absorbtion of atmospheric constituent adapted
           from Wolfe (1965).

Graves et al. (1972) successfully located white tailed deer with the 3-5 μm detector under certain conditions. Croon et al. (1968) and McCullough et al. (1969) recommended the use of a detector sensitive to the 8-14 μm spectral region because peak radiation from animals occurs in this range, and it coincides with an "atmospheric window".

The tone (lightness or darkness) on the thermal imagery is relative to the apparent temperatures of scene features. The lighter the tone the higher the relative apparent temperature. The temperature range on the imagery is determined by the operator during data collection. The optimal range would encompass only the total range of temperatures of landscapes. The thermal data can be processed into analog or digital image formats. The analog format is a continuous tone image representing a continuous temperature range. The contrast of the image can be controlled during image generation by a variable gain control.

The thermal data can also be processed into a digital format with 6 equal discreet apparent temperature increments between the blackbody temperatures (Figure 4). The breaks between temperature increments can more easily be delineated in the digital format. In this case the geese could not be distinguished on the full range digital data which indicates that the apparent temperature of the geese is within 1.7° C of the apparent temperature of the background and that both fall in the same temperature increment.

8.0 9.7   9.7 11.1   11.3 11.0   14.7-16.3   16.3-18.0   ≥18
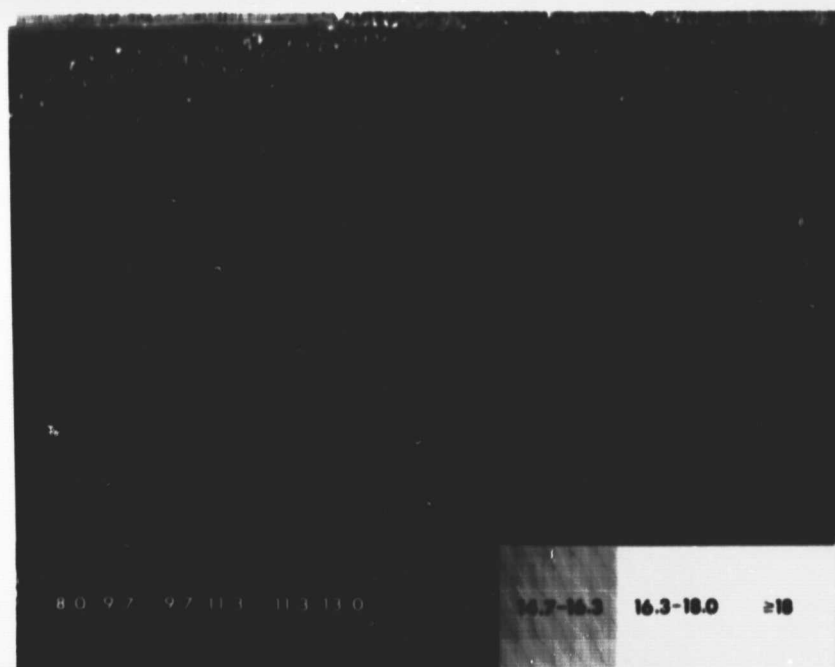
a. Full range digital thermal image

9.7 10.0   10.0 10.2   10.2 10.5   10.0-11.0   11.0-11.3   ≈11.3
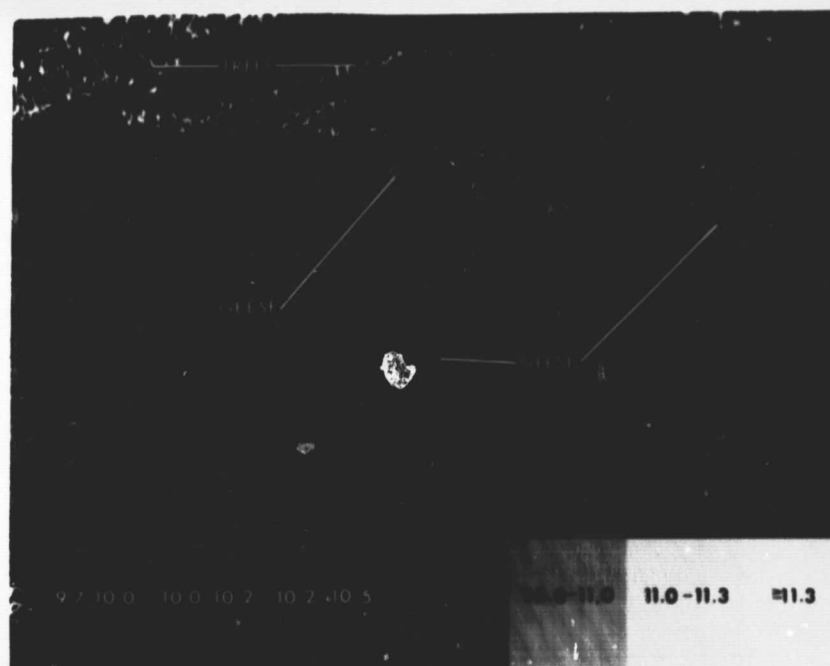
b. Level sliced digital thermal image

Figure 4. Illustration of digital image processing and level slicing
of thermal data. Note the increase in temperature resolution
in the level sliced data.

One or more of these temperature increments can be "sliced" into another 6 equal levels with a subsequent increase in temperature resolution (Figure 4). In Figure 4 the 9.7-11.3° C temperature level has been sliced with a subsequent increase in temperature resolution. The apparent temperature increments in Figure 4b are 0.3° C as compared to the 1.7° C of the full range digital data in Figure 4a. The geese now fall in a temperature level different from the background and can be identified. The geese appear in the 10.5-10.8° C apparent temperature range in these data. Single levels, isolevels, can be printed for easier delineation. The selection of the level containing geese is difficult if the location of some geese is not known.

Very low densities of geese resting on open water could be distinguished on thermal imagery collected with the trimetal detector from 1000 ft AGL (Figure 5). The temperature of the water background was slightly above 0° C and the apparent temperature of the geese was approximately 3.25° C. The small groups of geese appear as light "dots" on the thermal imagery. Larger groups have similar tones and appear in larger irregular shaped areas. Most groups of geese of two or more in close proximity could be distinguished from the water background. These small groups of geese could be individually counted on the imagery which will provide a very accurate estimate in low density areas. Geese resting on the shore could not be easily distinguished from the background which had a less uniform radiance.
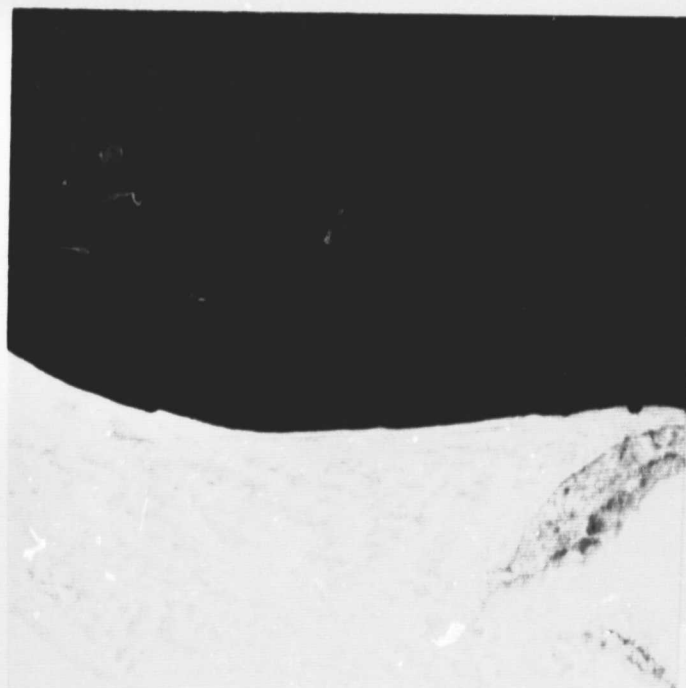
Aerial Photograph

Full range digital thermal imagery

Figure 5. Aerial photograph and thermal imagery (collected at 1000 ft.
AGL with trimetal detector) illustrating the detection of
low densities of geese with open water background.

High densities of geese were easily distinguished from water and ice background on aerial thermography collected at altitudes of 1500 ft or less (Figure 6). The thermal anomaly representing the geese has the lightest tones and warmest apparent temperature on the imagery. Differences in image texture within the area of geese are a result of differences in goose density. Densities of geese less than 2000 per hectare could not be consistantly interpreted on the imagery with snow and ice background (Figure 7). In six goose concentration areas on two different days only one had a significantly large area of low density geese. There was an 8.9% error between the areas of geese over 2000/hectare on the thermography and the area of geese over 2000/hectare measured on the aerial photography.

The average density of geese in six goose concentrations on two different days, as determined from aerial photography, was 4301 geese per hectare. This figure was used to calculate estimates of total geese from area measurement on thermography. There was a 10.98% error difference between the estimates from thermography and the actual number of geese determined from counts of the aerial photography. Improvements in this estimate may be possible if apparent goose density differences were delineated on the thermography and the empirical goose density calculations were refined.

Aerial photograph

High gain analog thermal imagery

Figure 6. Aerial photography and thermal imagery (collected at 1000 ft. AGL with trimetal detector) illustrating the detection of high densities of geese with a predominantly ice and snow background.
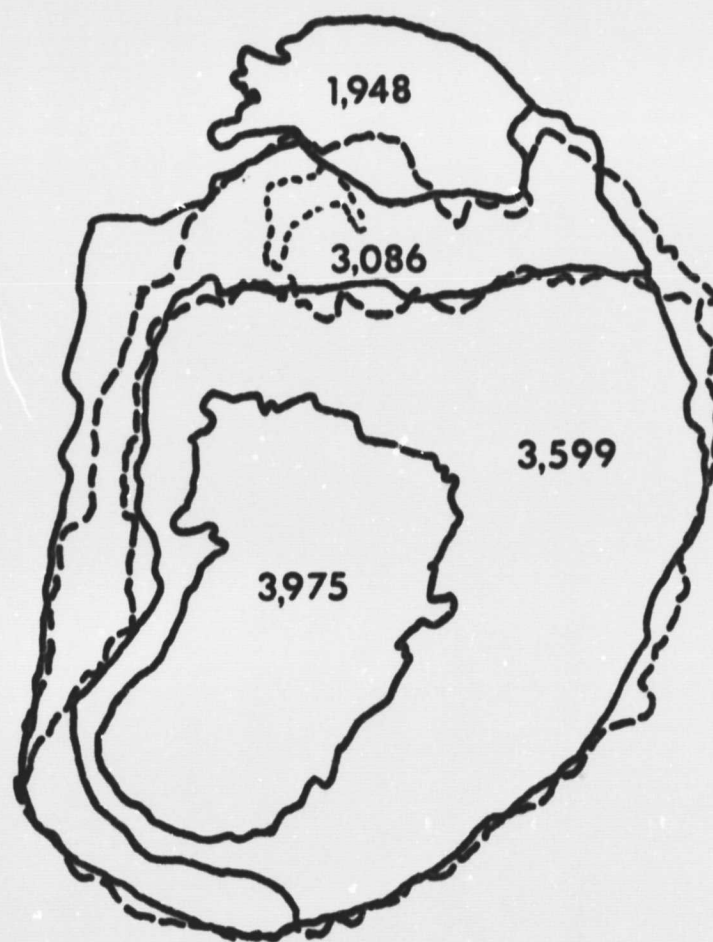
Figure 7. Diagram illustrating the comparison of delineation of goose
concentration on aerial photography and thermal imagery.
Solid line is delineation from aerial photography and dashed
line delineation from thermal imagery.

SUMMARY AND CONCLUSIONS

Canada geese can be distinguished from a water or ice background on aerial thermal infrared imagery. The techniques developed in this project could be used in an operational predawn census of Canada geese during fall migration when geese are concentrated on refuges. Low concentrations of geese can be counted on the imagery. Estimates of geese in high concentrations can be calculated from measurements of the area of geese made on thermal images and empirical goose densities derived from aerial photographs. Level slicing of the thermal data prior to generating an image increases the temperature resolution of the image which will improve the apparent temperature contrast on digital images. High gain analog or full range digital images are the easiest to produce and should be used except when contrast is very low. Computerized digital analysis of the data would further increase relative contrast in the thermal data and improve spatial resolution lost in the generation of imagery.

The spatial resolution of the thermal scanner that was used in this project limited the altitude for data collection to 1500 ft. AGL or less. The best results were obtained when data were collected at 1000 ft. AGL. The photo voltaic detector did not provide sufficient apparent temperature contrasts to distinguish geese from the background under the environmental conditions experienced during the test flight. Data collected with the trimetal detector produced imagery best suited to the objectives of this project.

An infrared emissivity .962 was measured for Canada geese. There were no statistically significant differences in emissivity between species of other central flyway geese. The relationship of ambient temperature and the apparent temperatures of Canada geese were analyzed. These data were used in conjunction with emissivity data and the results of test flights to determine the ambient temperature constraints for successful data collection.

These techniques could replace current census methods and provide more reliable census data. Accurate census data is necessary to formulate harvest regulations which provide both maximum recreational opportunity and more equitable distribution of harvest.

ACKNOWLEDGEMENTS

REFERENCES

Best, R.G. and R. Fowler. 1980a. Thermal infrared census of Canada geese in South Dakota, pages 21-53 in Remote sensing applications to resource problems in South Dakota. Semi-Annual Rpt. SDSU-RSi-80-02. 110pp.

Best, R.G. and R. Fowler. 1980b. Infrared emissivity and radiant heat loss from Canada geese. Submitted to J. Wildl. Manage.

Birkebak, R.C., E.A. LeFebure and D.G. Raveling. 1966. Estimated heat loss from Canada geese for varying environmental temperatures. Minnesota Museum Nat. Hist. Tech. Rept. 11. 25pp.

Brooks, J.W. 1970. Infrared scanning of polar bear in Bears and their management IUCN Pub. No. 23, Calgary, Canada.

Campbell, G.S. 1977. An introduction to environmental biophysics. Springer-Verlog. New York, New York. 157pp.

Chatten, J.E. 1952. Appraisal of California waterfowl concentrations by aerial photography. Trans. N. American Wild. Conf. Wildlife Management Inst., Washington, D.C. pp421-426.

Croon, G.W., D.R. McCullough, C.E. Olson, and J.M. Queal. 1968. Infrared scanning techniques for big game censusing. J. Wildl. Manage. 32:751-759.

Graves, H.G., E.D. Bellis, and W.M. Knuth. 1972. Censusing white-tailed deer by airborne thermal infrared imagery. J. Wild. Manage. 36:875-884.

Kelly, G.F., T.E. Bond, and H. Hertman. 1954. The role of thermal radiation in animal ecology. Ecology 35:562-569.

Lavigne, D.M. and K. Ronald. 1975. Improved remote sensing techniques for evaluating seal populations. ICES C.M. 1975. IN:12.

Marble, H.P. 1967. Radiation from big game and background: a control study for infrared scanner census. M.S. Thesis. Univ. Montana, Missoula. 86pp.

McCullough, G.W., C.E. Olson, and L.M. Queal. 1969. Progress in large animal census by thermal mapping. Pages 138-147 in P.L. Johnson ed. Remote Sensing in Ecology. Univ. Georgia Press. Athens.

Moen, A.N. 1974. Radiant temperatures of hair surfaces. J. Range Manage. 27:401-403.

Moen, A.N., and F.L. Jacobsen. 1974. Changes in radiant temperature of animal surfaces with wind radiation. J. Wildl. Manage. 38: 366-368.

Parker, H.D., Jr., and J.C. Harlan. 1972. Solar radiation affects radiant temperature of a deer surface. U.S. For. Serv. Res. Note Rm-213, Rocky Mt. For. and Range Exp. Stn., Fort Collins, Colo. 4pp.

Salt, G.W., and E. Zeuthen. 1960. The respiratory system. Pages 363-409. In A.J. Marshall ed. Biology and comparative physiology of birds. Vol. 1 Academic Press, New York. 518pp.

Wolfe, W.L. ed. 1965. Handbook of military infrared technology: U.S. Gov't Print. Office. Washington, D.C. 906pp.

Wride, M.C., and K. Baker. 1977. Thermal imagery for census of ungulates. Proc. II Int. Symp. of Remote Sensing of Environ. Univ. Michigan Ext. Service. 11:1091-1099.

Wyatt, C.L., M. Trivedi, D.R. Anderson. 1980. Statistical evaluation of remotely sensed thermal data for deer census. J. Wild. Manage. 44:397-402.

APPENDIX A

Robert G. Best   1
Remote Sensing Institute
South Dakota State University
Brookings, South Dakota 57007

INFRARED EMISSIVITY AND RADIANT HEAT LOSS FROM CANADA GEESE

R.G. BEST, Remote Sensing Institute, South Dakota State
         University, Brookings, SD 57007
R. FOWLER, South Dakota Department of Game, Fish and Parks,
         Pierre, SD 57501

Abstract: The thermal infrared emissivities of 2 subspecies of
Canada geese and 2 color phases of snow geese were measured.
The mean emissivity of the goose integument was .962 ± .017 and
there were no statistically significant differences between the
subspecies of Canada and the snow and blue color phases of snow
geese. The apparent temperature of 6 hand-reared Canada geese
was measured at ambient temperatures varying from -25 to 20°C.
There were no statistically significant apparent temperature
differences between geese. All measurements were included in an
analysis of the relationship of apparent goose temperature with
varying environmental temperature. There was an approximately
linear relationship (r^2 = .87) between apparent goose
temperature and varying ambient temperature with an increase in
the apparent temperature difference between goose and ambient
temperature as the ambient temperature decreased. Radiant heat
loss was calculated from apparent temperature measurements.

Thermal infrared emissivity and radiant heat loss measurements from Canada geese (*Branta canadensis*) are an integral part of energy balance calculations and can be used to determine the feasibility for aerial thermal infrared census. Radiant heat loss measurements from Canada geese can be used to determine if sufficient apparent temperature contrasts exist in order to discern them on thermal imagery (thermography). Heat loss of 2 subspecies of Canada geese at varying environmental temperatures and the effect of heat loss on their distribution has been studied by Birkebak et al (1966) and LeFebvre and Raveling (1967), respectively.

The major factors contributing to heat loss from a Canada goose are conduction, convection, radiation and evaporation. The temperature profile near the skin is determined solely by conduction (Birkebak et al. 1966). The conduction is along the fibers of the feathers or through air and water vapor trapped within the feathers. A major proportion of the heat loss from the surface of the integument can be attributed to a combination of convection and radiation. Latent (evaporative) heat loss is insignificant at low temperatures (Salt and Zeuthen 1960). Heat loss from the bill will be negligible for resting geese which generally place their bill under their wing during cold weather. Only the radiated component of heat loss can be detected with

thermal infrared sensors. However, the radiated component can be very significant with the environment acting as an infinite heat sink.

The thermal infrared energy emitted from the surface of a goose depends not only on the temperature of the feathers, but also the emissivity of the surface as expressed by the Stephan-Boltzman Law (Campbell 1977):

$$R = \epsilon \sigma T^4 \qquad [1]$$

where:

R = energy emitted by non-blackbody $W\ m^{-2}$

ϵ = emissivity of the surface

σ = Stephan-Boltzman constant $5.67 \times 10^{-8}\ W\ m^{-2}\ K^4$

T = absolute temperature in $^\circ K$

Most surfaces radiate slightly less than a perfect radiator (blackbody). Hammel (1956) measured the emissivity of the integument of 10 species of artic birds and mammals and found that within experimental error, the emissivities were not measurably different than 1.0. Hammel concluded that there was no advantage in heat conservation for animals with white integument. It was shown that animals which were white in visible wavelengths were not necessarily "white" in the thermal infrared wavelengths. Svihla (1956) found similar results in an experiment with dyed rats.

The objectives of this project were (1) to measure the emissivity of Canada geese, (2) to measure the apparent temperature (temperature measured remotely with a thermal infrared sensor) of Canada geese at varying ambient temperatures, (3) to determine the radiant heat loss from Canada geese at varying ambient temperatures, (4) to evaluate if sufficient apparent temperature differences are present to image Canada geese with an airborne thermal infrared sensor.

METHODS

Emissivity values of unpreserved goose integuments from 2 subspecies of Canada geese (*Branta canadensis interior* and *B.c. hutchinsonii*) and adult and immature snow (*Anser caerulenscens*) were calculated from measurements made with a

Barnes Precision Radiation Thermometer* (PRT). The filtered
sensitivity of the radiometer was 8-14 μm. Skins were removed
from freshly killed geese and frozen until measurements were
made. Skins were removed from the freezer to allow their
sensible temperature to equilibrate with environmental
temperatures. All measurements were made in a shaded area under
clear skies.

Two methods were used to estimate the emissivity. A rough
estimate was made by ratioing the 4th power of the apparent
temperature (°K) with the 4th power of the actual temperature
(°K). A second more precise technique developed by Fuchs and
Tanner (1966) for infrared thermometry of vegetation is based
on a form of the Stephan-Boltzman Law which considers background
radiance effects.

$$R_b = \varepsilon\sigma T^4 + (1-\varepsilon)B* \qquad\qquad [2]$$

where:

R_b = radiation received by the sensor

$(1-\varepsilon)B*$ = incoming thermal infrared reflected by the surface

$B*$ = background radiance

---

*Inclusion in this report of registered trade names or
trademarks does not constitute an endorsement by the authors or
the Remote Sensing Institute.

In this method the apparent temperature of an aluminum
plate of known emissivity is measured with the PRT. The actual
temperature is measured with a digital thermometer and
thermocouples embedded in the plate. The background radiation
is then calculated by solving equation [2] for background
radiance (B*).

$$B^* = \frac{R_b - \epsilon\sigma T^4}{1-\epsilon}$$

where:

$R_b = \sigma T^4$ (T is apparent temperature measured by PRT in °K)

Measurements of the apparent temperature of the goose skins
were made with the PRT and the actual temperature was measured
with the PRT by placing the goose skin under a specimen chamber
lined with aluminum foil, which simulates a blackbody cavity.
The emissivity of the goose skins were calculated by solving
equation [2] for ϵ.

$$\epsilon = \frac{R_b - B^*}{\sigma T^4 - B^*}$$ [4]

where:

T^4 = actual temperature °K measured with PRT under
blackbody cavity

Five measurements of apparent and actual temperature were
made on each of two different skins for each type of goose. An

average of background radiance, calculated from measurements made at regular intervals during the measurement of goose skins, was used in the calculations. Statistical means and standard deviations of emissivities were calculated for each individual skin and goose type. Analysis of variance was used to determine if statistically significant emissivity differences occurred between geese. Statistical analyses were performed using the Statistical Analysis System (SAS) procedures (Barr et al. 1976).

The apparent temperature of 6 hand-reared pinioned Canada geese was measured with a radiometer (PRT). Five replicate measurements of each goose were made at environmental temperatures ranging from -25 to 10°C. All measurements were made under cool clear skies. The background radiation was estimated from PRT measurements of an aluminum plate with a known emissivity in which thermocouples have been embedded to determine actual temperature. Mean apparent temperatures of each of the 6 geese were plotted against ambient temperatures. Linear regression analysis was used to statistically analyze the relationship. A similar technique was used by Moen (1968) to measure the surface temperature and radiant heat loss from white-tailed deer.

RESULTS AND DISCUSSION

The mean emissivities of 6 types of geese ranged from .957

to .966 (Table 1). Statistical analysis of variance indicated

that there was no statistically significant emissivity difference

between geese (P>.10). Based on these results the mean

emissivity for all geese is .962 + .017 (95% confidence interval).

Several authors (Hamilton, 1939 and Hesse et al. 1951) have

hypothesized that arctic mammals and birds may have a reduced

thermal emittance as a result of their white coloration. The

results of this study contradict this hypothesis. Adult snow

geese which are pure white have the same infrared emissivity as

the very dark colored Canada geese and both are very close to

that of a blackbody radiator. There would be an advantage, had

the emissivity been very low, because radiant heat loss is

proportional to emissivity. Emissivity values calculated

without consideration of background radiation ranged from .98

to .99 which would correspond very closely with emissivity

measurements of arctic mammals and willow ptormigan (*Lagopus*

lagopus) made by Hammel (1956). The effects of background

radiation are not considered in the emissivity measurement

technique developed by Hardy (1934) which was used by Hammel.

Radiant energy loss might still be small for geese, even

with an emissivity near 1.0 if the surface temperature of the

integument and the environment are nearly the same. However,

the apparent temperature of a clear sky will usually be

Table 1. Infrared emissivities of central flyway geese.

Species	Visible Color	Mean Emissivity
Canada goose	dark grey	.962
(*Branta canadensis interior*)		
Canada goose	dark grey	.966
(*B. hutchinsonii*)		
Adult snow goose	white	.963
(*Anser caerulescens*)		
Immature snow goose	light grey	.959
Adult blue goose	grey	.964
(*Anser caerulescens*)		
Immature blue goose	grey	.957
	Grand mean	.962

significantly colder than the air temperature. Hardy and Stoll (1954) found that the radiant temperature of the clear sky may be 30 to 40°C colder than air temperature. Clear sky will act as a heat sink for the exposed portion of the goose.

The relationship of the apparent temperature of Canada geese to varying environmental temperature is illustrated in Figure 1. The apparent goose temperatures were measured remotely with a radiometer and are an average of 5 readings from the back of each goose. Data for all 6 geese are included together in Figures 1 and 2 because an analysis of variance indicated that there were no significant differences (P>0.05) between geese for the apparent goose temperature/air temperature relationship. Surface temperatures of the geese can be determined from these data by using the Stephan-Boltzman law with the measured emissivity (.962). The surface temperature will be very close to the apparent temperature as measured with PRT because the emissivity is very close to 1.0 and background radiance is negligible. There appears to be a linear relationship between the apparent temperatures of the geese and the ambient temperatures based on these data. An estimate of the apparent temperature of the geese can be calculated from the following regression equation:

$$T_{app} = .692 \, T_{amb} + 6.103$$

where:

T_{app} = apparent goose temperature °C

T_{amb} = ambient temperature °C

This equation accounts for 87% of the variance (r^2 = .873) in the data.

The difference between the apparent temperature of the goose and the ambient temperature is, among other variables, an indication of the thermal conductivity of the integument when the emissivity is near 1.0. These data show that as ambient temperature decreases the apparent temperature difference of the goose increases. Convective heat losses should increase as the temperature difference increases.

These data can be used to determine if sufficient apparent temperature contrasts are present to discern geese from background and are essential for planning the collection of aerial thermography designed to image geese.

The radiant heat loss of Canada geese at varying ambient temperatures is illustrated in Figure 2. Heat loss by radiation can be calculated from the product of the 4th power of the apparent temperature (°K) as measured with PRT and Stephan-Boltzman constant in the form: $\sigma = 4.93 \times 10^{-8}$ kcal m^{-2} h^{-1} K^{-4}. Radiant heat loss decreases as the apparent temperature of the goose decreases with ambient temperature. It follows that

as ambient temperature decreases, heat loss by convection should
increase while radiant heat loss will decrease.

Numerous factors can have an effect on the "apparent"
temperature and radiant heat loss from an animal. The net
radiation loss can be affected by not only the downward flux
under different sky conditions (Moen 1968) but can also be
affected by absorbed solar radiation (Parker and Driscoll 1972)
and changes in wind velocity (Blaxter and Wainman 1964, Moen
1974, Moen and Jacobsen 1974). Knowledge of the radiation
profile or "effective surface" for the goose is essential for
calculating total radiant heat loss. The radiation profile is
used to adjust for geometrical consideration and is based on the
proportion of the body exposed to different environmental energy
flux. The radiation profile for Canada geese is not known.
When the radiation profile is determined the data can be used
in thermal energy exchange calculations. These data suggest
that sufficient apparent temperature contrasts may be present
in order to utilize aerial thermography for censusing Canada
geese when environmental conditions are suitable.

LITERATURE CITED

Barr, A.J., J.H. Goodnight, J.B. Sall and J.T. Helwig. 1976.
    A users guide to SAS. SAS Inc. Raleigh, North Carolina.
    320pp.

Birkebak, R.C., E. A. LeFebvre and D.G. Raveling. 1966.
    Estimated heat loss from Canada geese for varying
    environmental temperatures. Minnesota Museum Nat. Hist.
    Tech. Rept. 11. 25pp.

Blaxter, K.L. and F.W. Wainman. 1964. The effect of increased
    air movement on heat production and emission by steers.
    J. Agr. Sci. 62:207-214.

Campbell, G.S. 1977. An introduction to environmental
    biophysics. Springer-Verlog. New York, New York. 157pp.

Fuchs, M. and C.B. Tanner. 1966. Infrared thermometry of
    vegetation. Agronomy Journal 58:597-601.

Hamilton, W.J., Jr. 1939. American mammals, Ed. 1. McGraw-Hill
    Book Co. p.111.

Hammel, H.T. 1956. Infrared emissivities of some arctic fauna.
    Journal of Mammology 37:375-378.

Hardy, J.D. 1934. The radiation of heat from the human body.
    III. The human skin as a blackbody radiator. J. Clin.
    Invest. 19:615-620.

_____ and A.M. Stoll. 1954. Measurement of radiant heat load on man in summer and winter Alaskan climates. J. Appl. Physiol. 7:200-205.

Hesse, R., W.C. Allee, and K.P. Schmidt. 1951. Ecological animal geography, Ed. 2, John Wiley and Sons. p.616.

LeFebvre, E. A. and D.G. Raveling. 1967. Distribution of Canada geese in winter as related to heat loss at varying environmental temperatures. J. Wildl. Manage. 31:538-546.

Moen, A.N. 1968. Surface temperatures and radiant heat loss from white-tailed deer. Wildl. Manage. 32:338-344.

_____. 1974. Radiant temperatures of hair surfaces. J. Range. Manage. 27:401-403.

_____ and F.L. Jacobsen. 1974. Changes in the radiant temperature of animal surfaces with wind and radiation. J. Wildl. Manage. 38:366-368.

Parker, H.D., Jr. and R.S. Driscoll. 1972. An experiment in deer detection by thermal scanning. J. Range Manage. 25:480-481.

Salt, G.W. and E. Zeuthen. 1960. The respiratory system. 363-409pp. *in* A.J. Marshall Ed. Biology and Comparative Physiology of Birds. Vol. 1 Academic Press, New York. 5188pp.

Svihla, A. 1956. The relation of coloration in mammals to low temperature. Journal of Mammology 37:378-381.
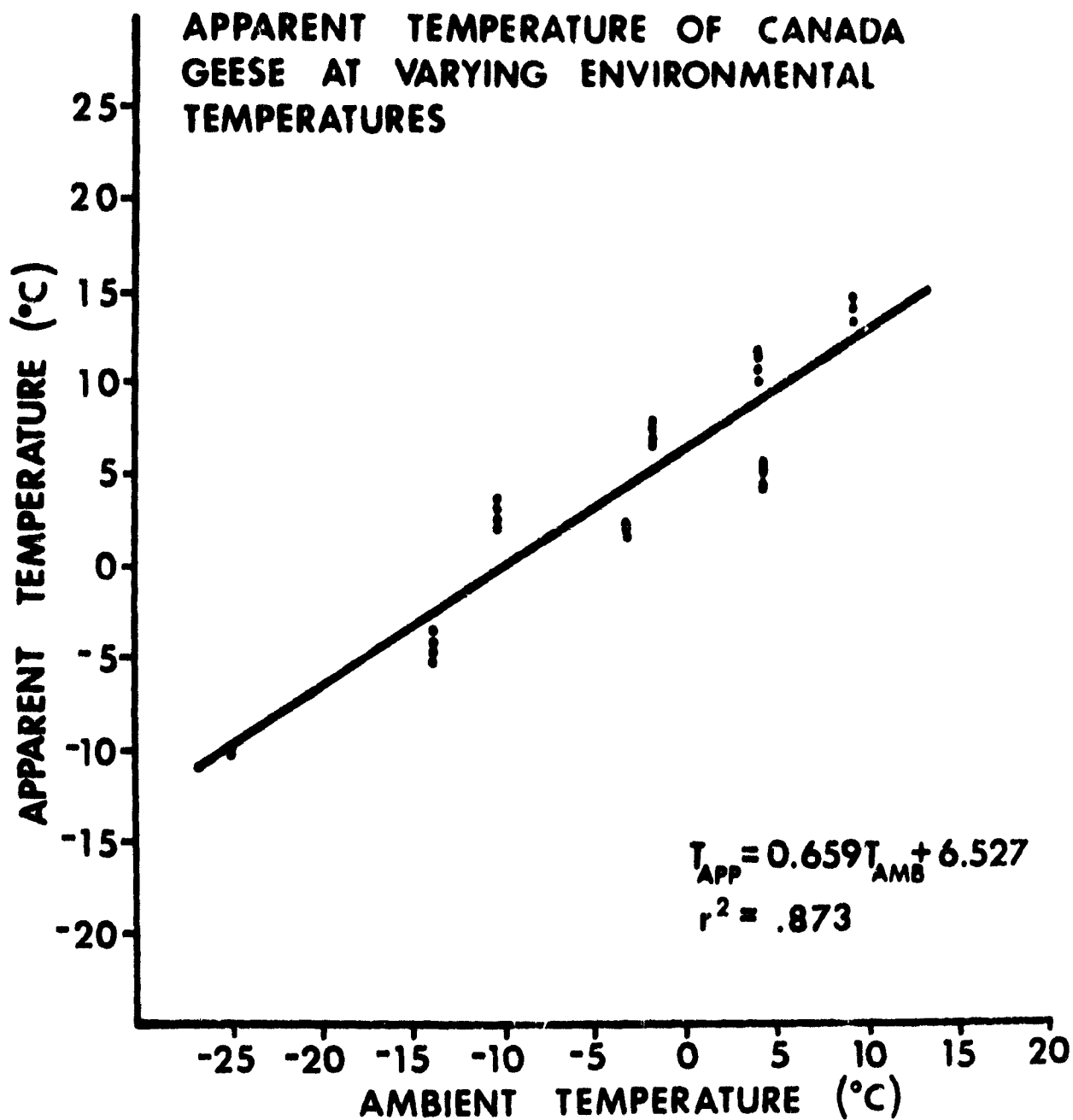
Figure 1. Relationship of apparent temperature of Canada geese to varying environmental temperature.
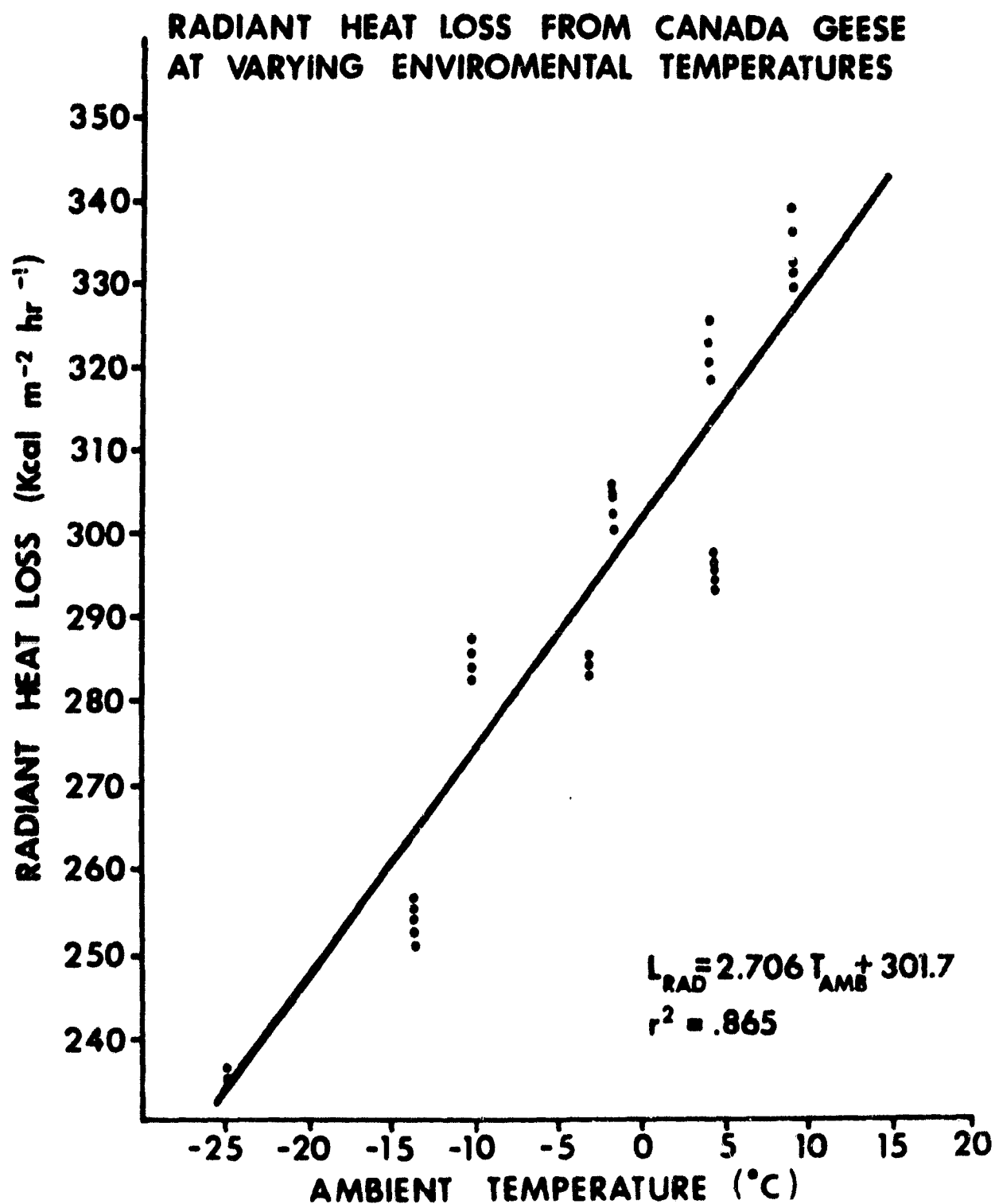
Figure 2. Relationship of radiant heat loss from Canada geese to varying environmental temperature.

APPLICATION OF REMOTE SENSING TECHNIQUES FOR DETECTING
DUTCH ELM DISEASE IN URBAN ENVIRONMENTS

INTRODUCTION

Dutch elm disease is a disease fatal to most elm species but especially the American elm (*Ulmus americana*). The disease is caused by a fungus (*Cerotocystis ulmi*) which invades and grows in the water conducting vessels of elm. The disease is generally transmitted by the European elm bark beetle (*Scolytus multistriatus*) and the native elm bark beetle (*Hylurgopinus rufipes*). The beetles overwinter as larvae and adults under the bark of dead or dying elms. In the spring the emerging adult beetles, contaminated with fungus spores, fly to dead or dying trees to reproduce and then on to healthy trees to feed. It is at this point that the infection is spread.

Sanitation by removal and destruction of dead and dying elm is the only way to slow disease spread within an elm population. Prompt identification and destruction can reduce losses to levels where severe economic impact is minimized. The Department of Game, Fish and Parks estimated that 28,000 elms were lost to Dutch elm disease in 1978. The economic loss, including removal of dead trees exceeded $22 million.

The severity of the tree loss problem prompted an investigation to test the feasibility of using remote sensing techniques for early detection of Dutch elm disease. French and Meyer (1977) used low

altitude color infrared aerial photography to detect diseased trees.
Waltz (1969) and La Perriere and Howard (1971) also recognized the
utility of color infrared photography for detection of diseased trees.
The investigators determined the disease is easiest to detect and has
the highest incidence in early July. It is also recommended that a
survey in late August would also be useful in detecting trees infected
by second generation adult beetles.

The concensus of the investigators was that aerial photography
was a fast, low cost survey method. Accuracy of detection ranged from
50-70 percent. Accuracy was influenced by difficulty of species
identification, difficulty in discriminating the target disease from
other kinds of moisture stress-inducing situations, difficulty in
mapping locations of infected trees and coordinating the photo with
the ground situation. It is expected accuracy can be improved in the
proposed project because many of the previous investigations were
performed in a natural forest rather than an urban forest. In a normal
urban environment it should be easier to identify species because the
crown density will be less.

The city of Watertown with the assistance of the South Dakota
Department of Game, Fish and Parks, Division of Forestry, has taken
significant steps that should facilitate Dutch elm disease detection.
In the past the Watertown city forester with the assistance of the
South Dakota Division of Forestry, has mapped and inventoried by
species all trees on most public land and street boulevards. The

inventory was performed to simplify the annual ground surveys necessary to identify diseased trees on public land.

The problem now facing the city of Watertown is how to identify early diseased elms on private property as well as to monitor for disease in the already identified elms on public property. The city has passed an ordinance permitting the city forester to condemn and remove diseased trees on private property at the owner's expense.

The process of identifying the diseased trees on private and public land by conventional ground survey is time consuming. The city officials and South Dakota Division of Forestry are hopeful that remote sensing techniques can significantly reduce the amount of time and expense needed to perform the inventory of private trees.

PROCEDURES

It was originally proposed to collect 1:4,500 scale color infrared aerial photography and thermal infrared data during early July and again in late August, 1979. However, in 1979 eastern South Dakota experienced an unusually wet summer. Consequently, cloud cover restricted any data collection until late July. An aborted attempt was made to collect data in late July but the airplane developed engine problems shortly after takeoff and was subsequently grounded for four weeks for repairs. Color infrared aerial photography was finally collected in early September. A camera malfunction severely overexposed approximately half of each frame of the film resulting

in the film being of minimal use for an operational disease detection program. No thermal infrared was collected because of a scanner malfunction.

RESULTS

Despite the initial problems in obtaining data both the city of Watertown and the South Dakota Division of Forestry were still interested in pursuing the project. It was mutually decided to utilize the data which had been collected to develop and refine interpretation procedures to be used in an operational program.

A meeting was held with the Watertown city forester and a representative of the Division of Forestry to determine what information and assistance was needed to utilize the existing data effectively. It was determined that the major use of the data would be to assist in training an interpreter to identify tree species. The 1979 film was reviewed to determine which portions of the city had suitable photographic coverage. The areas were delineated on a city base map. The map was given to the city of Watertown forester and he provided the corresponding inventory data.

The training was by comparison of the photography to the existing public land tree inventory and other interpretation keys developed for tree specie identification. The training enabled the interpreter to readily identify elm trees. However, difficulties still exist in determining individual trees in an overcrowded stand. Overlapping

tree canopies is the major reason for the problems. The agreed upon method of dealing with the problem is to merely identify that there is a potential disease problem associated with a group of trees. Ground inspection should identify the individual problem trees.

RECENT DEVELOPMENTS

On June 28, 1980, 1:4,500 scale color infrared stereo aerial photography and thermal infrared imagery was collected for the city of Watertown. The photography has been reviewed and appears to be excellent data for identifying elm trees infected with DED. The thermal imagery has not been reviewed at this time.

On June 23 a preliminary ground inspection was conducted to obtain ground truth information. At that time nearly 50 trees were identified as having DED.

Interpretation of the 1980 photography has begun. Pink and light gray areas in elm trees are suspected to be early indication of disease presence. All leafless trees are being identified as dead elm trees. The dead trees could be of a different species but it is impossible to discern this from the photography. Final determination will be made during the ground survey.

The major interpretation problem is the ability to distinguish the light pink areas of potentially infected elms from the pink tone of an ash tree. The similarity is confusing but can be dealt with by making an accurate interpretation of species. Figure 1 is a contact
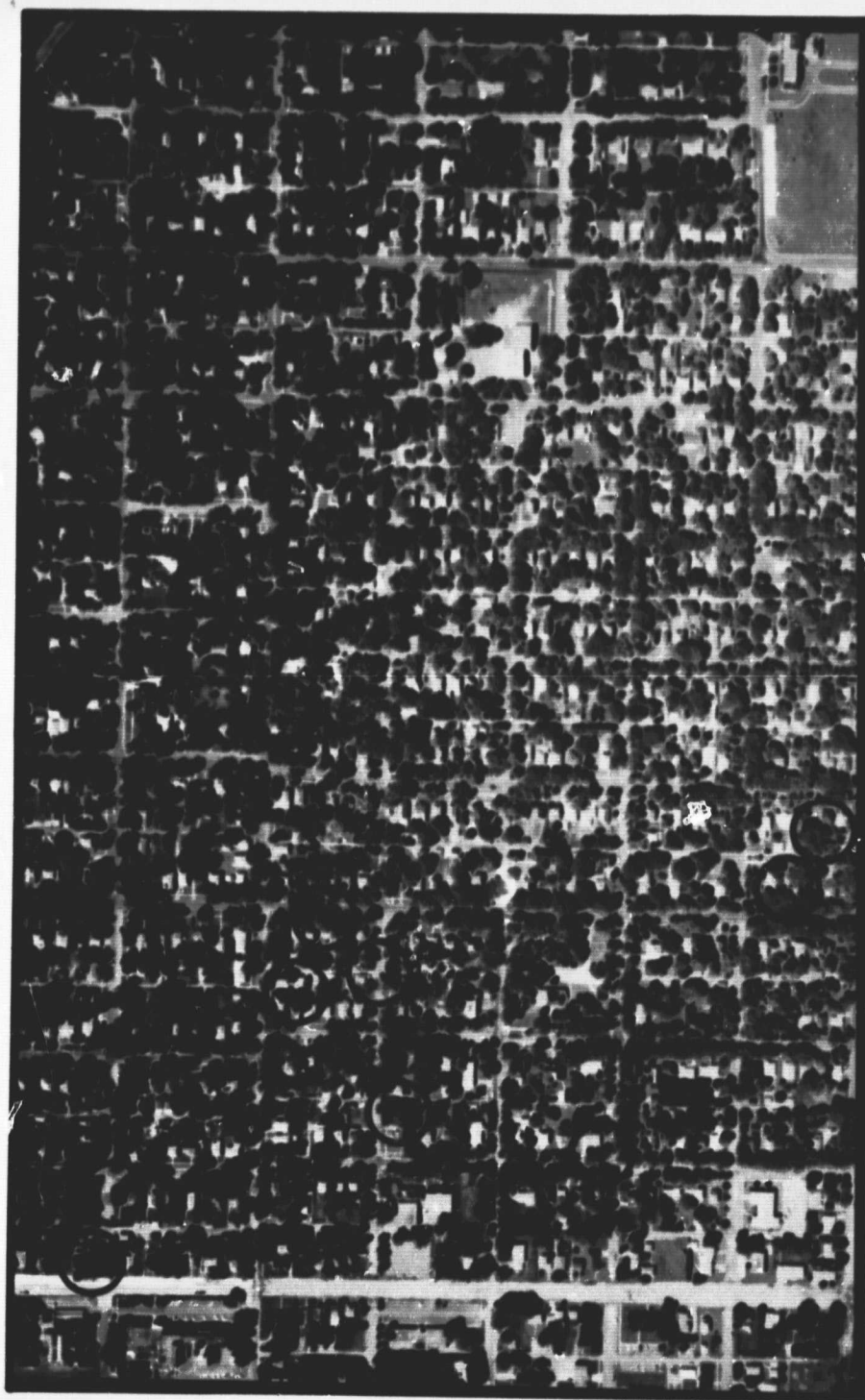
Fig. 1. Contact print (1:4500) of the 1980 photography with a sample of suspected elm trees annotated.

print of the 1980 photography. A sample of the suspected trees have been annotated. Many more will be identified in a detailed interpretation using a 2x enlargement and stereoscopic viewing of the film transparencies.

ANTICIPATED WORK

Work has already begun on interpreting the photography for DED. The plan is to annotate DED trees on contact prints of the photography. The photography will also have streets and avenues annotated to enable ground crews to find trees suspected of having the disease.

Currently the city forester is conducting the annual DED survey of public and for the first time private land. Records of infected and removed trees are being kept so a comparison of the ground inspection and remote sensing techniques can be made.

A followup ground inspection and aerial data collection will be conducted in late August. This survey will identify newly infected trees. More importantly, from the remote sensing standpoint, the late summer survey will assist in the evaluation of the potential of using color infrared photography for determination of previsual stress conditions due to DED. It is likely that some elm trees identified on the photography as potentially infected trees may not show symptoms until after the first ground inspection has been completed. The followup inspection will verify the usefulness of the data for previsual stress detection.

The thermal infrared imagery obtained will be analyzed to determine if there is any potential use of the data for discriminating infected trees under stress.

REFERENCES

French, D.W., Mark E. Ascerno, and Ward C. Steinstra. 1977. The Dutch elm disease. Agricultural Extension Service, University of Minnesota.

LaPerriere, L.R., and W.A. Howard. 1971. Discriminating previsual symptoms of stress associated with Dutch elm disease through color infrared photography. University of Denver, Department of Geography Technical Paper no. 17-1.

Waltz, F.A. 1969. Unpublished material. Remote Sensing Institute, South Dakota State University, Brookings, SD.

A FEASIBILITY STUDY FOR
MONITORING EFFECTIVE PRECIPITATION
IN SOUTH DAKOTA USING TIROS-N

INTRODUCTION

Improved estimates of soil moisture and rainfall distribution are important for agricultural and hydrological applications (yield forecasting, pest management, runoff modeling, flood forecasting, etc.). In drafting South Dakota's response to the National Climate Act, a Workshop of Climatic Data Users set establishment of a soil moisture information network as a top-priority for the state. The Workshop recognized that soil moisture budgeting will be an integral part of a soil moisture network.

Suitable soil moisture budget models have been developed. However, a weak link in the models is uncertainty in estimates of effective precipitation (infiltration), a major input of the models. Spatial evaluations of precipitation and soil moisture using ground measurements are difficult because of the requirement of dense networks. The possibility exists, however, of using satellite visible, near IR, and thermal IR data to monitor precipitation and soil moisture patterns associated with changes in evapotranspiration and thermal inertia as inputs into soil moisture models.

A study was proposed to evaluate the feasibility of using weather satellite (TIROS-N) data to monitor effective precipitation for use

in a soil moisture network in South Dakota. TIROS-N collects data (visible, near and thermal IR) twice daily (mid-afternoon and early morning) at a spatial resolution of 1.1 km.

MATERIALS AND METHODS

Daily rainfall estimates for July and August, 1979, were provided by the South Dakota Department of Water and Natural Resources (DWNR). DWNR operates a network of approximately 1500 rain gauges. A network of 81 soil sampling sites was established with sites selected to represent the major soil associations in the state. Land use categories were restricted to pasture and small grains. Soil samples for determining water content were collected at ten day intervals for each site during July and August, 1979. Percent cover was also estimated at each site.

TIROS-N imagery were received and were compared with rainfall and soil moisture estimates to locate apparent reflectance/emittance anomalies associated with moisture distribution patterns.

RESULTS

Standard TIROS-N imagery is produced to enhance cloud patterns at the expense of land surface features. This is particularly evident in thermal infrared. As a result, no discernible patterns associated with moisture variations were found on the standard products. Photographically enhanced imagery showed little improvement over the standard products.

Selected digital data were ordered, and are currently being used to produce digitally enhanced imagery. Because of delays in obtaining the data, and extensive reformatting required to make the data compatible with the RSI analysis system, the enhancement process is not completed. Thus, there are no results to report at this time. A detailed final report of results will be submitted upon completion of the the analysis of the digitally enhanced imagery.

SURVEY AND ANALYSIS OF POTENTIAL POLLUTION
FROM OPEN AND ABANDONED SOLID WASTE DUMP
SITES USING REMOTE SENSING TECHNIQUES

INTRODUCTION

There are numerous unauthorized open and abandoned solid waste dumps still in existence in South Dakota. The majority of these dumps have been and are still utilized without concern for sound environmental practices. Potential health and environment hazards that are created by open and abandoned dump sites may include pollution of ground and surface waters from leachates and runoff; the breeding of germs, insects, and disease carrying rodents; potential fire hazard; generation of methane gas; and the creation of an unsightly nuisance.

Several local, state and federal government agencies are cooperatively involved in solid waste management in South Dakota and in particular Spink County. The Fourth Planning and Development District is presently developing a regional solid waste management plan for its ten-county area including Spink County. The South Dakota Department of Environmental Protection is presently developing a state-wide solid waste management plan. This plan will identify the responsibilities and authorities for implementation of the State Plan. The plan will address the establishment of new open dumps, and the closing or upgrading of all existing open dumps, among other items. The U.S. Environmental Protection Agency (USEPA) is required by law to inventory all disposal facilities or sites in the United States which are open dumps, and

those that do not meet the requirements of a sanitary landfill will be placed on a compliance schedule for closure or upgrading.

The problem is to determine where and how many sites exist and potential pollution problems. Many of the sites are near small towns but many more are in rural areas where generally a small group of people dump waste. The conventional way to find the sites would be a "windshield survey" of the area. Unfortunately this method is very costly, extremely time consuming and ineffective in locating sites not near main roads. Remote sensing techniques, which are generally cost effective for large area reconnaissance, were used to locate and map open and abandoned dump sites in Spink County.

STUDY AREA

Spink County encompasses approximately 968,000 acres. There are 11 communities and, according to the 1970 census, a population of 10,595. The major land use in this area is agricultural. The James River and the James River Basin, with numerous meandering streams, are partially located within Spink County.

PROCEDURES

Existing and newly acquired 1979 NASA high altitude color infrared photography was interpreted to identify dump sites in Spink County. Initial interpretation was performed using June 1975 1:60,000 scale

C-2

photography. The 1975 photography provided about 75% coverage of the county.

Additional interpretation was performed using the 1979 color infrared 1:120,000 scale photography for the entire county. The photography was acquired in conjunction with other NASA projects. The quality of the data was considerably less than that of the 1975 data. Segments of many frames were overexposed and some clouds and cloud shadows were present.

Ground truth information for known existing open dumps was provided by the Fourth Planning and Development District. The information provided was the location of the dump sites near each of the towns within the county. The ground truth information helped train an interpreter to recognize possible dump sites.

The location of possible dump sites was determined by using two key indicators. They were the presence of a mottled texture and tone, which was distinct from the usually homogeneous texture and tone of the surrounding area, and the presence of a road or trail used by vehicles to deliver the waste, Another indicator was the white tone of metal containers which was evident on the imagery. Both dates of imagery were interpreted using a 7x magnifying eyepiece.

The accuracy of the interpretation was determined by field checking. Field checking was performed by trained observers flying at low altitude in a small plane from site to site. The light plane method was chosen because of the difficulty in reaching sites not near roads and because

considerable time and money was saved in comparison to driving to each site. It took only three hours to verify 72 sites.

Other resource information concerning each site's pollution potential such as land use was also considered. The proximity to surface water was the most important from a pollution standpoint since contamination of water supplies could be very dangerous. In addition contamination of livestock forage by residual pesticide and herbicide chemicals may present a danger to the livestock. The basic land use surrounding each dump site was interpreted from the 1979 high altitude photography. The land use was grouped into four basic categories: cropland, pasture, riparian, and farmstead. The distance to surface water was calculated from USGS 7 1/2 minute topographic maps. The maps were used because the poor quality of the 1979 film made it difficult to accurately determine the drainage. The surface water bodies were either streams, lakes or marshes. No information concerning location of shallow groundwater or any other geologic information was available.

RESULTS

A total of 146 possible dump sites were interpreted from the 1975 and 1979 imagery. A total of 72 sites were field checked, of which 33 were actual garbage dump sites (Fig. 1). Garbage dumps were composed of cans, bottles, paper, and other household refuse. Another 20 sites were rubble piles composed of lumber, automobiles, and machinery (Fig. 2), and 19 were not dump sites of any kind. Only one dump site which had

Fig. 1. Aerial view of typical garbage dump site.
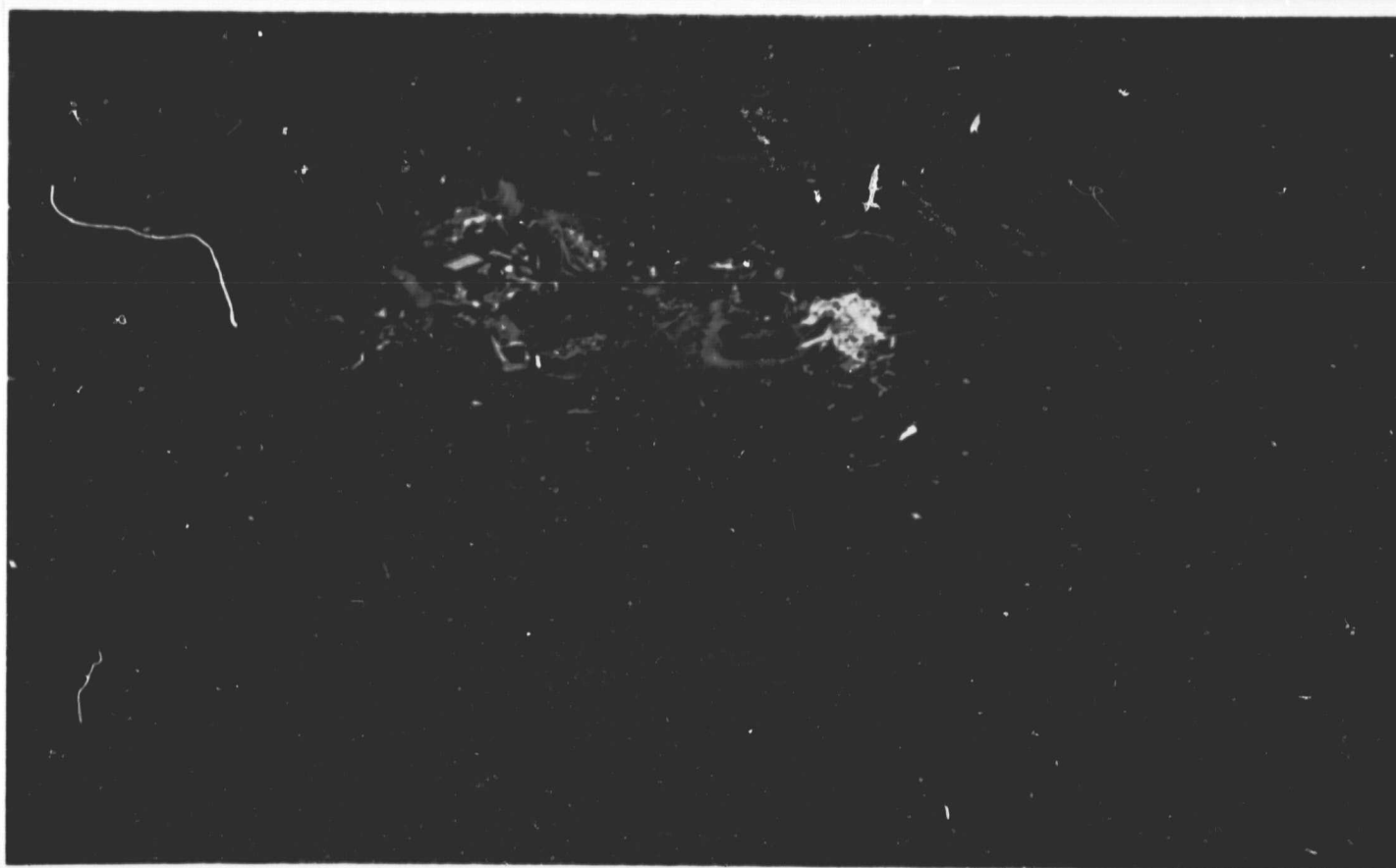
Fig. 2. Aerial view of typical rubble pile.

not been interpreted from the imagery was found during the field checking. This indicates that the interpretation detected almost every probable dump site.

Based on the interpreted dump sites, which were field checked, the level of accuracy for detecting probable garbage dump sites is 46%. If rubble sites which closely resemble garbage dump sites were included the accuracy increases to 75%.

A comparison of the accuracy results for dump sites interpreted from both scales of imagery was made to determine if one would be more advantageous. Of the 33 confirmed dump sites 19 were interpreted from the 1:60,000 scale imagery and 24 from the 1:120,000 scale photography. Consideration must be given to the fact that the 1:60,000 scale photography provided only 75% coverage of the county, the quality of the 1:120,000 scale imagery was poor and some sites could have been created after 1975. These three considerations make it difficult to make a complete evaluation of photographic scale.

The dump site inventory was put in tabular form. The tabular information included a site number, the location based on a township and range system, the name of the USGS 7 1/2 minute quadrangle map in which the site is located, whether or not it was verified, the surrounding land use type, proximity to surface water, type of surface water and date of imagery from which the site was delineated (see Appendix A). The sites were also annotated on the appropriate USGS 7 1/2 minute topographic map to facilitate finding the sites while in the field.

SUMMARY AND CONCLUSIONS

Interpretation of two dates and scales of imagery delineated
146 potential open or abandoned dump sites. The inventory of sites
and ancillary data were put into tabular form. Local government
agencies were provided the data to assist the refinement of the Spink
County solid waste management plan and as input into the implementation
of the State Plan.

Despite the acceptance of the data as being accurate, timely and
cost effective (see letter in Appendix B) the data have not been used
extensively. The primary reason is the sensitive nature of solid waste
management in Spink County. Spink County recently withdrew from a
multi-county solid waste program. Hence establishment of a new waste
disposal site in Spink County has become a political issue. Hopefully,
circumstances will change and the data will be used for planning purposes.

Efforts will continue to expose those in the state and federal
government to procedures developed. The study provides an economically
and technically feasible method to inventory waste disposal sites. All
indications are that similar inventories will be conducted nationally at
some time in the future.

APPENDIX A

SPINK COUNTY OPEN AND ABANDONED DUMP SITES

Site #	Location	Quadrangle	Type	Surrounding Land Use	Surface Water Proximity to	Type	Date of Discovery
1	SW Corner, SW¼, Section 9, T 120 N, R. 65 W.	Chelsea	Unknown	Cropland	3000 ft.	Stream	1975
2	SW Corner, SE¼, Section 21, T 118 N, R 65 W	Northville SW	Garbage	Cropland	2800 ft.	Stream	1979
3	NE Corner, NE¼, Section 8, T 117 N, R 65 W	Zell	Unknown	Cropland	800 ft.	Pond	1975
4	NW Corner, SW¼, Section 8, T 116 N, R 65 W	Zell	Unknown	Abandoned Farm	<800 ft.	Stream	1979
5	SE Corner, SE¼, Section 31, T 116 N, R 65 W	Redfield SW	Unknown	Pasture	750 ft.	Stream	1975
6	SE Corner, SE¼, Section 6, T 115 N, R 65 W	Redfield SW	Unknown	Pasture	750 ft.	Lake	1979
7	SE Corner, NE¼, Section 32, T 114 N, R 64 W	Tulare	Unknown	Pasture	1200 ft.	Stream	1979
8	NE Corner, NE¼, Section 28, T 114 N, R 64 W	Tulare	Unknown	Pasture	3100 ft.	Stream	1975
9	SE Corner, NE¼, Section 8, T 114 N, R 64 W	Tulare	Unknown	Pasture	500 ft.	Pond	1979
10	NW Corner, SE¼, Section 28, T 115 N, R 64 W	Tulare	City Dump	Cropland	>4000 ft.	Pond	1979
11	SW Corner, SW¼, Section 19, T 115 N, R 64 W	Redfield S	Unknown	Pasture	800 ft.	Stream	1979

SPINK COUNTY OPEN AND ABANDONED DUMP SITES

Site #	Location	Quadrangle	Type	Surrounding Land Use	Surface Water Proximity to	Type	Date of Inspection
12	NE Corner, SW¼, Section 18, T 116 N, R 64 W	Redfield S.	Unknown	Pasture	<500 ft.	Creek	1979
13	? Middle, NW¼, Section 18, T 116 N, R 64 W	Redfield S.	Unknown	Pasture	<500 ft.	Creek	1975
14	SE Corner, NE¼, Section 29, T 117 N, R 64 W	Redfield N.	Unknown	Abandoned Farm	3800 ft.	Stream	1979
15	NW Corner, NW¼, Section 7, T 117 N, R 64 W	Redfield N.	Unknown	Pasture	~3200 ft.	Pond	1979
16	NW Corner, NW¼, Section 32, T 118 N, R 64 W	Redfield N.	Unknown	Pasture	400 ft.	Stream	1979
17	Middle, NE¼, Section 5, T 116 N, R 64 W	Redfield N.	City dump	Cropland	1200 ft.	Stream	1975
18	SE Corner, SW¼, Section 2, T 116 N, R 65 W	Redfield N.	Unknown	Pasture	1000 ft.	Pond	1975
19	SE Corner, NE¼, Section 25, T 118 N, R 65 W	Athol	City dump	Urban/pasture	<500 ft.	Stream	1979
20	Middle, NE¼, Section 20, T 118 N, R 64 W	Athol	unknown	Cropland	<500 ft.	Stream	1975
21	NW Corner, NE¼, Section 29, T 119 N, R 64 W	Atnol	Unknown	Cropland	1500 ft.	Stream	1979
22	Middle, NW¼, Section 5, T 119 N, R 64 E	Northville	Garbage	Cropland	3000 ft.	Creek	1979

SPINK COUNTY OPEN AND ABANDONED DUMP SITES

Site #	Location	Quadrangle	Type	Surrounding Land Use	Surface Water Proximity to	Type	Date of Imagery
23	SE Corner, NE¼, Section 26, T 120 N, R 65 W.	Northville	Unknown	Pasture	800 ft.	Pond	1979
24	SW Corner, SE¼, Section 32, T 121 N, R 64 W	Northville	Unknown	Cropland	<500 ft.	Creek	1979
25	NE Corner, NE¼, Section 18, T 119 N, R 63 W.	Mellette	Unknown	Cropland	3000 ft.	Stream	1979
26	SE Corner, NW¼, Section 4, T 119 N, R 63 W.	Mellette	Garbage	Riparian	500 ft.	River	1979
27	SE Corner, SE¼, Section 35, T 120 N, R 64 W	Mellette	Garbage	Cropland	500 ft.	Pond	1979
28	SW Corner, NW¼, Section 34, T 120 N, R 63 W.	Mellette	Unknown	Pasture/Flood-Plain	1000 ft.	Stream	1979
29	NW Corner, NE¼, Section 22, T 120 N, R 63 W	Mellette	Unknown	Cropland	2000 ft.	James River	1979
30	SE Corner, SW¼, Section 10, T 120 N, R 63 W	Mellette	Unknown	Riparian	<500 ft.	River	1979
31	Middle, NE¼, Section 10, T 120 N, R 63 W	Mellette	Unknown	Riparian	500 ft.	River	1979
32	SW Corner, SE¼, Section 17, T 118 N, R 63 W	Gallup	Garbage	Pasture	<500 ft.	River	1979
33	SW Corner, SW¼, Section 3, T 118 N, R 63 W	Gallup	Unknown	Cropland	1500 ft.	Stream	1979

SPINK COUNTY OPEN AND ABANDONED DUMP SITES

Site #	Location	Quadrangle	Type	Surrounding Land Use	Surface Water Proximity to	Type	Date of Inspection
34	NW Corner, NW¼, Section 36, T 118 N, R 64 W	Ashton	Garbage	Pasture	200 ft.	River	1979
35	NW Corner, NW¼, Section 18, T 115 N, R 63 W	Frankfort SW	Unknown	Pasture	>4000 ft.		1979
36	Middle, NW¼, Section 26, T 116 N, R 64 W	Frankfort SW	Unknown	Pasture	4000 ft.	Pond	1979
37	NE Corner, NW¼, Section 27, T 116 N, R 63 W	Frankfort, SW	Unknown	Cropland	2300 ft.	Stream	1979
38	NE Corner, NW¼, Section 33, T 114 N, R 63 W	Hitchcock	City dump	Cropland	4000 ft.		1979
39	NE Corner, SE¼, Section 20, T 114 N, R 63 W	Hitchcock	Unknown	Pasture	>4000 ft.		1979
40	NW Corner, NE¼, Section 17, T 114 N, R 64 W	Hitchcock	Unknown	Pasture	>4000 ft.		1979
41	SW Corner, SW¼, Section 34, T 115 N, R 63 W	Hitchcock	Unknown	Cropland	2000 ft.	Stream	1979
42	SE Corner, SE¼, Section 28, T 115 N, R 63 W	Hitchcock	Unknown	Farmstead	22	Stream	1979
43	NW Corner, NE¼, Section 35, T 115 N, R 64 W	Spink	Unknown	Cropland	500 ft.	Stream	1979
44	Middle, NW¼, Section 34, T 115 N, R 62 W	Spink	Unknown	Riparian/ Pasture	<500 ft.	River	1979
45	NE Corner, NW¼, Section 28, T 115 N,	Spink	Unknown	Riparian	<500 ft.	River	1979

SPINK COUNTY OPEN AND ABANDONED DUMP SITES

Site #	Location	Quadrangle	Type	Surrounding Land Use	Surface Water proximity to	Type	Date of Closure
46	SE Corner, SE¼, Section 27, T 115 N, R 62 W	Spink	Unknown	Riparian	<500 ft.	River	1972
47	NE Corner, NE¼, Section 27, T 115 N, R 62 W	Spink	Unknown	Cropland	<500 ft.	Stream	1975
48	SW Corner, SE¼, Section 13, T 115 N, R 63 W	Glendale	Unknown	Pasture	<500 ft.	Stream	1975
49	NW Corner, NW¼, Section 18, T 115 N, R 62 W	Glendale	Unknown	Cropland	500 ft.	Stream	1975
50	SE Corner, SE¼, Section 7, T 115 N, R 62 W	Glendale	Unknown	Pasture	1000 ft.	Stream	1979
51	SW Corner, SE¼, Section 31, T 116 N, R 60 W	Glendale	Unknown	Cropland	<500 ft.	Stream	1975
52	SW Corner, NW¼, Section 6, T 116 N, R 62 W	Glendale	Garbage	Cropland	1500 ft.	Stream	1979
53	Middle, NW¼, Section 6, T 115 N, R 62 W	Frankfort	Garbage	Pasture	<500 ft.	Stream	1975
54	NW Corner, NW¼, Section 34, T 117 N, R 62 W	Frankfort	Unknown	Cropland	1000 ft.	Stream	1979
55	NE Corner, NE¼, Section 23, T 117 N, R 53 W	Frankfort	Unknown	Pasture	<500 ft.	Stream	1979
56	SE Corner, SE¼, Section 29, T 118 N, R 62 W	Brentford SE	Unknown	Riparian	<500 ft.	Stream	1979

SPINK COUNTY OPEN AND ABANDONED DUMP SITES

Site #	Location	Quadrangle	Type	Surrounding Land Use	Surface Water Proximity to	Type	Date of Inspection
57	Middle, NW¼, Section 21, T 118 N, R 62 W	Brentford SE	Unknown	Riparian/Pasture	<500 ft.	Stream	1975
58	NE Corner, NE¼, Section 1, T 118 N, R 63 W	Brentford SE	Unknown	Cropland	2200 ft.	Pond	1979
59	NW Corner, NW¼, Section 34, T 119 N, R 62 W	Brentford	Unknown	Cropland	<500 ft.	Stream	1979
60	NW Corner, SE¼, Section 22, T 120 N, R 62 W	Brentford	Garbage	Cropland	2200 ft.	Pond	1979
61	NW Corner, NW¼, Section 25, T 120 N, R 63 W	Brentford	Unknown	Riparian	2000 ft.	Stream	1975
62	Middle, NE¼, Section 13, T 120 N, R 63 W	Brentford	Unknown	Pasture	<500 ft.	Stream	1975
63	SE Corner, SW¼, Section 8, T 120 N, R 62 W	Brentford	Unknown	Pasture	<500 ft.	Stream	1975
64	NE Corner, SE¼, Section 33, T 120 N, R 61 W	Randolph	Garbage	Cropland	<500 ft.	Stream	1979
65	NW Corner, NW¼, Section 10, T 119 N, R 60 W	Conde	Unknown	Cropland	1200 ft.	Stream	1979
66	NE Corner, NE¼, Section 31, T 120 N, R 60 W	Conde	City Dump	Cropland	<500 ft.	Stream	1979

SPINK COUNTY OPEN AND ABANDONED DUMP SITES

Site #	Location	Quadrangle	Type	Surrounding Land Use	Surface Water Proximity to	Type	Date of Interest
67	NW Corner, NW¼, Section 25, T 120 N, R 61 W	Conde	Unknown	Cropland	<500 ft.	Stream	1975
68	NW Corner, NW¼, Section 28, T 120 N, R 60 W	Conde	Unknown	Pasture	<500 ft.	Pond	1975
69	SW Corner, SE¼, Section 22, T 120 N, R 60 W	Conde	Unknown	Pasture	2000 ft.	Stream	1975
70	Middle, SE¼, Section 23, T 118 N, R 62 W	Conde SW	Unknown	Pasture	500 ft.	Pond	1979
71	SW Corner, SE¼, Section 21, T 118 N, R 61 W	Conde SW	Unknown	Riparian	<500 ft.	Stream	1975
72	Middle, SE¼, Section 14, T 118 N, R 62 W	Conde SW	Unknown	Cropland	1000 ft.	Stream	1979
73	NW Corner, NE¼, Section 30, T 117 N, R 61 W	Doland NW	Garbage	Riparian	<500 ft.	Stream	1979
74	NW Corner, SE¼, Section 19, T 117 N, R 61 W	Doland NW	Garbage	Riparian	<500 ft.	Stream	1979
75	NW Corner, NE¼, Section 5, T 117 N, R 61 W	Doland NW	Unknown	Pasture	<500 ft.	Stream	1979
76	NW Corner, NW¼, Section 3, T 117 N, R 61 W	Doland NW	Unknown	Pasture	4200 ft.	Stream	1979
77	NE Corner, NW¼, Section 21, T 115 N, R 61 W	Doland SW	Unknown	Pasture	2500 ft.	Stream	1975

SPINK COUNTY OPEN AND ABANDONED DUMP SITES

Site #	Location	Quadrangle	Type	Surrounding Land Use	Surface Water Proximity to	Type	Date of Inspection
78	SW Corner, SW¼, Section 10, T 115 N, R 61 W	Doland SW	Garbage	Cropland	<500 ft.	Stream	1979
79	SE Corner, SE¼, Section 3, T 115 N, R 61 W	Doland SW	Unknown	Cropland	>4000 ft.		1979
80	SE Corner, SE¼, Section 25, T 114 N, R 60 W	Lake Byron NW	Unknown	Pasture	<500 ft.	Stream	1979
81	SE Corner, SE¼, Section 32, T 114 N, R 61 W	Lake Byron NW	Unknown	Cropland	<500 ft.	Creek	1979
82	SE Corner, NE¼, Section 35, T 114 N, R 61 W	Lake Byron NW	Unknown	Cropland	1200 ft.	Stream	1979
83	SE Corner, NE¼, Section 11, T 114 N, R 61 W	Lake Byron NW	Unknown	Cropland	2200 ft.	Stream	1975
84	NW Corner, NW¼, Section 28, T 115 N, R 61 W	Lake Byron NW	Unknown	Cropland	>4000 ft.	Stream	1979
85	Middle, NW¼, Section 29, T 118 N, R 60 W	Turton	Garbage	Pasture	1100 ft.	Stream	1975
86	Middle, SW¼, Section 20, T 118 N, R 60 W	Turton	Garbage	Riparian	500 ft.	Stream	1979
87	SE Corner, NE¼, Section 7, T 118 N, R 60 W	Turton	Garbage	Pasture	<4000 ft.	Stream	1979

SPINK COUNTY OPEN AND ABANDONED DUMP SITES

Site #	Location	Quadrangle	Type	Surrounding Land Use	Surface Water Proximity to	Type	Date of Interview
88	SE Corner, SW¼, Section 30, T 117 N, R 60 W	Doland	City Dump	Riparian	<500 ft.	Stream	1979
89	SE Corner, SE¼, Section 9, T 117 N, R 60 W	Doland	Dump	Riparian/Pasture	<500 ft.	Stream	1975
90	NW Corner, NW¼, Section 20, T 115 N, R 60 W	Doland SE	Garbage	Cropland	4000 ft.	Stream	1979
91	NW Corner, NW¼, Section 18, T 115 N, R 60 W	Doland SE	Garbage	Pasture	<500 ft.	Stream	1975
92	SW Corner, SW¼, Section 9, T 115 N, R 60 W	Doland SE	Garbage	Cropland	1000 ft.	Pond	1979
93	NE Corner, NW¼, Section 1, T 115 N, R 61 W	Doland SE	Unknown	Pasture	1000 ft.	Stream	1975
94	Middle, NE¼, Section 6, T 115 N, R 60 W	Doland SE	Garbage	Pasture	<500 ft.	Stream	1979
95	SE Corner, NW¼, Section 34, T 116 N, R 60 W	Doland SE	Unknown	Pasture	3000 ft.	Pond	1975
96	Middle, NE¼, Section 35, T 114 N, R 61 W	Bloomfield	Unknown	Pasture	3800 ft.	Stream	1975
97	Middle, NW¼, Section 32, T 114 N, R 60 W	Bloomfield	Unknown	Cropland	<500 ft.	Stream	1975
98	SW Corner, SW¼, Section 28, T 114 N, R 61 W	Bloomfield	Unknown	Farmstead	1000 ft.	Stream	1975

SPINK COUNTY OPEN AND ABANDONED DUMP SITES

Site #	Location	Quadrangle	Type	Surrounding Land Use	Surface Water Proximity to	Type	Date of Imagery
99	Middle SW¼, Section 24, T 114 N, R 61 W	Bloomfield	Garbage	Cropland	3800 ft.	Stream	1975
100	Middle NE¼, Section 2, T 114 N, R 61 N	Bloomfield	Garbage	Cropland	3000 ft.	Stream	1975
101	SE Corner, NE¼, Section 31, T 115 N, R 60 W	Bloomfield	Unknown	Riparian/Pasture	<500 ft.	Stream	1975
102	SW Corner, SE¼, Section 32, T 115 N, R 60 W	Bloomfield	Garbage	Riparian/Pasture	500 ft.	Stream	1975
103	Middle, SE¼, Section 33, T 115 N, R 60 W	Bloomfield	Garbage	Pasture	<500 ft.	Stream	1975
104	SE Corner, SE¼, Section 34, T 115 N, R 60 W	Bloomfield	Unknown	Pasture	2000 ft.	Stream	1979
105	Middle SW¼, Section 30, T 115 N, R 60 W	Bloomfield	Unknown	Pasture	<500 ft.	Stream	1979
33A	NW Corner, NW¼, Section 21, T 119 N, R 63 W	Gallup	Garbage	Riparian	<500 ft.	River	1975
33B	NW Corner, SW¼, Section 16, T 119 N, R 63 W	Gallup	Garbage	Riparian	<500 ft.	River	1975

APPENDIX B

Mr. Jeff Eidenshink
Remote Sensing Institute
South Dakota State
  University
Brookings, SD 57006

Dear Jeff:

The Fourth Planning and Development District would like to express its appreciation to the Remote Sensing Institute at South Dakota State University for its efforts in the "Survey and Analysis of Potential Pollution from Open and Abandoned Solid Waste Dump Sites Using Remote Sensing Techniques" in Spink County, South Dakota.

The data compiled in the report appears to be most impressive in terms of accuracy, expedience, and cost effectiveness for a project of this nature.

As to how this data will be utilized in Spink County is a matter that the local elected officials will have to examine and address.

It would appear that the Remote Sensing Institute, by the results of the Spink County Project, could take an active role related to Section 4005 of the Resource Conservation and Recovery Act (P.L. 94-580) in inventorying open and abandoned dump sites.

If this office could be of any further assistance, please feel free to contact us.

Sincerely,

G. Marvin O'Hara
Planner

GMO/sf

INFLUENCE OF SOIL REFLECTANCE ON
LANDSAT SIGNATURES OF CROPS

INTRODUCTION

The world economy in past decades to the present has exhibited an ever-increasing influence on modern American agriculture (Hueg, 1979). Agencies and individuals connected with agriculture now, more than ever, require a variety of information on a global basis. Accurate estimation of crop areas and yields are among the data which are crucial to decision makers at all levels.

Estimation of crop area in the U.S. and numerous other countries has been accomplished largely by two major procedures: 1) the Area Frame concept developed by the Economics, Statistics, and Cooperatives Service (ESCS) which employs statistically-based ground data collection and expansion for agricultural data, e.g. livestock, crops, etc. (Von Steen and Wigton, 1976); and 2) interpretation and classification of Landsat data (Paarlberg et al., 1978; Malila and Gleason, 1977). The ESCS has been involved in both of the above procedures (Starbuck, 1977; Wigton and Bormann, 1978).

The influence of soils, topography, and phenology has been cited as contributing to variability of crop signatures on Landsat data (Tucker and Miller, 1977; Wiegand et al., 1977: Westin and Lemme, 1978). Recent studies have investigated methods to negate the influence of the factors listed above by stratification (Dalsted

et al., 1979; Padmanabhan, 1980) and by transformation of Landsat digital data (Kauth and Thomas, 1976).

Holmes et al. (1979) reported moisture stress and soil brightness as likely causes of altered spectral signatures of wheat on Landsat data. They also noted that stratification was a "useful tool" leading to "greater overall efficiency in producing estimates . . .". Schubert et al. (1980) stratified five Landsat scenes in western Canada by Uniform Productivity Areas (UPAs), which were based on soil properties, in order to improve sampling strategy. They reported a stratification technique that both aided in the selection of Landsat training data and related to the yields of spring wheat. The yield data within each UPA were based on 10-year production records.

The objective of this study was to investigate the statistical implications of stratification upon crop signatures from Landsat CCT's. The stratification was based on manual photo-interpretation of multi-date Landsat coverage of an area in eastern South Dakota.

STUDY AREA

The region of investigation is shown in Fig. 1. Physiographic diversities and agricultural activities of this region have been detailed (Westin and Malo, 1978). Corn, wheat, oats, and barley are the major crops in this region. Sunflowers, however, are rapidly becoming a major crop in certain parts of this study area.

Fig. 1. Location of study area in crop-soil spectral study. Boundaries of the Landsat scene and the counties included in the study are outlined.

This region is characterized by hot summers and cold winters. Precipitation occurs predominantly in the spring and early summer months.

MATERIALS AND METHODS

The study area was divided into 10 strata by photo-interpretation of 1:500,000 1978 Landsat prints (14 May, 3 August, 8 September 1978 scenes). Locations of representative ground samples within each stratum were determined by ESCS techniques (Von Steen and Wigton, 1976). The samples or segments were generally one-quarter section in area and totaled 255 for the entire region. The number of segments per stratum was weighted according to the areal extent of the respective stratum.

Ground investigation was accomplished by an on-site description of the land use at each of the segments; this data collection took place during the last week of July and first week of August, 1979. Aerial photography (1:15,840 scale) was used as a base for outlining field boundaries and notating crops and crop phenology (Table 1) at each segment. The aerial photography used in the field investigation varied in date, the majority being in the 1975 to 1979 period.

The August 25 data were chosen for the initial analysis because of interest shown by ESCS personnel in using these data along with the RSI-acquired field information for verification of their sunflower acreage estimates. Time limitations precluded the use of the July 20

90

Table 1. Crop phenology (ad hoc) is listed by code and characterizing
features. These stages were noted at the time of ground data
collection, approximately two to three weeks before the
25 August Landsat data.

Code	Stage (row crops)
6	.3 - .6 m in height
7	.6 - 1.2 m in height
8	1.2 - 1.8 m in height
9	> 1.8 m in height
10	0 - 25% bloom or tasselling
11	25 - 50% bloom or tasselling
12	> 50% bloom or tasselling

data. The late-season date of the Landsat data utilized limited this study to the analysis of sunflower and corn data.

The segment data were extracted from the Landsat CCT using the ESCS-developed EDITOR computer software package (Steinberg, 1979; Institute for Advanced Computation, 1978), the Bolt, Baranek and Newman, Inc. DEC PDP-10 computer, and established ESCS techniques for map digitization and data verification. A master data set was created which contained the pixel values for MSS bands 4 through 7 and tagged each pixel by crop, strata, segment, field and stage of growth. Sub-sets of this master data set were created for the corn and sunflower data.

Various statistical procedures from the Statistical Analysis System (SAS) software package (SAS Institute, 1979) were used to analyze the corn and sunflower data sets. These procedures included MEANS

(means and other descriptive statistics), GLM (general linear models - analysis of variance), and DUNCAN (Duncan's multiple range test). A nested model was used for the GLM analysis with the segment and field variables being random and the strata and stage variables being fixed.

RESULTS AND DISCUSSION

The approach of this study was designed to develop a Landsat stratification procedure for application to other crop-producing regions of the world. To reduce bias (i.e. prior knowledge of the soils in the region) only Landsat imagery was used to establish the strata. An operational approach would utilize Landsat and physiography data in concert.

The strata boundaries were established using three Landsat dates; the August and September dates gave an indication of land use and land capability while the May date showed soil tones (Fig. 2). The May date was given priority for boundary location followed in order by the September date and August date.

Since an August 25, 1979 CCT was used, only corn and sunflowers were considered in the analysis. Analysis and interpretations in conjunction with ESCS are still in progress.

Corn

Mean digital count data by strata are shown in Table 2. All but stratum 1 are well represented in number of observations. Standard deviations values within each band were consistent with the exception of strata 6 and 9 for MSS 6 and 7; this indicated a reasonable level of accuracy from the field identifications and data extractions.
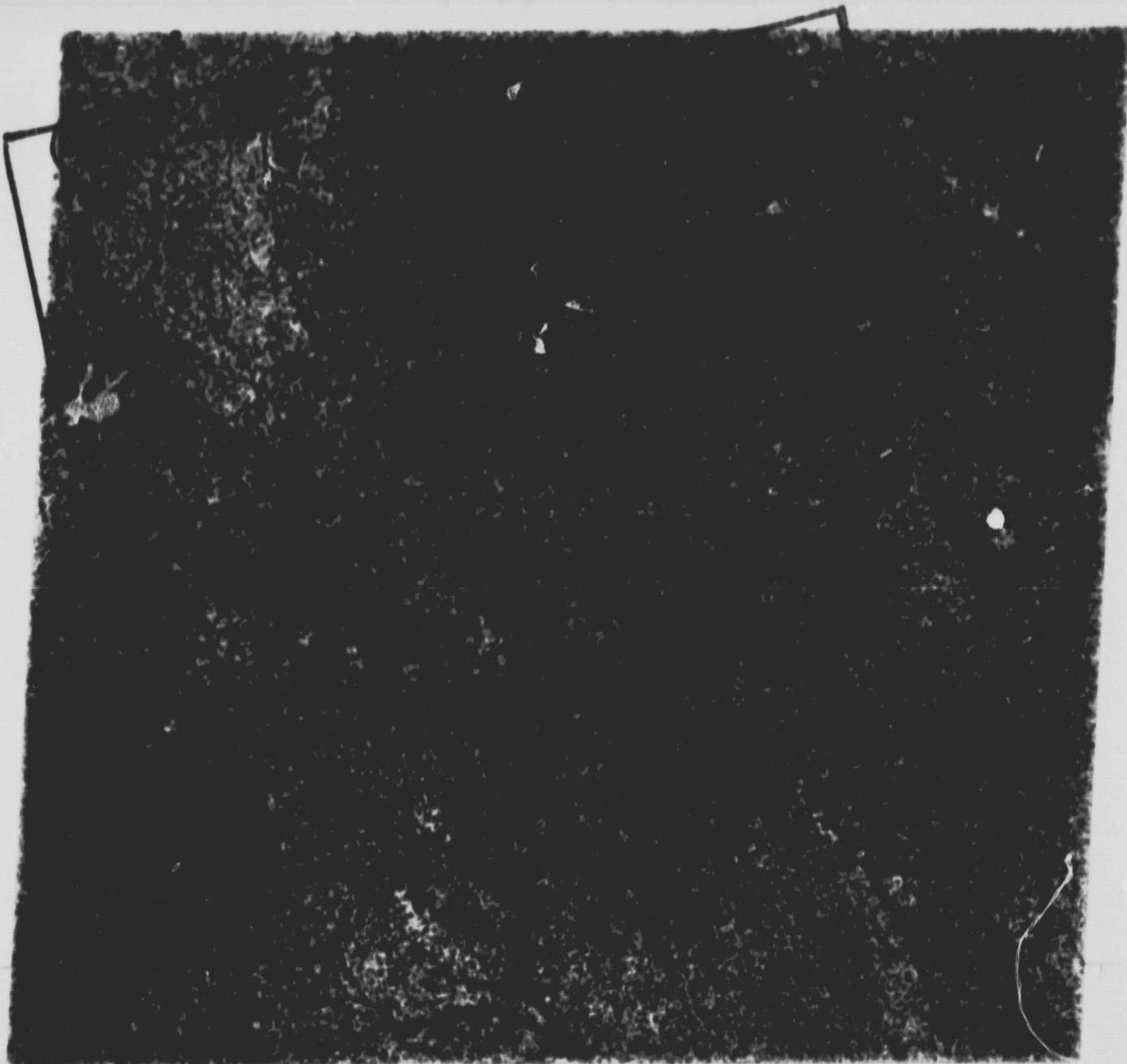
14MAY78 C N44-26/W097-42 D032-029 N N44-27/W097-43 M 5   D SUN EL52 A122 SIS· P·N L2 NASA LANDSAT E-21208-16141-5

Fig. 2. Delineation of strata is shown on the 14 May 1979 Landsat
band 5 print.

Table 2. Landsat digital means (25 August 1979 CCT) are listed by strata and Landsat band for corn.

MSS 4	Strata	N[+]	Mean	Standard Deviation
	1	117	18.1	0.9
	2	312	18.5	2.4
	3	641	17.1	1.3
	4	617	16.9	1.3
	5	532	16.1	1.3
	6	342	17.2	1.9
	7	1331	15.0	1.6
	8	449	14.5	1.2
	9	357	15.1	1.5
	10	366	15.2	1.2
MSS 5	1	117	17.7	1.6
	2	312	18.2	4.5
	3	641	16.4	2.4
	4	617	16.4	2.1
	5	532	15.5	2.0
	6	342	16.4	2.4
	7	1331	14.3	2.8
	8	449	13.6	1.5
	9	357	14.9	3.1
	10	366	14.3	1.8
MSS 6	1	117	43.0	3.9
	2	312	46.9	4.2
	3	641	43.0	3.1
	4	617	44.9	2.9
	5	532	43.7	5.6
	6	342	48.4	12.6
	7	1331	42.5	4.8
	8	449	39.6	4.8
	9	357	39.9	7.8
	10	366	42.1	4.1
MSS 7	1	117	43.8	5.4
	2	312	46.9	4.2
	3	641	44.8	4.0
	4	617	47.7	3.8
	5	532	45.4	7.1
	6	342	52.4	16.0
	7	1331	45.9	6.1
	8	449	42.6	6.1
	9	357	42.1	10.3
	10	366	43.9	5.6

[+]Observations, Landsat pixels

The mean digital data were also subdivided by crop stage (Table 3). This subdivision, which had 5 crop stages, did not recognize strata and provided a larger sample size/unit than did the subdivision by strata. Several general trends are visible in the data. The more mature classes (i.e. units 9 and 10) had higher digital values in Landsat band 4 and band 5. In Landsat band 6 and band 7 unit 10 had the lowest mean digital value, and unit 9 had the highest mean value. While the ground data recorded crop stage approximately two to three weeks in advance of the 25 August CCT, the data followed predictable trends. The greater the crop maturity the higher the digital count in the visible spectrum and the most advanced maturity (i.e. unit 10) had the lowest digital count in the near-infrared spectrum.

Table 3. Mean digital counts of corn data are shown by crop stage and Landsat band.

Stage	N	MSS 4	MSS 5	MSS 6	MSS 7
6	340	15.2	13.9	43.8	47.0
7	434	15.7	14.7	43.6	46.7
8	1069	15.6	14.9	42.9	45.7
9	518	16.1	15.4	44.9	47.2
10	2624	16.3	15.9	42.6	45.1

Analysis of Variance (ANOVA) results indicated significant differences among variables (Table 4). Since one or more stage and stratum were indicated as significantly different among the variables, a multiple comparison test was utilized to locate those differences by

Table 4. ANOVA results are shown for corn from the August 25, 1979
          CCT. A fixed model was employed.

Dependent Variable	Independent Variables F Values		
	Stage(5)[+]	Strata(9)	Stage* strata(19)
Band 4	20.68**	149.20**	33.55**
Band 5	28.31**	45.62**	32.26**
Band 6	81.61**	163.36**	147.75**
Band 7	68.38**	145.97**	143.47**

[+]Degrees of freedom

strata (Table 5). Strata are divided into five to seven significant

groups, dependent upon Landsat band. The interplay of the crop, soil,

crop stage, and wavelength sensitivity combined the various strata in

different configurations for each MSS band. Further statistical testing

is needed to establish one system of strata separation/combination, e.g.

multivariate analysis, covariance analysis, clustering, etc.

Duncan's New Multiple Range Test (DMR) was also used to indicate

the significant groupings of digital count means for corn stage (Table 6).

Landsat bands were shown to have differing sensitivities to crop stage.

The advanced maturity of stage 10 resulted in high digital count in

the visible bands (i.e. 4 and 5) and a low count in the near-infrared

band (i.e. 6 and 7). Since each crop stage did not occur within each

stratum, the data set is incomplete. Further multiple comparisons are

needed to examine the interaction of strata and crop stages. Phenology

Table 5. Duncan's New Multiple Range test for August 25 corn data by strata. Mean digital count decreases in magnitude from top to bottom.

$N^{\dagger}$	MSS 4		MSS 5		MSS 6		MSS 7	
312	$A^{\dagger\dagger}$	2	A	2	A	6	A	6
			A	1				
117	B	1	B	4	B	2	B	2
			B	6			B	
			B	3			B	4
342	C	6	C	5	C	4	C	7
641	C	3					C	
							D C	5
617	D	4	D	9	D	3		
							D	
							D	3
					E D	7		
532	E	5	E	7	E D	5	E	10
			E	10	E	7	E	
					E		E	1
					E			
					E	10		
366	F	10	F	8	F	9	F	8
319	F	9			F		F	
1323	F	7			F	8	F	9
449	G	8						

†Observations are aligned with the order of strata in band 4, i.e. unit 2 - 312 pixels, etc.

††Units with the same letter are not significantly different (.05 probability level).

Table 6. Duncan's New Multiple Range test for August 25 corn data by crop stage. Occurrence of stage within strata is also listed.

Band 4		Band 5		Band 6		Band 7	
A[†]	10[††]	A	10	A	9	A	9
		A				A	
B	9	A	9	B	6	B A	6
				B			
C	7	B	8	B	7	B	7
C		B		B			
C	8	B	7	B	8	C	8
				B			
D	6	C	6	B	10	D	10

[†]Units with the same letter are not significantly different (.05 level of probability).

[††]Occurrence of crop stage by strata is as follows: stage 6 - 5,7,9,10; stage 7 - 2,4,6,9,10; stage 8 - 3,4,5,6,7,8,9,10; stage 9 - 1,2,3,7,8 9,10; and stage 10 - 1,2,3,4,5,6,7,8.

differences within one c op across a region cause classification problems. Further strata comparisons with phenology held constant may provide additional information about the strata/crop stage interrelationship.

Sunflowers

Mean digital counts of sunflowers by strata are shown in Table 7. Strata 1, 5, and 10 were not represented. Several strata had a low number of observations; consequently, sensitivity of statistical tests will be reduced. However, the standard deviations appeared to be reasonably low.

Mean digital counts of sunflowers by crop stage are shown in Table 8. The advanced maturity of stage 12 was apparent by the low digital values.

Table 7. Landsat digital means (25 August 1979 CCT) are listed by strata and Landsat band for sunflowers.

MSS 4	Strata	N[†]	Mean	Standard Deviation
	2	763	20.0	1.3
	3	10	18.3	0.7
	4	73	18.1	1.2
	6	113	19.0	1.1
	7	357	17.3	1.2
	8	51	17.1	0.7
	9	95	17.6	1.3
MSS 5	2	763	19.1	1.8
	3	10	17.1	1.0
	4	73	18.3	2.1
	6	113	18.2	1.2
	7	357	16.3	1.8
	8	51	16.2	1.1
	9	95	17.4	1.4
MSS 6	2	763	63.1	5.9
	3	10	59.6	4.2
	4	73	57.6	5.5
	6	113	57.5	6.9
	7	357	53.4	9.0
	8	51	60.1	6.0
	9	95	52.7	8.4
MSS 7	2	763	63.5	6.5
	3	10	63.0	5.2
	4	73	60.1	6.2
	6	113	58.1	7.4
	7	357	54.7	10.1
	8	51	62.4	5.6
	9	95	51.8	8.8

[†]Observations, Landsat pixels

Table 8.   Landsat digital means (25 August 1979 CCT) are listed by
crop stage and Landsat band for sunflowers.

Stage	N	MSS 4	MSS 5	MSS 6	MSS 7
7	196	18.6	19.0	52.6	52.2
8	344	19.5	18.4	62.4	63.1
9	450	19.4	18.3	62.8	63.9
10	-	-	-	-	-
11	330	18.6	17.6	59.0	59.9
12	142	17.2	16.0	50.0	51.0

Analysis of variance and multiple comparison tests are in progress.
A comparison of these results with the results from the corn data will
provide an additional basis for evaluation of the procedure.

The sunflower ground data proved to be very valuable to the FSCS.
They were able to expand the information to produce an area estimate of
sunflowers, a crop whose rapid growth in the area was of significant
importance.

SUMMARY AND CONCLUSIONS

A stratification procedure for partitioning Landsat data into
homogeneous regions relative to crop identification was investigated.
Strata were evaluated on the basis of corn and sunflower data from an
August 25, 1979 CCT; the study area was a six-county area in eastern
South Dakota.

Results are not yet complete, but the following conclusions can be made relative to corn: 1) utilizing a fixed ANOVA model, there are differences among strata and crop stage in the digital count means; 2) five to seven strata, dependent upon Landsat band, were recognized as significantly different; 3) two to four groupings of crop stages out of a possible total of five crop stages were determined by multiple comparison. This indicated differing sensitivity of Landsat bands to crop stage. Further analysis is underway, i.e. holding crop stage constant while testing strata.

Analysis of sunflower data is in progress. The results will be compared to the corn results. Sunflower ground information was expanded to provide the ESCS with an area estimate of this crop which has rapidly increased in importance in South Dakota.

REFERENCES

Dalsted, K.J., B.K. Worcester, and M.E. DeVries. In Press. Influence of soils on Landsat spectral signatures of corn. Eighth Annual Remote Sensing of Earth Resources Conference, March 27-29, 1979. The Univ. of Tenn. Space Inst., Tullahoma.

Holmes, Q.A., R. Horvath, R.C. Cicone, R.J. Kauth, and W.A. Malila. 1979. Development of Landsat-based technology for crop inventories. Final Report SR-E9-00404. ERIM, Ann Arbor, Mich. 207p.

Hueg, W.F., Jr. 1979. Will you inform the decisionmaker? p.1-25. In J. Pesek (ed.) Agronomy: science in action. ASA Special Publ. No. 36. Am. Soc. Agron., Madison, WI.

Institute for Advanced Computation. 1978. EDITOR user's handbook. IAC Tech Memo No. 5662. NASA/Ames Research Center Institute, Moffett Field, Calif.

Kauth, R.J. and G.S. Thomas. 1976. The tasselled cap-a graphic description of the spectral temporal development of agricultural crops as seen by Landsat. Proc. Symp. Machine Proc. of Remote Sens. Data, 4B:41-51, LARS, Purdue Univ.

Malila, W.A., and J.M. Gleason. 1977. Investigations of spectral separability of small grains, early season wheat detection, and multicrop inventory planning. NASA CR-ERIM 122700-34-F. Environ. Res. Inst. of Mich., Ann Arbor.

Paarlberg, D. et al. 1978. Independent peer evaluation of the large area crop inventory. NASA, Lyndon B. Johnson Space Center, Houston.

Padmanabhan, K., K.L. Majumder, and D.S. Kamat. 1980. Estimation of areas under different cover types by spectral stratification. p183. In P.G. Buroff and D.B. Morrison (ed.) Machine Processing of Remotely Sensed Data Symposium. LARS, Purdue University, West Lafayette, Indiana. (abstract)

SAS Institute, Inc. 1979. SAS user's guide, 1979 edition. Edited by Jane T. Helwig and Kathryn A. Council. Raleigh, N.C.

Schubert, J., P. Chagarlamudi, J.A. Shields, and A.R. Mack. 1980. Stratification of Landsat data by uniformity productivity of soils. p186-194. In P.G. Buroff and D.B. Morrison (ed.) Machine Processing of Remotely Sensed Data Symposium. LARS, Purdue University, West Lafayette, Indiana. (abstract).

Starbuck, R.R. 1977. Overview and examples of the EDITOR system for processing Landsat data. Statistical Reporting Service, USDA, Washington, D.C.

Steinberg, S.M. 1979. A user's guide to EDITOR. New Techniques Section; Research and Development Branch; Statistical Research Division; Economics, Statistics, and Cooperatives Service, USDA, Washington, D.C.

Tucker, C.J. and L.D. Miller. 1977. Soil spectra contributions to grass canopy spectral reflectance. Photogram. Eng. and Remote Sens. Vol. 43(6):721-726.

Von Steen, D.H., and W.H. Wigton. 1976. Crop identification and acreage measurement utilizing Landsat imagery. Statistical Reporting Service, USDA, Washington, D.C.

Westin, F.C., and G.D. Lemme. 1978. Landsat spectral signatures: studies with soil associations and vegetation. Photogram. Eng. and Remote Sens. Vol. 44(3):315-325.

Westin, F.C., and D.D. Malo. 1978. Soils of South Dakota. Bull. 656, South Dakota State Univ., Brookings.

Wiegand, C.L., et al. 1977. Soil, water, and vegetation conditions in south Texas. Type III Final Report for Goddard Space Flight Center, Greenbelt, MD.

Wigton, W.H., and P. Bormann. 1978. A guide to area sampling frame construction utilizing satellite imagery. ESCS, USDA, Washington, D.C.

APPLICATION OF REMOTE SENSING IN
THE NATIONAL MODEL IMPLEMENTATION PROGRAM,
LAKE HERMAN WATERSHED

INTRODUCTION

In 1978 Lake Herman watershed near Madison, South Dakota was selected as one of seven water resources systems in the United States to participate in the national Model Implementation Program (MIP). MIP is a three year pilot cooperative program by the United States Department of Agriculture (USDA) and the United States Environmental Protection Agency (USEPA). The program is designed to test and evaluate various water resources quality improvement methods.

Several South Dakota groups are cooperating in the Lake Herman MIP program. They include: Lake Herman Development Association, First Planning and Development District, East Dakota Conservancy District, South Dakota Department of Natural Resource Development, South Dakota State University Extension Service, USDA, Agricultural Stabilization and Conservation Service, USDA Soil Conservation Service (SCS), and the Remote Sensing Institute (RSI).

At the outset of the MIP, remote sensing techniques were employed as a means of monitoring land use and hydrologic changes throughout the watershed. In 1978, NASA and SCS funded data collection and analysis and provided technical expertise for establishment of an inventory of the baseline condition of the watershed. SCS is the

major user of the data. Baseline landcover data for the 1978 growing season and detailed soil survey data were coded into RSI's Area REsource Analysis System (AREAS), a computerized cellular information system (Wehde, 1979). The data were analyzed to produce tabular and map information concerning location, quantity and severity of soil erosion (Myers, et al. 1979).

The results of the first year of activity began to address several of the MIP objectives. Among them are the need to establish the baseline condition of the watershed, identify land in need of treatment, identify sites for sediment control structures, monitor changes within the watershed resulting from MIP and to document the achievements of MIP. Continual updating of the landcover data is necessary to address many of the objectives of MIP. The results of the second year of activity continued to address these objectives.

PROCEDURES

Initially, it was intended to utilize NASA high altitude photography acquired during the 1979 growing season for interpreting the landcover. Unfortunately, weather conditions prohibited data collection during the time period requested. Consequently, 70 mm 1:61,000 scale color and color infrared photography was acquired on 29 August using the RSI low altitude aircraft.

Groundtruth data for the watershed were collected prior to the interpretation of the photography. Twelve landcover categories

identical to those used for the 1978 data were interpreted. The groundtruth data were obtained by recording the landcover type that occurred in each quadrant at most road intersections within the watershed. The information was used to train the interpreters and verify interpretation results.

The 1979 landcover data were computerized using a method similar to the 1978 process (Myers et al. 1979). The photographic data were enlarged to approximately 1:11,000 using an International Imaging System (I^2S) color additive viewer.* The enlarged data were overlaid with a cell grid. Each cell represented .25 hectares (.625 acres). Each cell was classified, based on category dominance within the cell. The digitized data were verified for all category boundaries and classes.

Land Treatment

Several hundred acres of land were terraced during the first year of MIP. Much of the land was identified as in need of treatment from maps generated from analysis of the 1978 landcover data and detailed soil data within the information system. The land treatment data set was updated to reflect the improvements. Information concerning the location of the newly constructed terraces was provided by SCS. A revised map of land in need of treatment was produced for SCS.

---

*Inclusion in this report of registered tradenames or trademarks does not constitute an endorsement by the author or the Remote Sensing Institute.

Sediment Delivery Modeling

The latest application of the information system is being directed toward modeling sediment delivery to the lake. SCS has delineated four major tributary areas which are delivering sediment to the lake. The subdivision of the natural surface drainage network of streams accounts for three areas. The fourth area is the immediate lake shore. The fourth area and associated drainage network was delineated and encoded into the information system.

The tributary areas, drainage network, land cover and capability class data sets were used in the two approaches which were investigated to estimate sediment delivery to the lake. The first approach was to assign a weight to each cell of cropland on capability class IIE, IIIE, and IVE within the watershed. Cropland on these classes is considered to be the primary source of sediment by SCS. The weight was based on the shortest distance of the cell to the lake shore. Consequently, a cell on the lake shore would be weighed much more heavily than one on the outer extremity of the watershed. Theoretically the potential for sediment reaching the lake would decrease as the distance to the lake increased (Fig. 1).

The estimated sediment yield rate for the soils within the watershed was estimated in tons per acre. The estimates were made by SCS using the rainfall factor (R), erodibility factor (K), slope length and gradient factors (LS), vegetative cover factor (C), and the erosion control practice factor (P) of the universal soil loss
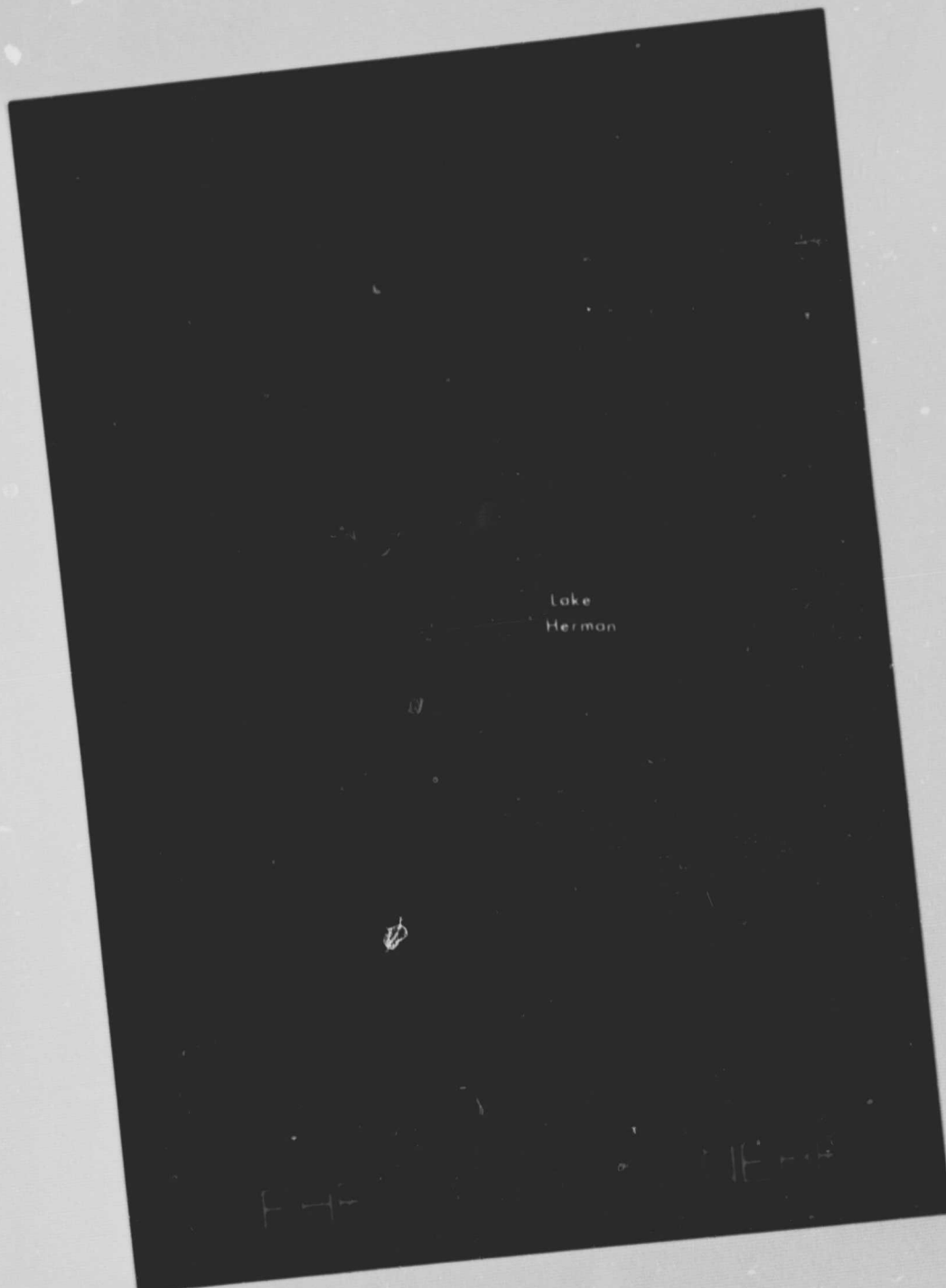
Lake
Herman

Fig. 1. Graphic representation of weighting based on distance to lake.

equation. Estimates were calculated for row crops, small grains, and grassland on capability class IIE, IIIE, and IVE land. The estimates do not take into consideration any existing land treatment.

The SCS estimates of sediment yield rate were used in a formula to calculate total sediment delivery. The formula is:

$$\Sigma_{cc/lu} \; A_{cc/lu} \; *YR \; *Wp = T/A$$

where:

$A_{cc/lu}$ is the acreage of a landcover class on a capability class

YR is the yield rate

Wp is the weight based on proximity to the lake

The second approach involved weighing each cell of cropland and grassland. This time however the cells were weighed on the distance to drainage rather than the lake itself. The basic assumption in the model was that any sediment entering the drainage would eventually enter the lake (Fig. 2).

RESULTS

Sediment Control Structure Site Planning

One of the major MIP activities of SCS is the planning and construction of sediment control structures. At least three major structures and several minor structures will be constructed. During the summer of 1979 SCS was involved in planning a major sediment control structure in the drainage entering the southern tip of Lake Herman.
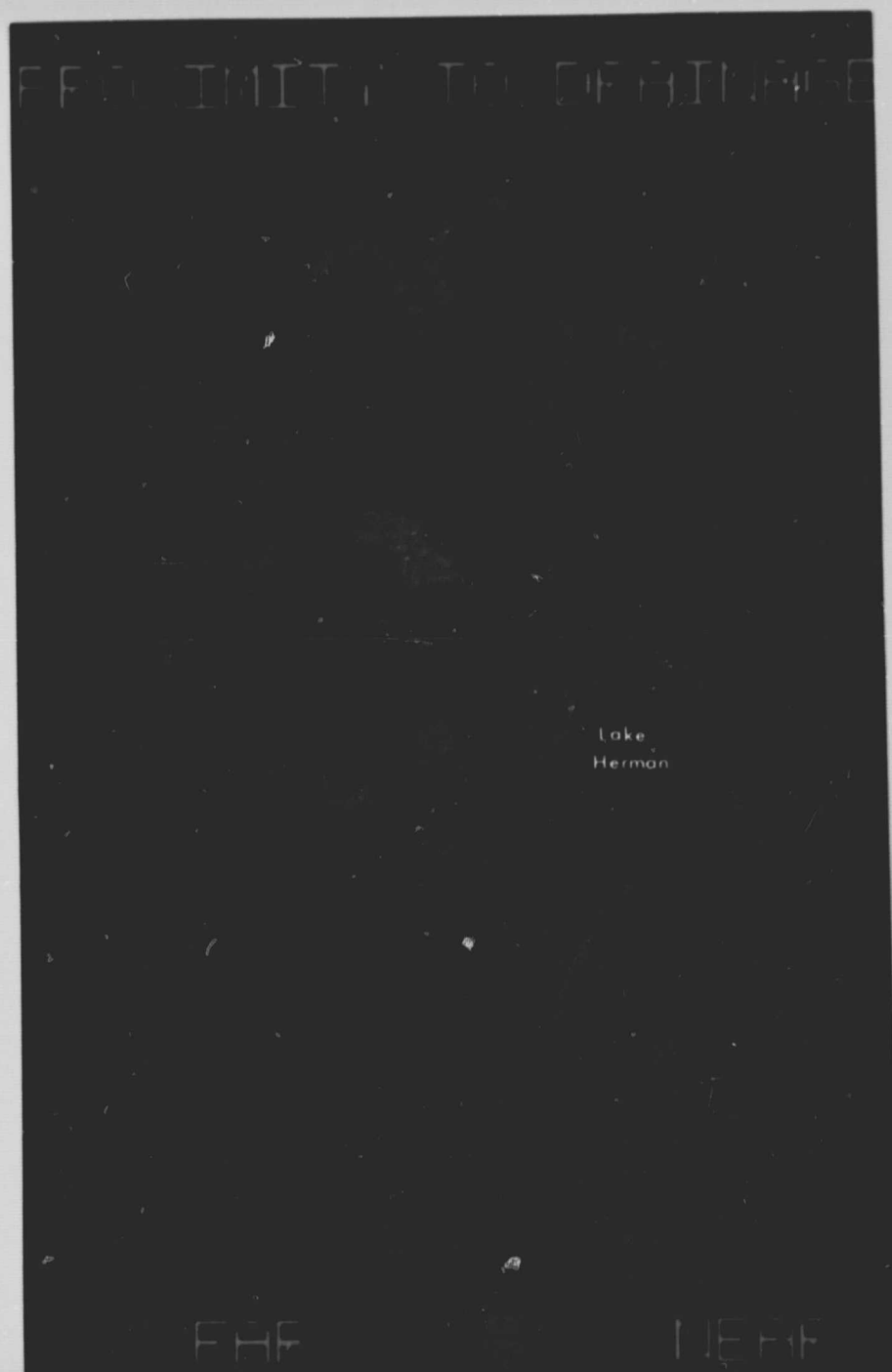
Fig. 2. Graphic representation of weighting based on distance to drainage.

The SCS utilized specific map and tabular information derived from AREAS throughout the planning and design of the sediment control structure. One of the major uses of the information was to determine the necessary size of the structure. The SCS utilized landcover, land treated, land in need of treatment and soil capability class information to estimate potential runoff and soil erosion.

Another use of the information was to determine potential sites. Sites were determined from a slope map of the watershed generated from the detailed soil data. The map delineated areas of steep slopes suitable for construction sites. The final sites were selected from field surveys. Figure 3 delineates the areas of steep slopes with existing and proposed sites annotated.

Sediment Delivery Modeling

Two sedimentation models have been evaluated to date. The first approach which was based on the distance of a parcel of land from the lake shore, utilized the SCS sediment yield estimates for cropland and capability classes (Table 1) to estimate sediment delivery to the lake.

Table 1. Estimated sediment yield (tons/acre) for landcover type and capability class.

	IIE	IIIE	IVE
Row Crops	5.3	10.2	15.3
Small Grains	1.8	3.9	6.3
Grassland	.2	.9	1.8
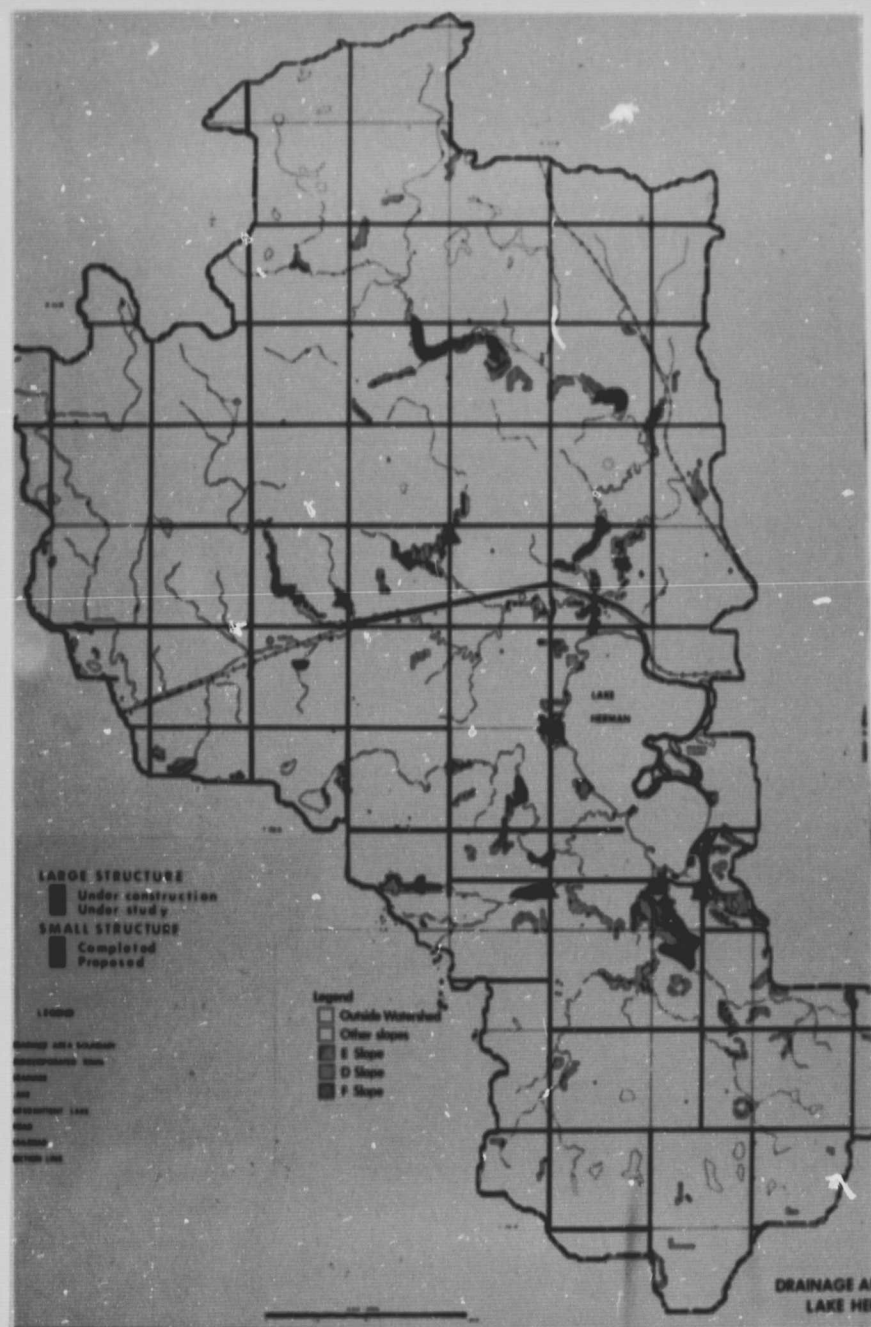
Fig. 3. Areas of significant slopes suitable for sediment control
structures with existing and proposed sites annotated.

The estimate of sediment delivery to the lake from the first approach for all four tributary areas was 42,800 tons or 32.7 acre feet. This estimate was relatively close to the results obtained from a study conducted by USDA Science and Education Administration. Sedimentation Laboratory (ESCS, 1979). The study involved collecting several core samples of sediment from the lake bottom. The age and rate of sedimentation was determined by measuring the amount of Cesium 137 in the core samples. The presence of the radioactive Cesium 137 was the result of nuclear testing conducted in 1954. The study measured a 25 year average sediment delivery rate of 22 acre feet annually. The estimate of the first approach would be closer to the ESCS measurement if existing land treatment is considered.

A breakdown by tributary area indicated as expected that the largest area was the greatest contributor. However, the breakdown showed that the average yield in tons per acre from cropland and grassland was the greatest in the second largest area. This indicated to SCS that perhaps a more intensive soil conservation effort was needed in that area.

The second approach which was based on the distance to drainage approach derived a sediment yield estimate of 72,900 on 55.8 acre feet. This is nearly 58 percent higher than the first estimate. The results of the second approach lead one to believe that the assumption that all sediment entering drainage reaches the lake is incorrect. Consequently, a new approach is being investigated which not only weighs

the distance to drainage but also weighs the distance of the drainage point from the lake along the drainage path. It is anticipated that this method will provide a more reasonable estimate.

CONCLUSIONS

Over the past two years SCS has been using a geographical information system to address the objectives of MIP. The objectives include establishing the baseline condition of the watershed, identifying land in need of treatment, constructing sediment control structures and documenting the achievements of MIP.

The map and tabular information derived from the information system have greatly facilitated the aspects of MIP. SCS has been able to utilize the map and tabular data to reduce the amount of field work and concentrate in areas where land treatment is most necessary and to delineate areas most suitable for sediment control structures.

The sediment yield model has provided new insight into the effects of land management on sediment delivery. Although it is difficult to assess the accuracy of the model repeated use of the same model over-time will provide a relative evaluation of the overall reduction of sediment yield as a result of land treatment or other management practices. Further refinement will improve the usefulness of the model for overall watershed management and sediment control structure design.

SCS has realized the benefits of utilizing natural resource data acquired from remote sensing and other techniques in an information system approach. Consequently, SCS is providing major funding support to continue the work through the remaining year of MIP.

In the future the landcover and land treatment data sets will be updated to facilitate the evaluation of the impact of the MIP program. Crop rotation and land treatment practices will be studied and further improvements will be made within the watershed. In general, it is anticipated that the use of natural resource information systems of this design could be used to address land and water quality management problems nationwide.

REFERENCES

Wehde, Mike, B.K. Worcester, and K.J. Dalsted. 1979. Computerized
  resource management. Submitted to Journal of Soil and Water
  Conservation, Soil Conservation Society of America.

Myers, V.I., R.G. Best, K.J. Dalsted, M.E. DeVries, J.C. Eidenshink,
  J.L. Heilman, S. Sather-Blair, F.A. Schmer, K. Solomon, and
  B.K. Worcester. 1979. Remote sensing applications to resource
  problems in South Dakota. Annual Report to NASA, July 1, 1979 -
  June 30, 1979. pp.96-113.

SIX-MILE CREEK INVESTIGATION FOLLOW-ON

INTRODUCTION

An investigation was initiated in 1978 to evaluate the geo-hydrology and the environment of Six-Mile Creek Watershed near Brookings, South Dakota to evaluate the impact of a proposed dam and reservoir site (Myers, et al., 1979). Thermal and color IR data were used by SCS and RSI personnel to evaluate the ground water situation, complete a land use inventory, and characterize erosion potential for preparation of an environmental impact statement. Specific objects were to:

1) Select sites for drilling observation wells

2) Evaluate water-table depths

3) Evaluate soil moisture

4) Evaluate erosion potential

These objectives were met in FY 79. An extension of the Six-Mile Creek Investigation was requested so that results of the drilling program (objective 1) could be fully documented. Refer to the 1979 Annual Report SDSU-RSI-79-14 for a complete discussion of the investigation.

RESULTS

A ground water investigation of the proposed dam and recreation site on Six-Mile Creek Watershed (Fig. 1) is required to evaluate
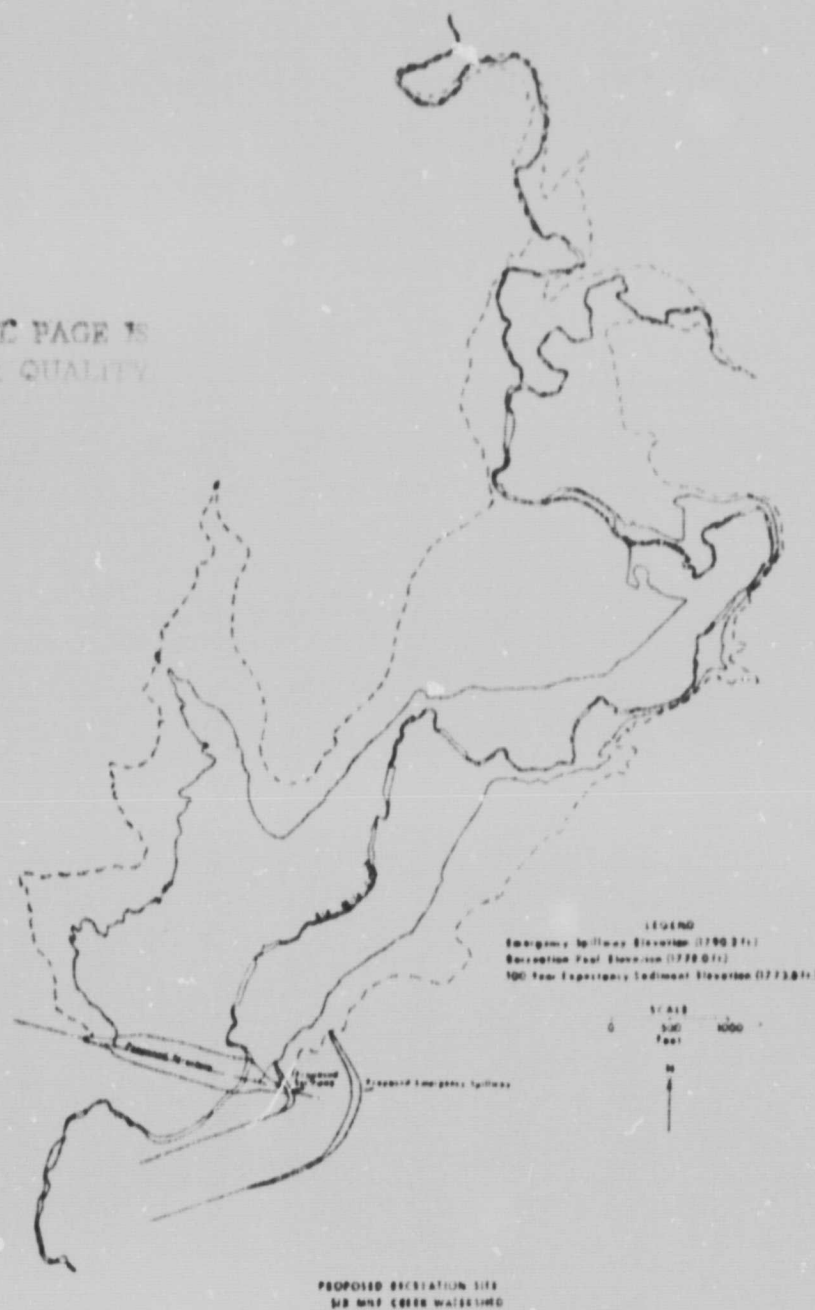
Fig. 1. Description of proposed recreation site on Six-Mile Creek Watershed.

potential seepage losses. The investigation consists of drilling and logging of observation wells to evaluate the vertical extent and layering of permeable aquifer material. Wells are installed so that ground water heads can be measured independently in each aquifer at multiple lateral locations. Relative and actual permeability and boundaries of permeable material must be known to design seepage cutoff and drainage control under the structure.

The geohydrologic investigation of the site was initiated in 1978 with the drilling of 11 observation wells along the proposed structure site and near the northern end of the pool area. Potential sites for drilling remaining wells were selected on the basis of the remote sensing imagery acquired in early September, 1978 (Myers et al., 1979). Thermal imagery of the recreation site revealed a broad cool pattern surrounding Six-Mile Creek (Fig. 2). The shape and location of the apparent thermal anomaly were typical of thermal patterns produced by shallow aquifers.

Test holes 805, 806, and 807 (Fig. 2), later renumbered 801, 802, and 803, respectively by SCS, were drilled in August 1979. Results of the drilling are summarized in Table 1 and Fig. 3-5. Drilling verified the presence of permeable alluvium at all three locations. Depth to water ranged from 1 to 5 feet below the soil surface. Observation wells and piezometers were installed at the three locations to monitor ground water fluctuations and head pressure.

Fig. 2. Daytime thermal image of proposed dam and recreation site on Six-Mile Creek Watershed. An apparent anomaly is delineated by dashed lines. Numbers are potential drilling sites. Approximate scale 1:16,000; dark is cool.

Table 1. Log of test boring for Six-Mile Creek.

LOG OF TEST BORING

JOB NO __620-1446__   VERTICAL SCALE __1" = 5'__   BORING NO __801__

PROJECT __OBSERVATION WELL INSTALLATION - PROPOSED RECREATION AREA - WHITE, SOUTH DAKOTA__

DEPTH IN FEET	DESCRIPTION OF MATERIAL (SURFACE ELEVATION)	GEOLOGIC ORIGIN	N	WL	SAMPLE NO	SAMPLE TYPE	LABORATORY TESTS W	D	AL WL	Qu
2	SILTY CLAY, dark gray (CL)	TOPSOIL			1	FA				
6	SANDY CLAY, trace of gravel, dark gray (CL)	TILL			2	FA				
9½	SANDY CLAY with gravel, dark gray, rather stiff, laminations of sand at 7'-8½' (CL)				3	SS				
13	SILTY SAND, dark gray, medium dense, laminations of medium grained sand at 11½'-13' (SM)	MIXED ALLUVIUM	11		4	SS				
	LEAN CLAY, a little gravel, dark gray, stiff, laminations of fine grained waterbearing sand (CL)	TILL	18		-	SS				
					6*	WS*				
					7*	WS**				
					8*	WS*				
					9*	WS*				
37					10	WS*				
40	LEAN CLAY, a little gravel, brownish gray, very stiff, laminations of fine grained sand (CL)									
	CONTINUED ON NEXT PAGE									

*No Sample Retained
**Washed Sample

SOIL EXPLORATION

SE 3 (7 76)

LOG OF TEST BORING

JOB NO ___620-1446___ VERTICAL SCALE ___1" = 5'___ BORING NO ___801___ (CONT.)

PROJECT ___OBSERVATION WELL INSTALLATION - PROPOSED RECREATION AREA- WHITE SOUTH DAKOTA___

DEPTH IN FEET	DESCRIPTION OF MATERIAL	GEOLOGIC ORIGIN	N	WL	SAMPLE		LABORATORY TESTS			
					NO	TYPE	W	D	LL/PL	Qu
40	SAME AS PREVIOUS PAGE	TILL	31		11	SS				
					12	*WS**				
46	SILTY SAND, gray, very stiff (SM)	MIXED ALLUVIUM								
51			41		13	SS				
	END OF BORING									
	* No Sample Retained ** Washed Sample									

WATER LEVEL MEASUREMENTS							START _8-5-79_ COMPLETE _8-5-79_
DATE	TIME	SAMPLED DEPTH	CASING DEPTH	CAVE IN DEPTH	BAILED DEPTHS	WATER LEVEL	METHOD 4C 0-7' @ 2:33
8-9	3:05	51'	None		to	5'	D.M. 7'-49½'
					to		
					to		
					to		CREW CHIEF HANSON

SE 2 (77-81) 5   SOIL EXPLORATION

LOG OF TEST BORING

JOB NO __620-1446__   VERTICAL SCALE __1" = 5'__   BORING NO __802 A & B__

PROJECT __OBSERVATION WELL INSTALLATION - PROPOSED RECREATION AREA - WHITE, SOUTH DAKOTA__

DEPTH IN FEET	DESCRIPTION OF MATERIAL SURFACE ELEVATION	GEOLOGIC ORIGIN	N	WL	SAMPLE NO	SAMPLE TYPE	W	D	LL/PL	Qu
1	SILTY CLAY, black (CL)	TOPSOIL		∨	1	FA				
	SANDY CLAY, a little gravel (CL)	TILL		∠	2	FA				
3½	SAND, coarse and medium grained, some cobbles, brown, laminations of SANDY CLAY	COARSE ALLUVIUM			3*	WS**				
	(SP)				4	WS**				
8½	SANDY CLAY, some gravel, red and brown mottled, stiff, lenses of waterbearing sand, gravel, and cobbles	TILL	16		5	SS				
					6*	WS**				
	(CL)				7*	WS**				
14½	SANDY CLAY, a little gravel, dark gray, stiff, laminations of waterbearing sand at 31', cobbles at 14½'-17½'				8	.S**				
	(CL)				9	WS**				
31			30		10	SS				
32	***SEE NOTE #1				11	SS				
	LEAN CLAY, a little gravel, brownish gray, stiff									
	(CL)		30		12	SS				
36½	END OF BORING *No Sample Retained **Washed Sample ***NOTE #1 - SILT, light gray, laminations of waterbearing sand (ML)									

		WATER LEVEL MEASUREMENTS					START __8-6-79__ COMPLETE __8-7-79__
DATE	TIME	SAMPLED DEPTH	CASING DEPTH	CAVE IN DEPTH	BAILED DEPTHS	WATER LEVEL	METHOD 4C 0-7' @ 12:45
8-9	3:03	36½'	None	-	to	1'	D.M. 7'-35'
					to		
					to		CREW CHIEF HANSON
					to		

SE-2 (77 81 5)   SOIL EXPLORATION COMPANY

LOG OF TEST BORING

JOB NO 620-1446   VERTICAL SCALE 1" = 5'   BORING NO 803

PROJECT OBSERVATION WELL INSTALLATION - PROPOSED RECREATION AREA - WHITE, SOUTH DAKOTA

DEPTH IN FEET	DESCRIPTION OF MATERIAL ⌐SURFACE ELEVATION	GEOLOGIC ORIGIN	N	WL	SAMPLE NO	TYPE	W	D	LL PL	Qu
	SILTY CLAY, dark brown (CL)	TOPSOIL			1	FA				
2½	*** SEE NOTE #1	TILL		▽	2	FA				
3½										
	SANDY CLAY, trace of gravel, brown, samll cobbles and layers of medium and coarse grained sand at 6'-8' (CL)				3*	WS**				
8										
	SANDY CLAY, trace of gravel, brown, very stiff, cobles at 9½' and 11½' (CL)		52		4	SS				
12½										
	LEAN CLAY, trace of gravel, dark gray, stiff to very stiff, cobbles at 41.2' (CL)				5*	WS**				
			19		6	WS*				
	***NOTE #1 - SANDY CLAY, trace of gravel, grayish brown, cobbles at 3' (CL)				7*	WS*				
					8	WS**				
					9*	WS**				
35	CONTINUED ON NEXT PAGE									
	*No Sample Retained **Washed Sample									

LOG OF TEST BORING

| JOB NO | 620-1446 | VERTICAL SCALE | 1" = 5' | BORING NO | 803(CONT.) |

PROJECT OBSERVATION WELL INSTALLATION- PROPOSED RECREATION AREA - WHITE, SOUTH DAKOTA

DEPTH IN FEET	DESCRIPTION OF MATERIAL — SURFACE ELEVATION	GEOLOGIC ORIGIN	N	WL	SAMPLE		LABORATORY TESTS			
					NO	TYPE	W	D	LL PL	Qu
35	SAME AS PREVIOUS PAGE	TILL								
41.2	OBSTRUCTION		43.7		10	SS				

WATER LEVEL MEASUREMENTS

DATE	TIME	SAMPLED DEPTH	CASING DEPTH	CAVE-IN DEPTH	BAILED DEPTHS		WATER LEVEL
8-9	3:00	41.2'	None	-	10		3½'
					10		
					10		
					10		

START	8-7-79	COMPLETE	8-7-79

METHOD 4C 0-6'   @

D.M. 6'-40'

CREW CHIEF HANSON

SE-2(77-8)-5

soil exploration company

GENERAL NOTES

DRILLING & SAMPLING SYMBOLS

SYMBOL	DEFINITION
C.S	Continuous Sampling
P.D.	2-3/8" Pipe Drill
C.O.	Cleanout Tube
3¼ HSA	3¼" I.D. Hollow Stem Auger
4 FA	4" Diameter Flight Auger
6 FA	6" Diameter Flight Auger
2½ C	2½" Casing
4C	4" Casing
D.M.	Drilling Mud
J. W.	Jet Water
H. A.	Hand Auger
NXC	Size NX Casing
BXC	Size BX Casing
AXC	Size AX Casing
SS	2" O.D. Split Spoon Sample
2T	2" Thin Wall Tube Sample
3T	3" Thin Wall Tube Sample

LABORATORY TEST SYMBOLS

SYMBOL	DEFINITION
W	Moisture content - percent of dry weight
D	Dry density-pounds per cubic foot
LL, PL	Liquid and plastic limits determined in accordance with ASTM D 423 and D 424
Qu	Unconfined compressive strength-pounds per square foot in accordance with ASTM D 2166-66

Additional insertions in Qu column

Pq	Penetrometer reading-tons/square foot
Ts	Torvane reading-tons/square foot
G	Specific gravity - ASTM D 854-58
SL	Shrinkage limit - ASTM D 427-61
pH	Hydrogen ion content-meter method
O	Organic content-combustion method
M.A.*	Grain size analysis
C*	One dimensional consolidation
Qc*	Triaxial compression

*See attached data sheet and/or graph

WATER LEVEL

SYMBOL – ▽

Water levels shown on the boring logs are the levels measured in the borings at the time and under the conditions indicated. In sand, the indicated levels can be considered reliable ground water levels. In clay soil, it is not possible to determine the ground water level within the normal scope of a test boring investigation, except where lenses or layers of more pervious waterbearing soil are present and then a long period of time may be necessary to reach equilibrium. Therefore, the position of the water level symbol for cohesive or mixed texture soils may not indicate the true level of the ground water table. The available water level information is given at the bottom of the log sheet.

DESCRIPTIVE TERMINOLOGY

DENSITY

TERM	"N" VALUE
Very loose	0-4
Loose	5-8
Medium Dense	9-15
Dense	16-30
Very Dense	Over 30

CONSISTENCY

TERM	"N" VALUE
Soft	0-4
Medium	5-8
Rather Stiff	9-15
Stiff	16-30
Very Stiff	Over 30

Standard "N" Penetration: Blows per foot of a 140 pound hammer falling 30 inches on a 2 inch OD split spoon.

RELATIVE PROPORTIONS

TERM	RANGE
Trace	0-5%
A Little	5-15%
Some	15-30%
With	30-50%

PARTICLE SIZES

Boulders	Over 3"
Gravel	
Coarse	¾"-3"
Fine	#4-¾"
Sand	
Coarse	#4-#10
Medium	#10-#40
Fine	#40-#200
Silt and Clay	Determined by plasticity Characteristics

Note: Sieve sizes shown are U.S. Standard

SE-4170A1

CLASSIFICATION OF SOILS FOR ENGINEERING PURPOSES

ASTM Designation: D 2487 – 69 AND D 2488 – 69

(Unified Soil Classification System)

Major divisions			Group symbols	Typical names	Classification criteria	
Coarse-grained soils More than 50% retained on No. 200 sieve*	Gravels 50% or more of coarse fraction retained on No. 4 sieve	Clean gravels	GW	Well-graded gravels and gravel-sand mixtures, little or no fines	$C_u = \dfrac{D_{60}}{D_{10}}$ greater than 4; $\quad C_z = \dfrac{(D_{30})^2}{D_{10} \times D_{60}}$ between 1 and 3	Classification on basis of percentage of fines Less than 5% pass No. 200 sieve ...... GW, GP, SW, SP More than 12% pass No. 200 sieve ...... GM, GC, SM, SC 5 to 12% pass No. 200 sieve ...... *Borderline classifications requiring use of dual symbols*
			GP	Poorly graded gravels and gravel-sand mixtures, little or no fines	Not meeting both criteria for GW	
		Gravels with fines	GM	Silty gravels, gravel-sand-silt mixtures	Atterberg limits below "A" line or P.I. less than 4 / Atterberg limits plotting in hatched area are *borderline* classifications requiring use of dual symbols	
			GC	Clayey gravels, gravel-sand-clay mixtures	Atterberg limits above "A" line with P.I. greater than 7	
	Sands More than 50% of coarse fraction passes No. 4 sieve	Clean sands	SW	Well-graded sands and gravelly sands, little or no fines	$C_u = \dfrac{D_{60}}{D_{10}}$ greater than 6; $\quad C_z = \dfrac{(D_{30})^2}{D_{10} \times D_{60}}$ between 1 and 3	
			SP	Poorly graded sands and gravelly sands, little or no fines	Not meeting both criteria for SW	
		Sands with fines	SM	Silty sands, sand-silt mixtures	Atterberg limits below "A" line or P.I. less than 4 / Atterberg limits plotting in hatched area are *borderline* classifications requiring use of dual symbols	
			SC	Clayey sands, sand-clay mixtures	Atterberg limits above "A" line with P.I. greater than 7	
Fine-grained soils 50% or more passes No. 200 sieve*	Silts and clays Liquid limit 50% or less		ML	Inorganic silts, very fine sands, rock flour, silty or clayey fine sands		
			CL	Inorganic clays of low to medium plasticity, gravelly clays, sandy clays, silty clays, lean clays		
			OL	Organic silts and organic silty clays of low plasticity		
	Silts and clays Liquid limit greater than 50%		MH	Inorganic silts, micaceous or diatomaceous fine sands or silts, elastic silts		
			CH	Inorganic clays of high plasticity, fat clays		
			OH	Organic clays of medium to high plasticity		
Highly organic soils			Pt	Peat, muck and other highly organic soils		

Plasticity Chart

For classification of fine-grained soils and fine fraction of coarse-grained soils.

Atterberg Limits plotting in hatched area are *borderline* classifications requiring use of dual symbols.

Equation of A-line:
$$PI = 0.73 \, (LL - 20)$$

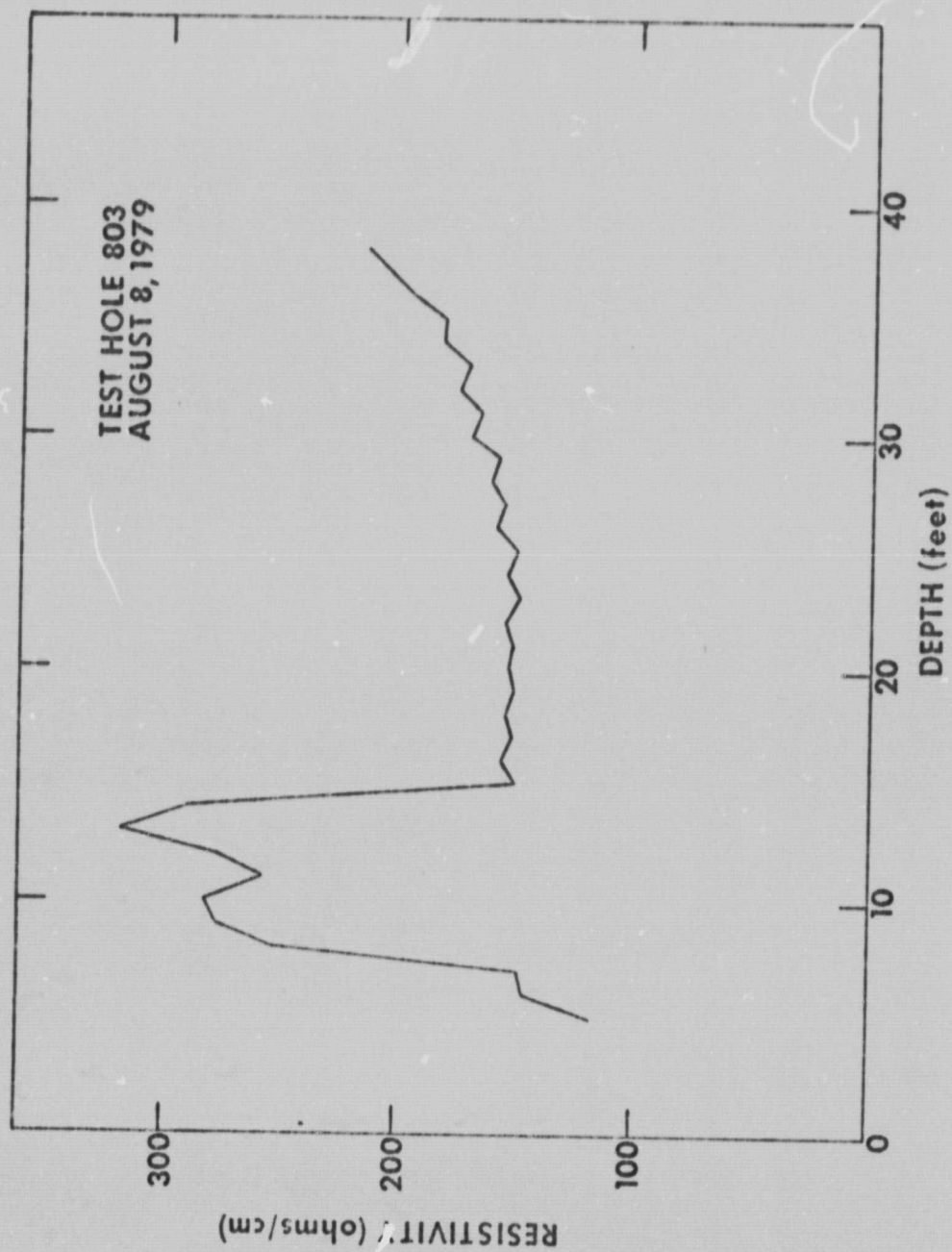*Based on the material passing the 3 in. (76 mm) sieve.

Fig. 3. Resistivity log for test hole 801. A high resistivity is indicative of permeable material.
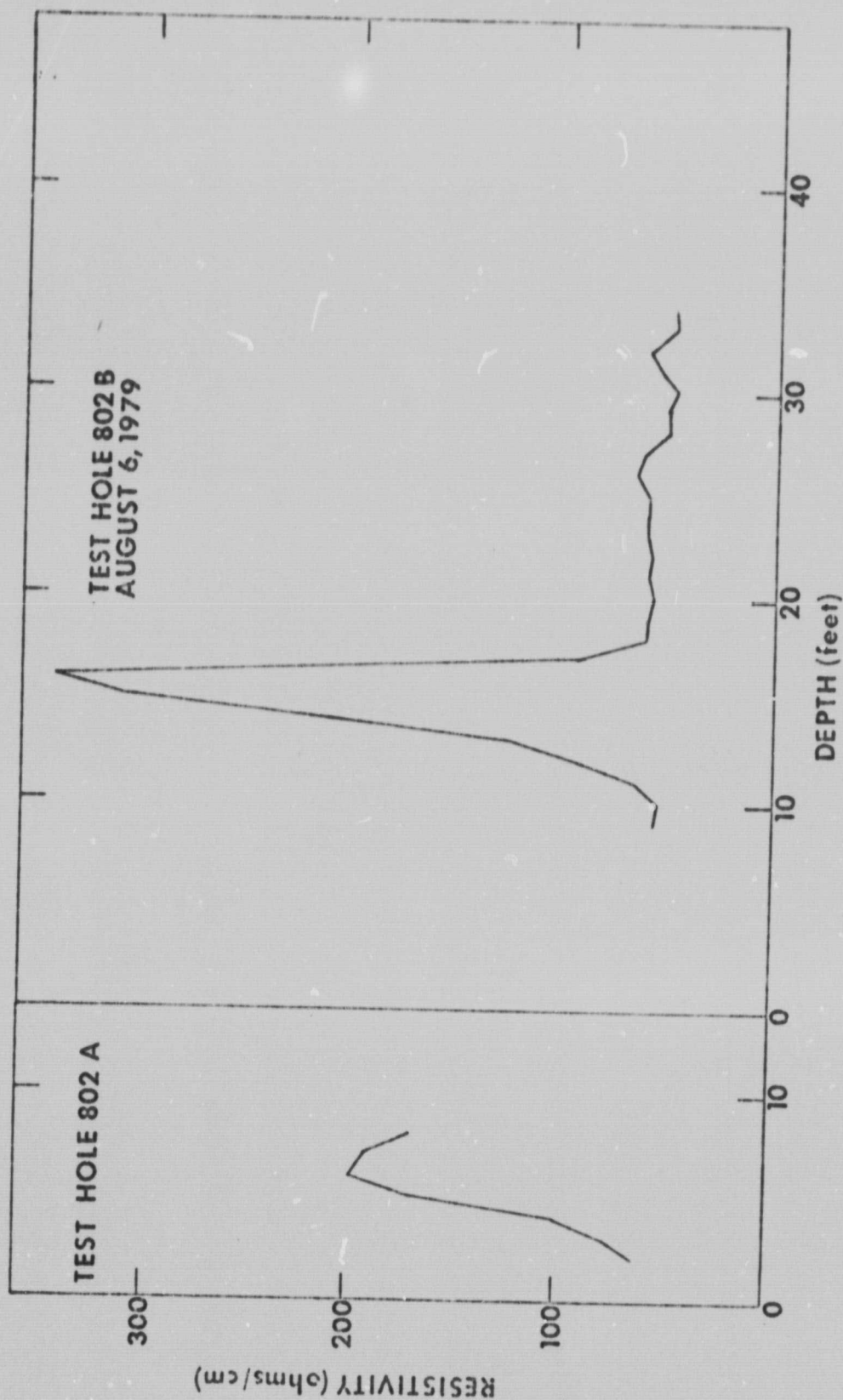
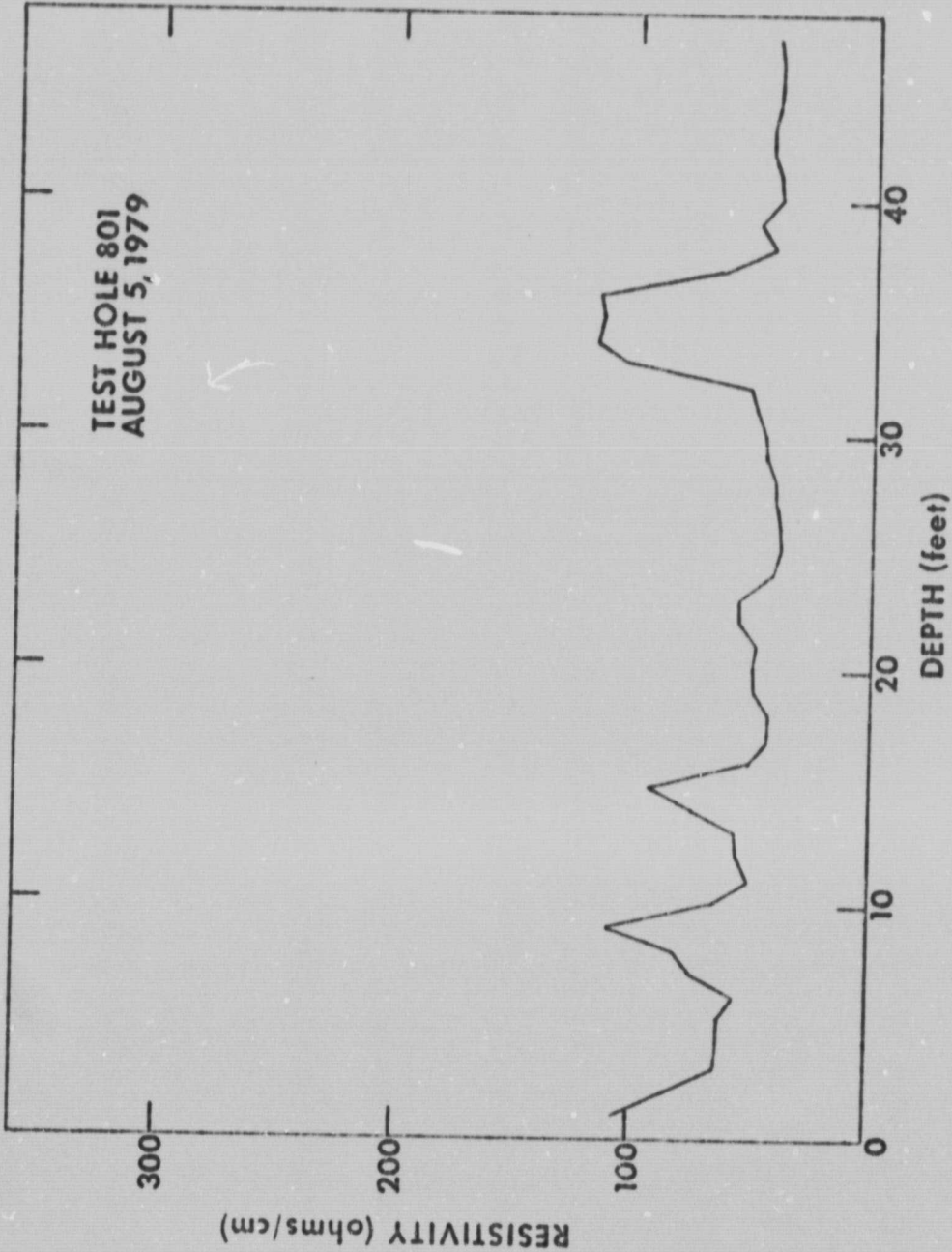Fig. 4. Resistivity log for test holes 802A and B.

Fig. 5. Resistivity log for test hole 803.

SUMMARY

This completes the Six-Mile Creek Investigation. The attached letter from the State Conservationist summarizes the cooperative study between the Soil Conservation Service and the Remote Sensing Institute. This project has been a successful demonstration of the use of remote sensing in watershed planning and development. Information obtained from the investigation will be used to prepare the Preliminary Investigation Report (PIR) which will form the basis for the final Working Plan and Environmental Impact Statement. The PIR will be submitted to NASA upon completion.

**United States
Department of
Agriculture**

Soil
Conservation
Service

Federal Building
200 Fourth Street S. W.
Huron, South Dakota 57350

November 26, 1979

Mr. Victor Myers, Director
Remote Sensing Institute
South Dakota State University
Brookings, South Dakota 57007

Dear Mr. Myers:

We wish to thank you and your staff for the fine cooperation and help
you have given us.

The cooperative study between the Remote Sensing Institute and the Soil
Conservation Service on Six Mile Creek Watershed has been extremely
useful and timely in the preparation of the watershed plan for flood-
damage reduction and the development of water-based recreation.

Identification of land use and land-treatment needs are integral parts
of the environmental assessment of the watershed. The remotely sensed
data obtained by RSI is being used in this identification process.
Digitized imagery has been analyzed and put in tabular form by RSI
for soils mapping units and land used. The land use data has been
superposed on watershed maps by RSI. SCS will pick out key soils which
RSI will superpose on the land use maps. This data will be used by SCS
to locate and quantify flood-prone areas and land treatment needs.

The proposed multipurpose reservoir designated SM-1B, located north of
White, South Dakota, is being investigated as both a flood-water
retarding and recreation reservoir. These combined purposes require
both safety and waterholding capability considerations. Understanding
the ground-water regime of the watershed and present and potential
subsurface-water movement to and from the proposed reservoir are
required in both safety and water holding capability considerations.

Infrared and near surface temperature scan data obtained by RSI were
used to locate the boundaries of near surface permeable alluvium.
Preliminary drilling was used to identify the subsurface materials.
The location of the drill holes was selected using both the remotely
sensed data and traditional site exploration methods. Ground-water
observation wells and piezometers were installed to monitor the
fluctuations in ground-water levels and head pressure. The monitoring
is being continued by SCS to obtain adequate data on seasonal changes.

The remotely sensed data has made it possible to reduce the time and
expense of subsurface drilling needed to identify the earth material
characteristics. SCS has been able to more efficiently study the ground
water conditions because the remotely sensed data has been used in
decisions on the location and number of ground-water observation
stations.

Cost and time efficiency have been improved by the use of remotely sensed
data in the environmental assessment through reduction of time required
for land use and land treatment inventories.

R. D. Swenson
State Conservationist

cc: Kenneth Huber, WRPSL, SCS, Huron
      James Hyland, Geologist, SCS, Huron

REFERENCES

Myers, V.I., et al., 1979. Remote sensing applications to resource problems in South Dakota. Report no. SDSU-RSI-79-14 to NASA Office of University Affairs, Washington, D.C.